Derivatization Methods for Improved Metabolome Analysis by LC-MS/MS

by

Paige A. Malec

A dissertation submitted in partial fulfillment
of the requirements for the degree of
Doctor of Philosophy
(Chemistry)
in The University of Michigan
2018

Doctoral Committee:

Professor Robert T. Kennedy, Chair
Professor Philip C. Andrews
Professor Charles F. Burant
Associate Professor Brandon T. Ruotolo

Paige A. Malec

pmalec@umich.edu

ORCID iD: 0000-0002-9853-6078

DEDICATION

I dedicate this work to Joe. I could not achieve what I have without his support.

ACKNOWLEDGEMENTS

I am truly blessed to be surrounded by such a strong support system. This support is what brought me to graduate school and has guided me through these past five years. From the start, my parents were my biggest supporters, raising me to believe I could accomplish anything I set my mind to. My teachers over the years encouraged my love of learning and science. My friends have always been there for me to fall back on when I became overwhelmed. My labmates, old and new, have been great resources for knowledge, troubleshooting, and entertainment. I thank everyone who has supported me in my academic journey.

I especially must acknowledge Joe, my husband. He has been by my side through the ups and downs of graduate school. His positive energy kept me focused and motivated even when everything seemed to be going wrong. I could not have reached this milestone in my life without his love and support.

Finally, I acknowledge my advisor, Robert Kennedy. Under his watch, I was able to work on a project I truly enjoyed. I do not think I could have achieved many of my accomplishments throughout graduate school without his guidance. His support and encouragement greatly helped bring me to this point.

It is challenging to watch this chapter of my life come to a close, but I am not afraid to face whatever adventures life has in store for me next because I have so many people I can count on for support.

TABLE OF CONTENTS

LIST OF TABLES

LIST OF FIGURES

LIST OF ABBREVIATIONS

2DG	2-deoxyglucose
2HPA	2-hydroxyphenylacetate
2-HQ	2-hydroxyquinoline
2PG	2-phosphoglycerate
3HAA	3-hydroxyanthranilic acid
3HK	3-hydroxykynurenine
3MT	3-methoxytyramine
3-OMD	3-O-methyldopa
3PG	3-phosphoglycerate
4HPA	4-hydroxyphenylacetate
4HPP	4-hydroxyphenylpyruvate
5HIAA	5-hydroxyindoleacetic acid
5HT	serotonin
5HTOL	5-hydroxytryptophol
5HTP	5-hydroxytryptophan
6PG	6-phosphogluconate
ACh	acetylcholine
ACN	acetonitrile
aCSF	artifical cerebrospinal fluid
Ado	adenosine
ADP	adenosine diphosphate
Agm	agmatine
aKG	α-ketoglutarate
Ala	alanine
AMP	adenosine monophosphate
Ans	anserine
Arg	arginine
Asn	asparagine
Asp	aspartate
ATP	adenosine triphosphate
BAla	β-alanine
Bn	benzyl group

BnA	benzylamine
BQB	ω-bromoacetonylquinolinium bromide
Bz	benzoyl group
BzCl	benzoyl chloride
CA	cysteic acid
CA	citrate
cAc	cis-aconitate
Cad	cadaverine
Caf	caffeic acid
Carn	carnosine
Ch	choline
Cit	citrulline
COMT	catechol-O-methyltransferase
Cou	p-coumaric acid
CRR	counterregulatory response
Cys	cysteine
DA	dopamine
DMSO	dimethylsulfoxide
DnsCl	dansyl chloride
DOMA	3,4-dihydroxymandelic acid
DOPAC	3,4-dihydroxyphenylacetic acid
DOPEG	3,4-dihydroxyphenylglycol
E	epinephrine
EDC	N-dimethylaminopropyl-N'-ethylcarbodiimide
ESI	electrospray ionization
ETA	ethanolamine
F16P	fructose-1,6-bisphosphate
F6P	Fructose-6-phosphate
Fer	ferulic acid
G6P	glucose-6-phosphate
GABA	γ-aminobutyric acid
Gal	gallic acid
GC	gas chromatography
Glc	glucose
Gln	glutamine
Glu	glutamate
Gly	glycine
GSH	glutathione
HC	healthy control
HCA	homocysteic acid

HCY	homocysteine
HGA	homogentisate
HILIC	hydrophilic interaction liquid chromatography
His	histidine
Hist	histamine
HMDB	Human Metabolome Database
HPLC	high pressure liquid chromatography
HSer	homoserine
HTau	hypotaurine
HVA	homovanillic acid
HY	Hoehn and Yahr
ICA	isocitrate
KA	kynurenic acid
Kyn	kynurenine
Kyo	kyotorphin
LC	liquid chromatography
LDOPA	3,4-dihydroxyphenylalanine
Leu	leucine
LOD	limit of detection
Lys	lysine
m/z	mass to charge ratio
Mal	malate
MALDI	matrix assisted laser desorption ionization
MAO	monoamine oxidase
Met	methionine
MOPEG	3-methoxy-4-hydroxyphenylglycol
MRC^2	Michigan Regional Comprehensive Metabolomic Resource Core
MRM	multiple reaction monitoring
MS	mass spectrometery
MS/MS	tandem mass spectrometry
NAP	N-acetylputrescine
NAS	N-acetylserotonin
NAT	N-acetyltransferase
NE	norepinephrine
NM	normetanephrine
NPLC	normal phase liquid chromatography
OA	octopamine
Orn	ornithine
PA	phenylacetate
PCA	protocatechuic acid

PD	Parkinson's disease
Phe	phenylalanine
PhEt	phenylethylamine
PP	phenylpyruvate
Pro	proline
Put	putrescine
QQQ	triple quadrupole
RPLC	reversed phase liquid chromatography
RSD	relative standard deviation
Ser	serine
Sin	sinapic acid
Spd	spermidine
Spm	spermine
STD	standard deviation
Suc	succinate
Syn	synephrine
Tau	taurine
TEA	triethylamine
TIC	total ion chromatogram
Thr	threonine
TOF	time of flight
TOH	tyrosol
Trp	tryptophan
TrpA	tryptamine
Tyr	tyrosine
TyrA	tyramine
UPLC	ultra high pressure liquid chromatography
VA	vanillic acid
Val	valine
VMA	vanillylmandelic acid
VN	vanillin
WT	wild type
Xle	leucine/isoleucine

ABSTRACT

Metabolomics, the study and characterization of small molecule metabolites, faces challenges due to the size and diversity of the metabolome. No current instrumentation is capable of measuring the entire metabolome. Liquid chromatography with mass spectrometry detection is widely used in metabolomics for its sensitivity and selectivity. Detection is limited to metabolites which are compatible with the selected column chemistry. Many small molecule neurochemicals are polar and thus not well retained with the popular reversed phase chromatography. Hydrophilic interaction liquid chromatography is better suited for this application, but the observed limits of detection are not sufficient for trace neurochemicals.

One way to overcome this limitation is through the use of chemical derivatization. Polar metabolites are labeled with a hydrophobic moiety, increasing retention and ionization efficiency in reversed phase chromatography, allowing for lower limits of detection. Additionally, internal standards are easily produced using stable isotope labeled derivatization reagents, allowing for improved quantification. Previous work in the Kennedy lab has been performed with benzoyl chloride, which reacts primarily with amines and phenols. This reaction is virtually instantaneous at room temperature and increases sensitivity by up to 1,000 fold. Benzoyl chloride derivatization was previously described for analysis of 17 neurochemicals in microdialysate with reversed phase liquid chromatography and triple quadrupole mass spectrometry.

In this work, benzoyl chloride derivatization is expanded upon in both metabolome coverage and applicability. To allow benzoyl chloride derivatization of proteinaceous samples such as plasma or tissue, a sample preparation method was developed and optimized. The resulting solvent precipitation method is fast, simple, and compatible with very small sample volumes. This was demonstrated in two brief applications monitoring epinephrine in mouse plasma and serotonin in *Drosophila* tissue.

With sample preparation optimized, we then aimed to expand metabolome coverage and subsequently developed a method for the analysis of 70 benzoylated neurochemicals. With nanomolar limits of detection and internal standards for each metabolite, this method has many advantages over other methods of comparable scale. We make use of this expanded coverage by investigating plasma metabolic changes in Parkinson's disease as well as wine analysis. Thirteen metabolites were found to be linked to Parkinson's disease or disease severity, though current evidence suggests L-DOPA treatment plays a major role in these findings. Using a 56-metabolite panel, we were able to distinguish wines based on their varietal and area of production.

Finally, we move away from benzoyl chloride and introduce a novel derivatization reagent, benzylamine. Benzylamine derivatization is complementary to benzoyl chloride, reacting with carboxylic acids, carbonyls, and phosphates. Moreover, the two reagents are compatible so derivatized samples can be mixed for analysis within a single run. Two short methods are introduced, using benzylamine as a standalone reagent to monitor energy metabolites, or in conjunction with benzoyl chloride to monitor phenylalanine metabolism. Together, the two reagents have the potential to cover the majority of the metabolome.

CHAPTER 1

Introduction

Introduction to metabolomics

There is a wealth of information contained within the biomolecular makeup of a living organism, so a variety of approaches have been developed for the analysis of these biomolecules. Often referred to as the "omics cascade," these techniques help to establish a connection between biochemistry and the observed phenotype (Figure 1-1). Significant work has been done in the analysis of large biomolecules, including proteins and nucleic acids, as early sequencing techniques have been established for over 50 years.[1–3] The analysis of small molecules in biological samples is not new, but it was not given the name "metabolomics" until recently. As an established "omics" technique, metabolomics has been rapidly gaining popularity in the past 20 years.[4]

A major challenge facing metabolomics is the sheer size of the metabolome. The Human Metabolome Database (HMDB) contains over 40,000 entries for known or expected endogenous

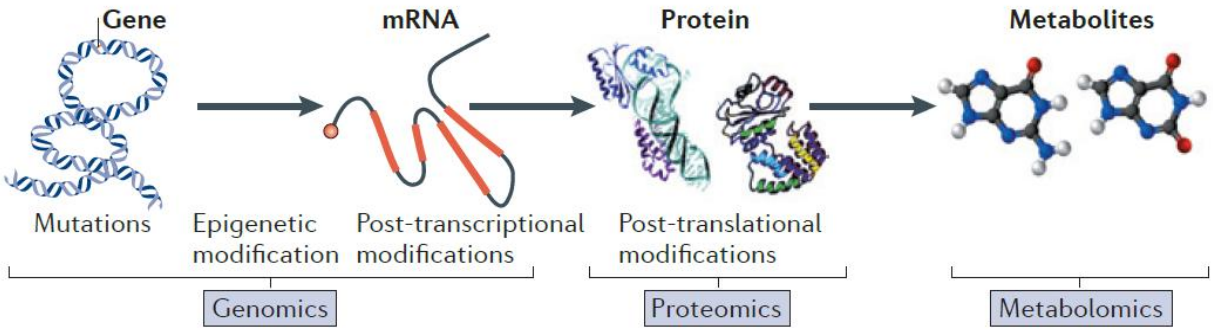

Figure 1-1: The "omics cascade" illustrates the relationship between complementary approaches to the analysis of biomolecules. Reproduced from Patti *et. al.*, 2012.

metabolites and approximately 70,000 more entries for external metabolites.[5] Depending on the biological matrix, these metabolites can range from sub-nanomolar to millimolar concentrations, and the physical properties of the metabolites are widely varied. To measure all metabolites, the ideal methodology would be sensitive, selective, and reproducible, with a large dynamic range and unbiased detection. Currently, no instrumentation is capable of measuring the entire metabolome, so different approaches have been developed, each encompassing some of these desired qualities.[6,7]

The goal of "untargeted" metabolomics is to measure as many metabolites as possible. Untargeted methods are created without prior knowledge of which metabolites are in the sample and are thus capable of identifying novel or unexpected metabolites. A general workflow for untargeted metabolomics is shown in Figure 1-2a. Metabolic fingerprinting is one subset of untargeted metabolomics which does not seek to identify specific metabolites but rather to distinguish sample groups based on the results, which are typically NMR or liquid chromatography - mass spectrometry (LC-MS) spectra. Metabolic profiling, on the other hand, attempts to identify metabolites to determine specific differences between sample groups which can lead to greater understanding of the metabolic pathways involved.

Identification of metabolites from untargeted methods can be challenging. A vast amount of data is generated, so rather than attempt to identify everything, the first step is generally to determine which features differ between groups. In LC-MS metabolomics, a "feature" is defined by a specific m/z and retention time which provides good Gaussian peak shape in the chromatogram. Thousands of features may be detected with untargeted methods.[8,9] Additional validation is required to confirm features as metabolites, as a single metabolite can produce multiple chromatographic features due to isotopes, adducts, or in-source fragmentation. Once

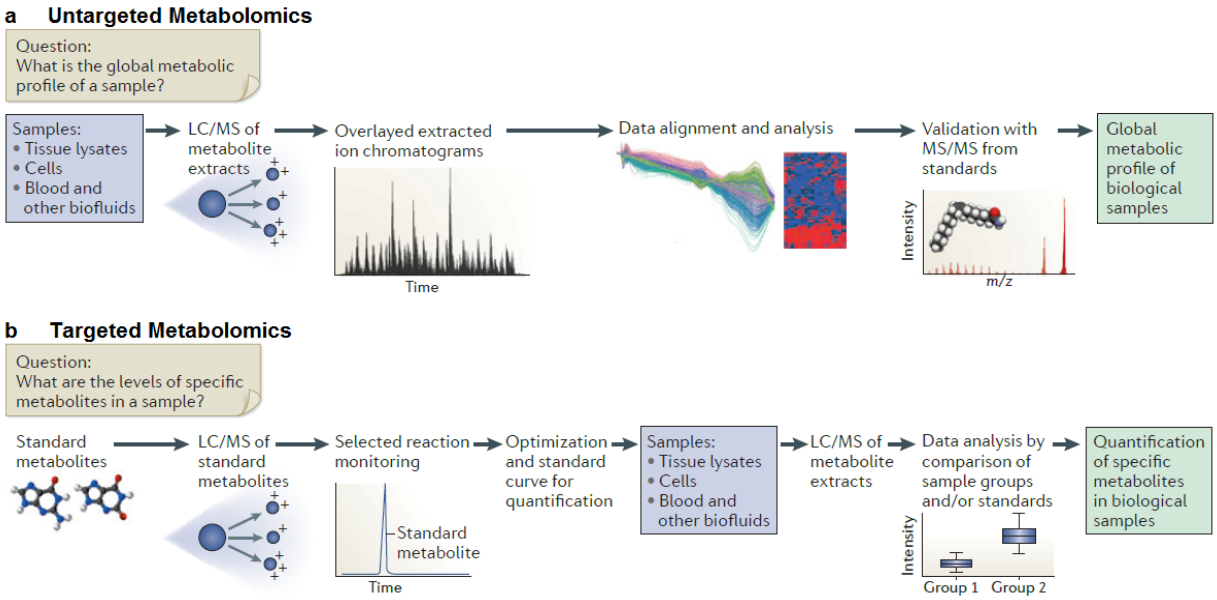

Figure 1-2: Approaches to metabolomics. a. Untargeted metabolomic seeks to analyze all metabolites within a sample and requires separate MS/MS analysis for metabolite identification. b. Targeted metabolomics develops methods based on authentic standards are can provide quantitative comparison of samples. Reproduced from Patti *et. al.*, 2012.

features of interest are identified, database searches can be performed to putatively identify metabolites. A number of metabolite databases exist for this purpose.[5,10,11] Finally, following putative identification, authentic standards can be used to compare retention times and tandem mass spectrometry (MS/MS) fragmentation patterns.

Although untargeted metabolomics cannot currently measure the entire metabolome, it is still a powerful technique. Analysis is not limited to metabolites for which standards are available. Method development is typically fast, as generic methods are used to allow detection of as many metabolites as possible. As a result, a large number of metabolites can be detected. Data analysis is time consuming, however, due to the large amount of data generated, and quantification is limited due to the lack of calibration. With these properties, untargeted metabolomics is best suited for hypothesis generating applications such as biomarker discovery.[12–14]

In contrast to untargeted metabolomics, "targeted metabolomics" focuses on specific, known metabolites.[15] Methods are generated through the use of authentic standards, so no identification is required following sample analysis. A workflow for targeted metabolomics is shown in Figure 1-2b. LC-MS/MS is typically used, though gas chromatography or capillary electrophoresis may also be used when compatible with the metabolites of interest. Analysis is limited to only metabolites which are known or selected, but the resulting methods are sensitive and selective. Up to hundreds of metabolites have been targeted in a single method.[16–18] Compared to untargeted metabolomics, method development for targeted metabolomics is slower, as conditions are optimized for the selected metabolites. Data analysis is much simpler, however. Metabolome coverage is limited in scope, but calibration curves can be prepared to allow for absolute quantification. Targeted metabolomics is most suited for hypothesis testing applications.

Instrumentation for metabolomics

Nuclear magnetic resonance spectroscopy (NMR) is commonly used in metabolomics.[19,20] NMR spectra are produced from the free induction decay of nuclei excited in a magnetic field. Proton NMR is the most common, but ^{13}C and ^{15}N are amongst other NMR active nuclei. For metabolomics, NMR offers unbiased detection, as anything with protons can be observed. The resulting spectra are very reproducible, and can provide structural and quantitative information. One of the major limitations for NMR in metabolomics, however, is sensitivity. Limits of detection for NMR are typically in the mid to high micromolar range.[20] Additionally, the spectra that result from the biological samples typical of metabolomics are

quite complex, making metabolite identification challenging. Despite these limitations, NMR can still be suitable for some untargeted metabolomics applications.[13,21]

Mass spectrometry (MS) has grown to become the most popular instrumentation for metabolomics.[6] A chromatographic separation is usually employed prior to MS detection to increase peak capacity and to remove salts and interfering compounds from the chromatographic regions of interest. Gas chromatography (GC) is one separation technique that can be used for metabolomics.[22] In GC, samples are volatilized and carried through a column by an inert carrier gas. The interior of a GC column is coated with the stationary phase, as rapid diffusion in the gas phase allows sufficient interaction between the analytes and the stationary phase despite the reduced surface area compared to packed columns. GC columns can be meters long, and thus provide good resolution of metabolites. However, metabolites which are not volatile require additional sample preparation to be compatible with GC, and degradation of thermally unstable metabolites may occur.

Liquid chromatography (LC) allows for separation in the liquid phase. LC columns are packed with small (typically $\leq$ 5 μm) particles which are coated with stationary phase. The packing material is generally silica based, and may be left bare or functionalized to create specific selectivity. The mobile phase is a solvent or mixture of solvents which is used to carry the sample through the column. Elution can occur with a constant mobile phase composition, called "isocratic" elution, or solvent composition can change over time through use of multiple pumps, called "gradient" elution. Analytes are separated based on their interactions between the stationary phase on the packing material and the mobile phase carrying them through the column. The specific combination of stationary phase and mobile phase determines the selectivity of the separation.

Compared to GC, LC is typically slower, requiring minutes to hours for analysis time. GC also provides better resolution. However, LC does not require analytes to be volatile and is less prone to sample degradation. A wide range of LC stationary phases exist and based on the selected stationary and mobile phases, different separation modes can be achieved. Reversed phase liquid chromatography (RPLC) is widely used, and employs a hydrophobic stationary phase (often C18) and a polar stationary phase. Gradients composed of water and polar organic solvents such as acetonitrile or methanol are commonly used. Hydrophobic analytes are well resolved with RPLC. However, many metabolites are polar and are not retained well with RPLC.

Normal phase liquid chromatography (NPLC) uses polar stationary phases such as silica or alumina, and nonpolar mobile phases such as hexanes to efficiently separate polar analytes. However, polar metabolites may have poor solubility in the nonpolar, organic mobile phases used. Additionally, water readily adsorbs to the polar stationary phases which can lead to poor retention time reproducibility. Biological samples are typically aqueous, so standard NPLC is not well suited for metabolomics.

A subtype of NPLC called hydrophilic interaction liquid chromatography (HILIC) was introduced in 1990.[23] This technique uses polar stationary phases, like NPLC, with blends of water and water-miscible organic mobile phases, similar to RPLC. Water preferentially adsorbs to the polar stationary phase, creating a water-enriched region at the stationary phase, with an adjacent water-depleted organic region in the mobile phase. Analytes are separated based on partitioning between the regions. Polar metabolites are generally soluble in HILIC mobile phases so the separation is not adversely affected by water in aqueous biological samples, and the mobile phases are more compatible with MS than NPLC. This makes HILIC a suitable choice for metabolomics, and indeed, it has been widely used for metabolomic studies.[24–28]

A variety of detection techniques are compatible with LC, including spectrophotometric and electrochemical techniques as well as MS. In MS, analytes are ionized and resolved on basis of their mass to charge ratio, m/z. With limits of detection at nanomolar concentrations or lower, MS has greater sensitivity than NMR. MS selectivity is better than spectrophotometric techniques, as coeluting compounds can be resolved based on their m/z. MS instruments vary in their ionization strategy and mechanism for resolving ions based on m/z. The initially developed ionization techniques, such as electron impact, are considered "hard," meaning they cause fragmentation of analytes in-source. While this can be useful for structure determination of single analytes, it increases spectral complexity and makes analysis of mixtures complicated. For metabolomics, "soft" ionization methods are typically used, which limit in-source fragmentation of the analytes.

Matrix-assisted laser desorption ionization (MALDI) is one such "soft" technique, in which a sample is mixed with a matrix which readily absorbs laser photons. The sample is ionized by ablation of the matrix with a pulsed laser. MALDI is relatively unaffected by the salt content of the original sample and can illustrate spatial distributions of metabolites. However, the MALDI matrix is also detected, which can cause significant background in the low m/z range where metabolites are typically detected. As a pulsed technique, it is not especially compatible with the continuous flow of LC. MALDI can be used with LC by spotting the effluent onto MALDI plates, but this leads to offline analysis and can be slow.

Flow based techniques, such as electrospray ionization (ESI), are better suited for LC-MS analysis. In ESI, the sample solution is passed through a nebulizer with a voltage applied to the spray tip, producing charged droplets. Solvent evaporates from the droplets in the heated source. As the droplets shrink, the charge-to-volume ratio increases until it hits the Rayleigh limit,

causing Coulombic fission of the droplets. This repeats as the droplets get smaller and smaller. The exact mechanism for the final production of individual gas phase ions through ESI is not fully understood but there are a few well-supported theories. One is called the "charge residue model" which claims increasingly smaller and smaller droplets are formed until they contain on average a single ion per droplet (Figure 1-3a).[29] The ion enters the gas phase as the remaining solvent evaporates. Another theory, the "ion evaporation model," proposes the field strength at the surface of the droplet increases as the droplets shrink until it becomes high enough to desolvate and eject analyte ions from the droplet (Figure 1-3b).[30,31] Evidence suggests small molecules, such as metabolites, are primarily ionized by ion evaporation.[32]

Atmospheric pressure chemical ionization (APCI) is another soft, flow based ionization technique.[33] In APCI, the LC effluent is passed through a heated nebulizer, leading to vaporization but not ionization. A corona discharge electrode is placed between the nebulizer tip

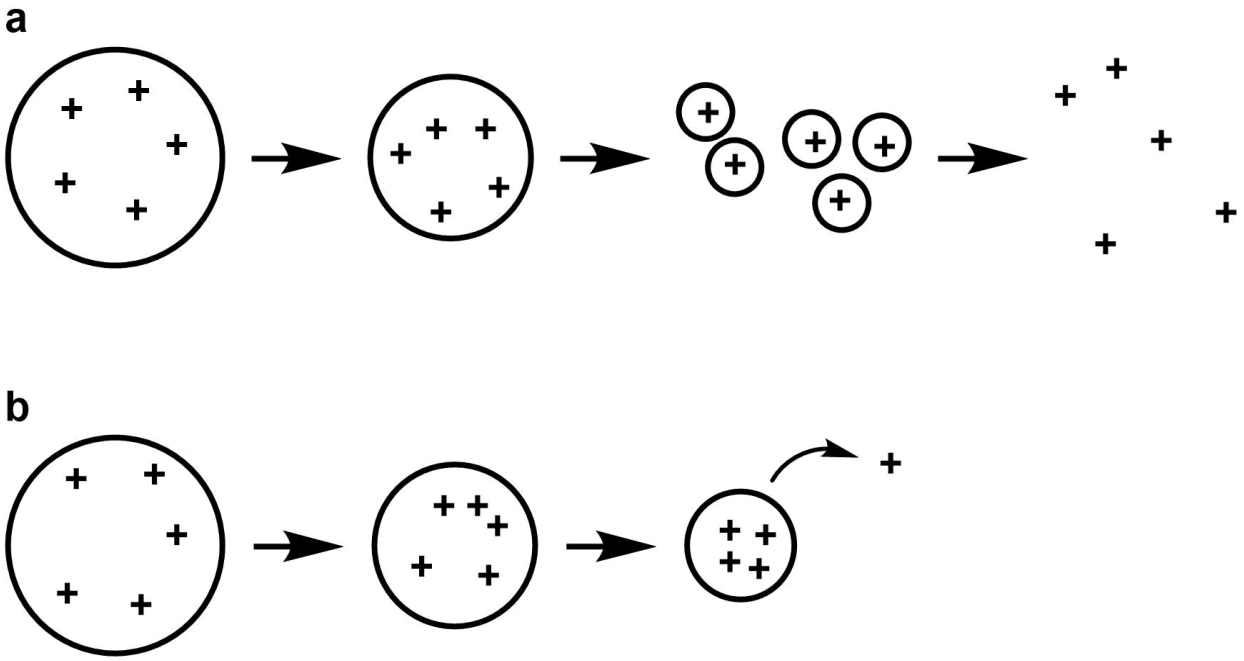

Figure 1-3: Proposed mechanisms for electrospray ionization. a. The charge residue model. Solvent evaporation and fission leads to progressively smaller droplets, until droplets contain on average a single ion. Ions enter the gas phase as any remaining solvent evaporates off. b. The ion evaporation model. As droplets shrink from solvent evaporation and fission, electrostatic repulsion grows until ions are ejected from the droplet into the gas phase.

and the MS inlet. The mobile phase, which is in excess relative to the analytes, is ionized by the corona discharge, and charged analyte ions are produced via proton transfer. APCI ionization efficiency is very high and is less subject to matrix effects than ESI. APCI is compatible with low-polarity mobile phases so it is better suited for low-polarity analytes. Metabolites which are polar or ionized in solution, such as amino acids, are more compatible with ESI. Thermal stability of the metabolites must also be considered, as labile metabolites may degrade during the thermal vaporization of APCI. Both APCI and ESI have applications in metabolomics, but this work will focus exclusively on ESI.

Various mass analyzers are used in mass spectrometers. The different qualities of each mass analyzer, such as mass resolution and scan rate, lead to advantages in different applications. Mass resolution is the ability for a mass spectrometer to distinguish between two similar m/z values. This can be calculated from equation 1-1, where R is the resolution, m is the m/z value of the peak, and Δm is the peak width:

$$R = \frac{m}{\Delta m} \qquad \text{(Equation 1-1)}$$

Peak width is often calculated as the full width at half maximum (FWHM), but other metrics can be used and should be specified. Mass accuracy is how close to the exact mass of an ion the mass spectrometer is capable of achieving, typically measured in ppm.

One common type of mass analyzer is the quadrupole.[34,35] A quadrupole consists of four parallel rod electrodes. A positive DC current is applied to one set of rods opposite each other, while a negative DC current is applied to the other two rods. An AC voltage is superimposed on both sets of rods. As ions traverse the quadrupole, the field leads to a spiraling pattern of the ions through the length of the quadrupole. Based on the applied voltages, only ions with a specific m/z can traverse the entire quadrupole without hitting one of the electrodes. The applied voltages

can be set to allow a wide m/z range to pass through, or it can be limited to let only a specific m/z pass.

Placing three quadrupoles in series produces the triple quadrupole (QQQ) mass spectrometer. This arrangement leads to great flexibility in analysis modes. For basic mass spectrometry, the first or third quadrupole can scan through a mass range producing a comprehensive mass spectrum. The second quadrupole can be used as a collision cell for tandem mass spectrometry, introducing additional scan types. A product ion scan selects a specific mass in the first quadrupole and scans for the product ions in the third quadrupole. A precursor ion scan, alternatively, scans through precursor ions in the first quadrupole, and selects for a specific product ion in the third quadrupole. In single or multiple reaction monitoring mode (SRM or MRM), specific precursor and product ions are selected.

MRMs can be considered the "gold standard" for targeted metabolomics.[6] They are sensitive, as noise in the mass spectrum is greatly reduced. QQQ mass spectrometers are limited to unit mass resolution, but MRMs are still selective as unique m/z transitions can be chosen for each metabolite. The acquisition rate of a QQQ is relatively slow and depends on the mass range or number of MRMs are being cycled through. MRMs can be time segmented, so MRMs are only scanned for at during a specified time window, reducing the number of MRMs being scanned at a given time point. Fewer MRMs allow for faster scan rates overall. All of the work in this thesis utilizes time segmented MRMs, also called "dynamic" MRMs in Agilent instrumentation.

In contrast to QQQ mass spectrometers, time-of-flight (TOF) mass spectrometers are considered to be high resolution mass spectrometers (HRMS).[36] TOF instruments operate by accelerating ions in an electric field, giving ions with the same charge the same kinetic energy.

Ions with a higher mass will have a slower velocity in the following field-free flight tube, so m/z is determined by measuring the time it takes ions to reach the detector.

To further increase mass resolution, a reflectron can be added, which acts as a mirror for ions.[37] This allows the path length to be increased without significantly increasing the size of the instrument. Additionally, a reflectron compensates for kinetic energy distributions. If two ions with the same m/z have differences in kinetic energy, they will arrive at the detector at different times. An ion with greater kinetic energy will penetrate deeper into the reflectron than an ion with lower kinetic energy, increasing path length for the higher energy ion, so the two can reach the detector at the same time.

TOF mass spectrometers have a very fast acquisition rate. The acquisition rate does not depend on the selected mass range, which can be particularly advantageous as TOF instruments have a wide mass range. Mass resolution of around 10,000 is typical. The high scan rate makes TOF mass spectrometers compatible with fast separations, while the high mass resolution is advantageous for untargeted metabolomics. For especially complex samples where even greater resolution is needed, an Orbitrap mass spectrometer can be used.[38]

In an Orbitrap instrument, ions first enter a curved, rf-only quadrupole called a C-trap. Ions are then ejected from the C-trap into the Orbitrap mass analyzer by a DC pulse. The mass analyzer contains a central spindle shaped electrode, enclosed by two split outer electrodes. Ions oscillate along the length of the spindle while moving around the spindle in a circular orbit. As ions oscillate, they induce a current in the outer electrodes. A Fourier transform is performed to convert the induced current to a mass spectrum.

Orbitrap instruments are expensive, but cheaper and easier to maintain than other Fourier transform based mass spectrometers such as the Fourier transform ion cyclotron resonance (FT-

ICR) instrument. Orbitrap instruments can provide mass resolution of 100,000 or higher and mass accuracy within 2 ppm or less. Orbitraps are a relatively new instrument, being commercially introduced in 2005.[39] Newer hybrid models of the instrument include linear ion traps and quadrupoles to allow for MS/MS, increasing the versatility of the instrument.[40] For many applications, the high resolution of an Orbitrap may be unnecessary, making the more inexpensive TOF mass spectrometer an appealing choice. However, for extremely complex samples, the mass resolution and mass accuracy of an Orbitrap may be necessary. Both untargeted and targeted metabolomics provide important information about a biological system, but the work in this dissertation will focus specifically on targeted metabolomics using LC with QQQ mass spectrometry.

Chemical derivatization in metabolomics

Although it is desirable to minimize sample preparation to reduce analysis time, chemical derivatization is an example of additional sample preparation which can increase sensitivity for polar metabolites. Polar metabolites typically elute at or near the void volume in RPLC, where ESI efficiency is low due to the high aqueous content. Metabolites can be labeled with a hydrophobic moiety, allowing them to be better retained with RPLC. By eluting later, with higher organic content in the mobile phase, and fewer components to cause ion suppression, ESI efficiency is increased.[41] Additionally, hydrophobic analytes are more likely to be found at the surface of droplets produced in ESI. These analytes at the surface are more likely to be ionized than the polar metabolites located at the center of the droplets.[42,43] Combined, these effects can lead to increases in sensitivity of 10-1,000 fold.[41,43]

As an additional benefit of derivatization, internal standards can be readily produced for all targeted metabolites through use of a stable isotope labeled (SIL) derivatizing reagent. Without derivatization, SIL metabolites or analogous exogenous compounds are used for internal standards. Analogues do not always behave the same chromatographically or in the presence of run to run ionization differences. SIL metabolites behave similarly to the target metabolites, but obtaining SIL metabolites for each targeted metabolite can be prohibitively expensive. With derivatization, only the derivatization reagent needs to be SIL. A mixture of all targeted metabolites can be derivatized with the SIL derivatization reagent to prepare SIL internal standards for all targeted metabolites in a single reaction.

Because of these advantages, a number of derivatization reagents have been explored for metabolomics. Alkylation and silylation are commonly used in GC-MS metabolomics to increase volatility of metabolites.[44] Reductive amination has been used for the analysis of polar metabolites including sugars, sugar phosphates, and amino acids.[45,46] A number of derivatization reagents, including O-phthaldialdehyde, have been used to allow for fluorescence or UV detection of otherwise undetectable metabolites, and have more recently been explored for LC-MS metabolomics.[47–49] One of the most widely used is dansyl chloride (DnsCl).[41,50,51] DnsCl reacts with amine and phenol containing metabolites, increasing hydrophobicity and subsequently retention in RPLC (Figure 1-4a). DnsCl also features a dimethylamino group which can be readily ionized in ESI, thereby increasing ionization efficiency and resulting sensitivity. DnsCl has been used for a wide range of applications,[41,50,52–54] but the reaction procedure is long. Recent advances have decreased the reaction time, but it still requires an hour.[54] Additionally, samples are heated during DnsCl derivatization, which could lead to degradation of the samples during the labeling process.

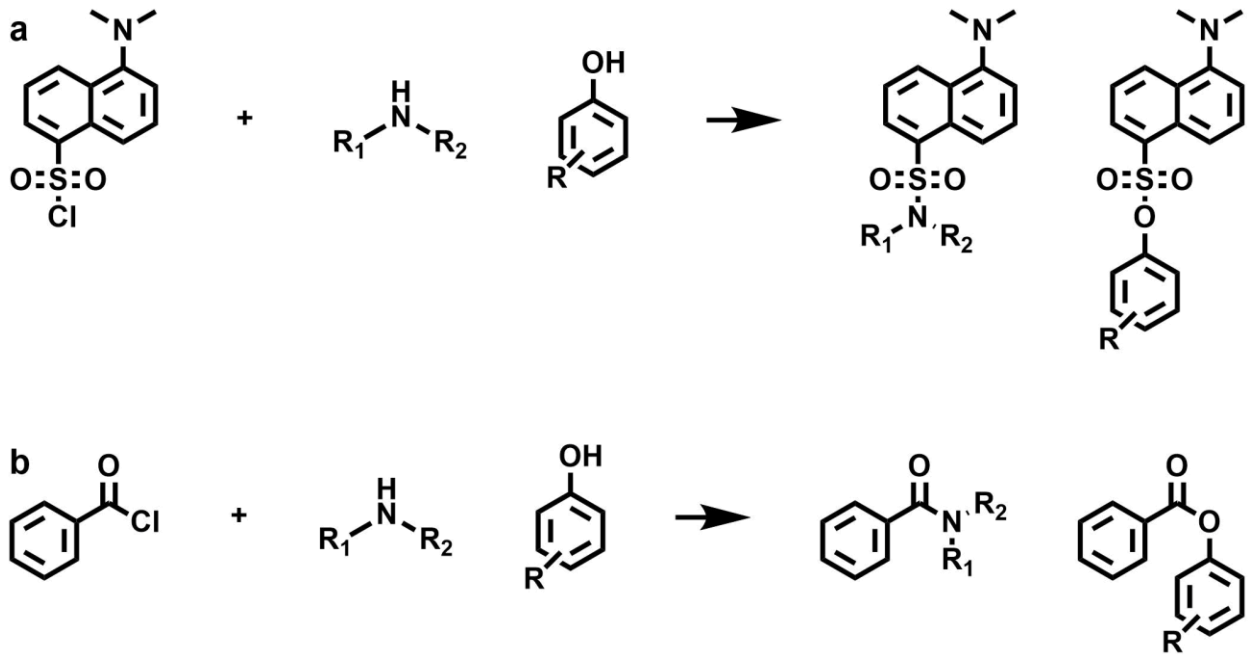

Figure 1-4: Reaction schemes for derivatization reagents. a. Dansyl chloride reacts with amines and phenols, requiring an hour at 40 °C. b. Benzoyl chloride reacts with amines and phenols requiring less than a minute at room temperature.

In searching for an alternative to DnsCl, the Kennedy group explored benzoyl chloride (BzCl).[55,56] BzCl has been commonly used for derivatization of amines and hydroxyls for LC with UV detection (Figure 1-4b). By optimizing reaction conditions, a method was developed for derivatization of amines, phenols, and ribosyl hydroxyls.[57] The reaction time is virtually instantaneous at room temperature, so sample degradation is less of a concern than with DnsCl. Individual samples can be processed in less than a minute, causing minimal increases in analysis time. The benzoylated metabolites are well retained with RPLC and ionization efficiency is increased up to 1,000-fold, greatly increasing sensitivity. The resulting derivatives are stable for at least a week at room temperature. [57]

Neurochemical metabolomics

One application where derivatization has been especially advantageous is neurochemical metabolomics. Neurochemical analysis can provide important information for understanding

behavior and disease. Common sample matrices include brain tissue, cerebrospinal fluid (CSF), and blood plasma. However, there are many challenges associated with the analysis of neurochemicals. Many of the model systems used are small, leading to limited sample size availability. Larger samples can be produced by pooling samples from multiple animals, but this obscures information about variation between individuals, and it is preferable to limit the number of animals used in a study if possible. Limited sample availability is especially important for low abundance metabolites. Depending on the matrix, neurochemicals are often at nanomolar or lower concentrations. Thus, method sensitivity is especially important for neurochemical analysis.

Additionally, many neurochemicals are polar and not well retained with RPLC. HILIC allows for good retention of polar neurochemicals. However, there are a variety of HILIC column chemistries and retention is not as predictable as in RPLC. Thus, HILIC method development can be more time consuming than RPLC method development as column optimization is required[58]. . Additionally, the sensitivity afforded by HILIC-MS is not always sufficient to detect low abundance (i.e. < 5 nM) neurochemicals.[25,26] Derivatization can be used to increase sensitivity as well as compatibility with RPLC. Most common neurotransmitters and their metabolites contain amine or phenol groups, making them compatible with BzCl derivatization. Previously in the Kennedy lab, a targeted method was developed for the analysis of 17 targeted neurochemicals and metabolites in microdialysate samples (Figure 1-5).[57]

Dissertation overview

Based upon the success of BzCl derivatization for LC-MS/MS neurochemical analysis, the goal of the work in this dissertation is to improve and expand upon this initial work. In

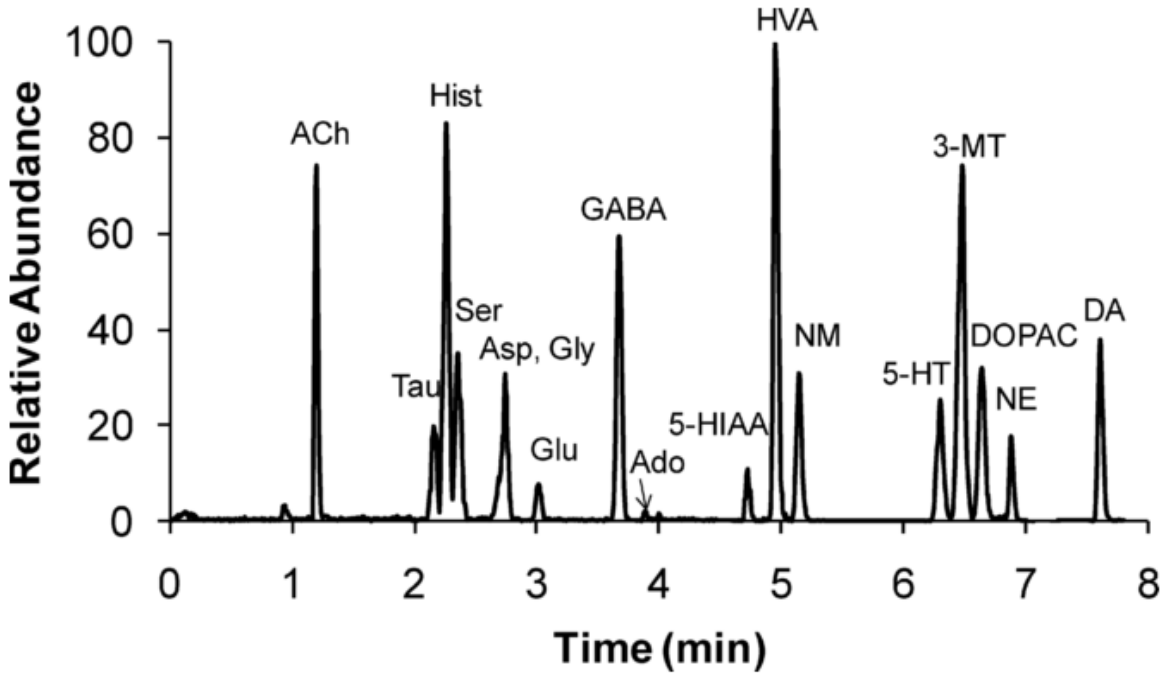

Figure 1-5: Ion chromatogram of 17 neurotransmitters and metabolites using benzoyl chloride derivatization. Reproduced from Song *et. al*., 2012.

Chapter 2, additional sample preparation is explored to allow analysis of proteinaceous samples with BzCl. Previous work in our lab with BzCl has only been performed in microdialysis samples, which are filtered during collection and can be considered relatively clean. High protein concentrations, such as those found in tissue or plasma, can be detrimental for both LC separations and MS sensitivity. Various methods for protein removal are investigated, and two applications are described. The first investigates the role of epinephrine in the counter regulatory response to hypoglycemia (Figure 1-6),[59,60] while the second explores the role of serotonin in the protein valuation process.

Chapter 3 describes a significant increase in scope of targeted neurochemical analysis with BzCl. The previously described method for 17 neurochemicals was expanded upon to include 70 neurotransmitters and metabolites. Using the sample preparation detailed in Chapter 2, this method was applied to a variety of sample matrices, including rat brain dialysate and

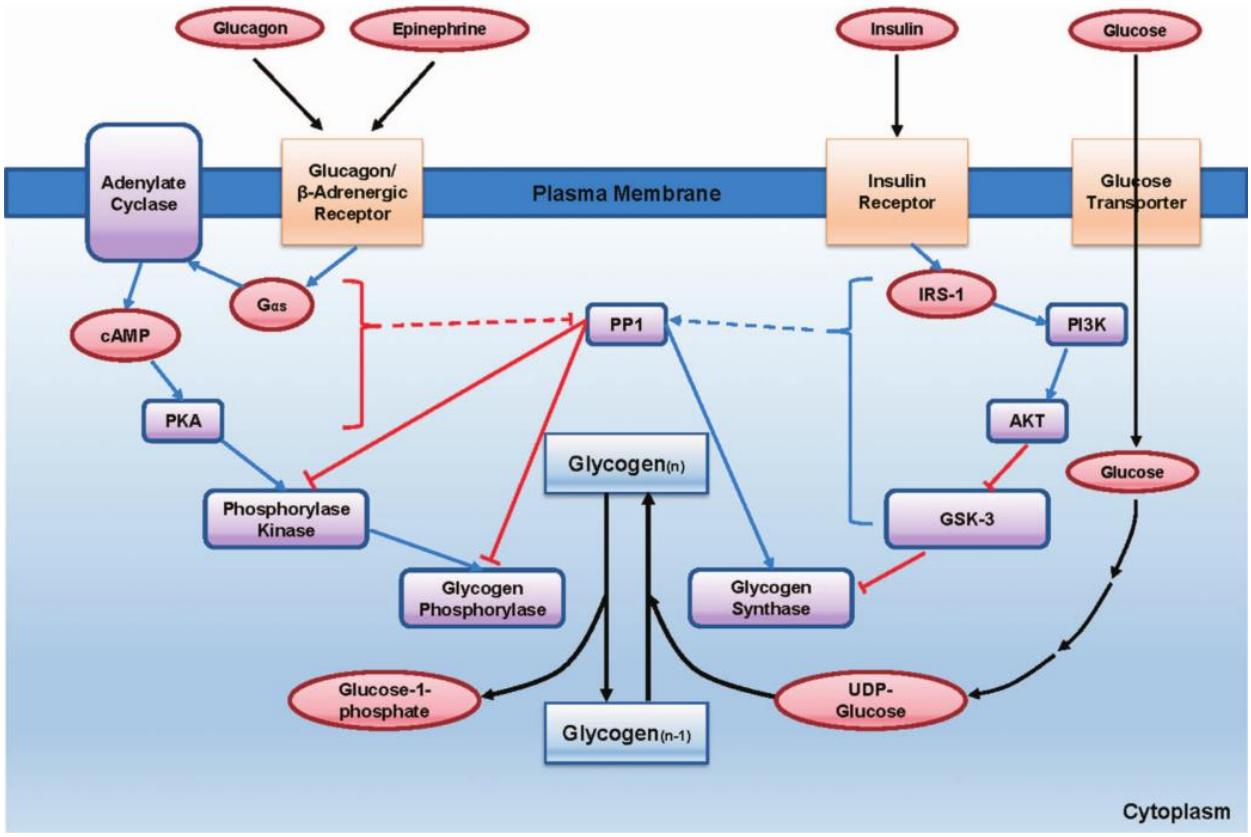

Figure 1-6: Schematic of glucose regulation in the liver. Insulin reduces blood glucose by promoting glycogen synthesis. Counter regulatory hormones, such as epinephrine, increase blood glucose by promoting glycogenlysis. Reproduced from Han *et. al.*, 2016.

Drosophila hemolymph. Chapter 4 combines advancements from Chapters 2 and 3 to explore plasma metabolomics in Parkinson's disease. Parkinson's disease is characterized by the loss of dopamine neurons in the brain, and differences in cysteine and polyamine metabolism have been noted as well.[61–64] Plasma samples from approximately 100 each of Parkinson's patients and healthy controls were compared with a specific focus on dopamine, cyteine, and polyamine metabolism. The observed differences may further the understanding of Parkinson's disease progression as well as the metabolic effects of Parkinson's treatment.

Chapter 5 moves away from neurochemical analysis and uses BzCl derivatization for a new application - food metabolomics. In a similar vein to Chapter 3, a method was developed for over 50 relevant amines and phenolic acids in wine. This method was able to distinguish

different wines by their location of origin and varietal using the observed metabolite profiles. This work in this chapter demonstrates that BzCl derivatization is extremely versatile and not limited to bioanalysis.

Chapter 6 describes a new derivatization reagent, benzylamine (BnA). BnA has complimentary reactivity to BzCl and can thus be used for applications where BzCl cannot label the desired metabolites. In this chapter, a BnA method is developed for the analysis of sugar phosphates and citric acid cycle metabolites. Additionally, the combination of BzCl and BnA is demonstrated in the context of phenylalanine metabolism. Combining the two techniques has the potential to greatly increase metabolome coverage with derivatization without significant increases in analysis time.

Chapter 7 concludes this dissertation by proposing two approaches to use BzCl derivatization outside of targeted metabolomics. Both approaches make use of dual derivatization with ^{12}C- and ^{13}C-BzCl to produce peak pairs from labeled metabolites in the resulting mass spectra. Untargeted metabolomics using high resolution mass spectrometry as well as "pseudotargeted" metabolomics with QQQ mass spectrometry are described, and preliminary work shows the approaches are viable. These methods could even further expand the versatility of BzCl derivatization for metabolomics.

References

(1) Holley, R. W.; Everett, G. A.; Madison, J. T.; Zamir, A. *J. Biol. Chem.* **1965**, *240* (5), 2122–2128.
(2) Ankeny, R. A. *Endeavour* **2003**, *27* (2), 87–92.
(3) Min Jou, W.; Haegeman, G.; Ysebaert, M.; Fiers, W. *Nature* **1972**, *237* (5350), 82–88.
(4) Kell, D. B.; Oliver, S. G. *Metabolomics*. 2016.
(5) Wishart, D. S.; Feunang, Y. D.; Marcu, A.; Guo, A. C.; Liang, K.; Vázquez-Fresno, R.; Sajed, T.; Johnson, D.; Li, C.; Karu, N.; Sayeeda, Z.; Lo, E.; Assempour, N.; Berjanskii,

M.; Singhal, S.; Arndt, D.; Liang, Y.; Badran, H.; Grant, J.; Serra-Cayuela, A.; Liu, Y.; Mandal, R.; Neveu, V.; Pon, A.; Knox, C.; Wilson, M.; Manach, C.; Scalbert, A. *Nucleic Acids Res.* **2017**.

(6) Dettmer, K.; Aronov, P. A.; Hammock, B. D. *Mass Spectrom. Rev.* **2007**, *26* (1), 51–78.

(7) Patti, G. J.; Yanes, O.; Siuzdak, G. *Nat. Rev. Mol. Cell Biol.* **2012**, *13* (4), 263–269.

(8) Denihan, N. M.; Kirwan, J. A.; Walsh, B. H.; Dunn, W. B.; Broadhurst, D. I.; Boylan, G. B.; Murray, D. M. *J. Cereb. Blood Flow Metab.* **2017**, 1–16.

(9) Wu, S.; Tohge, T.; Cuadros-Inostroza, Á.; Tong, H.; Tenenboim, H.; Kooke, R.; Méret, M.; Keurentjes, J. B.; Nikoloski, Z.; Fernie, A. R.; Willmitzer, L.; Brotman, Y. *Mol. Plant* **2018**, *11*, 118–134.

(10) Gowda, H.; Ivanisevic, J.; Johnson, C. H.; Kurczy, M. E.; Benton, H. P.; Rinehart, D.; Nguyen, T.; Ray, J.; Kuehl, J.; Arevalo, B.; Westenskow, P. D.; Wang, J.; Arkin, A. P.; Deutschbauer, A. M.; Patti, G. J.; Siuzdak, G. *Anal. Chem.* **2014**, *86* (14), 6931–6939.

(11) Smith, A.; O 'maille, G.; Want, E. J.; Qin, C.; Trauger, S. A.; Brandon, T. R.; Custodio, D. E.; Abagyan, R.; Siuzdak, G. *Proc. 9Th Int. Congr. Ther. Drug Monit. Clin. Toxicol.* **2005**, *27* (6), 747–751.

(12) Kang, J.; Zhu, L.; Lu, J.; Zhang, X. *J. Neuroimmunol.* **2015**, *279*, 25–32.

(13) Graça, G.; Desterro, J.; Sousa, J.; Fonseca, C.; Silveira, M.; Serpa, J.; Carvalho, T.; da Silva, M. G.; Gonçalves, L. G. *Metabolomics* **2017**, *13* (11).

(14) Roede, J. R.; Uppal, K.; Park, Y.; Lee, K.; Tran, V.; Walker, D.; Strobel, F. H.; Rhodes, S. L.; Ritz, B.; Jones, D. P. *PLoS One* **2013**, *8* (10), e77629.

(15) Vinayavekhin, N.; Saghatelian, A. *Curr. Protoc. Mol. Biol.* **2010**, No. SUPPL. 90, 1–24.

(16) Yuan, M.; Breitkopf, S. B.; Yang, X.; Asara, J. M. *Nat. Protoc.* **2012**, *7* (5), 872–881.

(17) Yan, Z.; Yan, R. *Anal. Chim. Acta* **2015**, *894*, 65–75.

(18) Cai, Y.; Weng, K.; Guo, Y.; Peng, J.; Zhu, Z. J. *Metabolomics* **2015**, *11* (6), 1575–1586.

(19) Markley, J. L.; Brüschweiler, R.; Edison, A. S.; Eghbalnia, H. R.; Powers, R.; Raftery, D.; Wishart, D. S. *Curr. Opin. Biotechnol.* **2017**, *43*, 34–40.

(20) Emwas, A. H. M.; Salek, R. M.; Griffin, J. L.; Merzaban, J. *Metabolomics* **2013**, *9* (5), 1048–1072.

(21) Armiñán, A.; Mendes, L.; Carrola, J.; Movellan, J.; Vicent, M. J.; Duarte, I. F. *J. Drug Target.* **2017**, *25* (9–10), 845–855.

(22) Koek, M. M.; Jellema, R. H.; van der Greef, J.; Tas, A. C.; Hankemeier, T. *Metabolomics*. 2011, pp 307–328.

(23) Alpert, A. J. *J. Chromatogr. A* **1990**, *499*, 177–196.

(24) Fei, F.; Bowdish, D. M. E.; McCarry, B. E. *Anal. Bioanal. Chem.* **2014**, *406* (15), 3723–3733.

(25) Virgiliou, C.; Sampsonidis, I.; Gika, H. G.; Raikos, N.; Theodoridis, G. A. *Electrophoresis* **2015**, *36* (18), 2215–2225.

(26) Tufi, S.; Lamoree, M.; de Boer, J.; Leonards, P. *J. Chromatogr. A* **2015**, *1395*, 79–87.

(27) Johnsen, E.; Leknes, S.; Wilson, S. R.; Lundanes, E. *Sci. Rep.* **2015**, *5* (1), 9308.

(28) Tang, D.-Q.; Zou, L.; Yin, X.-X.; Ong, C. N. *Mass Spectrom. Rev.* **2016**, *35* (5), 574–600.
(29) Dole, M.; Mack, L. L.; Hines, R. L.; Mobley, R. C.; Ferguson, L. D.; Alice, M. B. *J. Chem. Phys.* **1968**, *49* (5), 2240–2249.
(30) Thomson, B. A.; Iribarne, J. V. *J. Chem. Phys.* **1979**, *71* (11), 4451–4463.
(31) Iribarne, J. V.; Thomson, B. A. *J. Chem. Phys.* **1976**, *64* (6), 2287.
(32) Kebarle, P.; Verkcerk, U. H. *Mass Spectrom. Rev.* **2009**, *28* (6), 898–917.
(33) Thomson, B. A. *J. Am. Soc. Mass Spectrom.* **1998**, *9* (3), 187–193.
(34) Chernushevich, I. V.; Loboda, A. V.; Thomson, B. A. *J. Mass Spectrom.* **2001**, *36* (8), 849–865.
(35) Yost, R. A.; Enke, C. G. *Anal. Chem.* **1979**, *51* (12), 1251–1264.
(36) Boesl, U. *Mass Spectrom. Rev.* **2017**, *36* (1), 86–109.
(37) Mamyrin, B. A.; Karataev, V. I.; Shmikk, D. V; Zagulin, V. A. *Sov. Phys. - JETP* **1973**, *37* (1), 45–48.
(38) Eliuk, S.; Makarov, A. **2015**.
(39) Makarov, A.; Denisov, E.; Kholomeev, A.; Balschun, W.; Lange, O.; Strupat, K.; Horning, S. .
(40) Williamson, J. C.; Edwards, A. V. G.; Verano-Braga, T.; Schwämmle, V.; Kjeldsen, F.; Jensen, O. N.; Larsen, M. R. *Proteomics* **2016**, *16* (6), 907–914.
(41) Guo, K.; Li, L. *Anal. Chem.* **2009**, *81* (10), 3919–3932.
(42) Cech, N. B.; Enke, C. G. *Anal. Chem.* **2000**, *72* (13), 2717–2723.
(43) Mirzaei, H.; Regnier, F. *Anal. Chem.* **2006**, *78* (12), 4175–4183.
(44) Villas-Bôas, S. G.; Smart, K. F.; Sivakumaran, S.; Lane, G. A. *Metabolites* **2011**, *1* (1), 3–20.
(45) Han, J.; Tschernutter, V.; Yang, J.; Eckle, T.; Borchers, C. H. *Anal. Chem.* **2013**, *85* (12), 5965–5973.
(46) Guo, K.; Ji, C.; Li, L. *Anal. Chem.* **2007**, *79* (22), 8631–8638.
(47) Qureshi, G. A.; Baig, M. S. *J. Chromatogr.* **1988**, *459*, 237–244.
(48) Zarghi, A.; Shafaati, A.; Foroutan, S. M.; Khoddam, A.; Madadian, B. *Sci. Pharm.* **2010**, *78* (4), 847–856.
(49) Song, M.; Hang, T.-J.; Wang, C.; Yang, L.; Wen, A.-D. *J. Pharm. Anal.* **2012**, *2* (1), 19–28.
(50) Nirogi, R.; Komarneni, P.; Kandikere, V.; Boggavarapu, R.; Bhyrapuneni, G.; Benade, V.; Gorentla, S. *J. Chromatogr. B Anal. Technol. Biomed. Life Sci.* **2013**, *913–914*, 41–47.
(51) Cai, H. L.; Zhu, R. H.; Li, H. D. *Anal Biochem* **2010**, *396* (1), 103–111.
(52) Soufleros, E. H.; Bouloumpasi, E.; Zotou, A.; Loukou, Z. *Food Chem.* **2007**, *101* (2), 704–716.
(53) Achaintre, D.; Buleté, A.; Cren-Olivé, C.; Li, L.; Rinaldi, S.; Scalbert, A. *Anal. Chem.* **2016**, *88* (5), 2637–2644.
(54) Han, W.; Sapkota, S.; Camicioli, R.; Dixon, R. A.; Li, L. *Mov. Disord.* **2017**, *0* (0), 1–9.
(55) Novotny, M.; Alasandro, M.; Konishi, M. *Anal. Chem.* **1983**, *55* (14), 2375–2377.

(56) Redmond, J. W.; Tseng, A. *J. Chromatogr. A* **1979**, *170* (2), 479–481.
(57) Song, P.; Mabrouk, O. S.; Hershey, N. D.; Kennedy, R. T. *Anal. Chem.* **2012**, *84*, 412–419.
(58) Chirita, R. I.; West, C.; Finaru, A. L.; Elfakir, C. *J. Chromatogr. A* **2010**, *1217* (18), 3091–3104.
(59) Beall, C.; Ashford, M. L.; McCrimmon, R. J. *Am. J. Physiol. Regul. Integr. Comp. Physiol.* **2012**, *302* (2), R215–R223.
(60) Han, H.-S.; Kang, G.; Kim, J. S.; Choi, B. H.; Koo, S.-H. *Exp. Mol. Med.* **2016**, *48* (3), e218.
(61) Lewandowski, N. M.; Ju, S.; Verbitsky, M.; Ross, B.; Geddie, M. L.; Rockenstein, E.; Adame, A.; Muhammad, A.; Vonsattel, J. P.; Ringe, D.; Cote, L.; Lindquist, S.; Masliah, E.; Petsko, G. A.; Marder, K.; Clark, L. N.; Small, S. A. *Proc. Natl. Acad. Sci. U. S. A.* **2010**, *107* (39), 16970–16975.
(62) Gomes-Trolin, C.; Nygren, I.; Aquilonius, S.-M.; Askmark, H. *Exp. Neurol.* **2002**, *177* (2), 515–520.
(63) Hassin-Baer, S.; Cohen, O.; Vakil, E.; Sela, B.-A.; Nitsan, Z.; Schwartz, R.; Chapman, J.; Tanne, D. *Clin. Neuropharmacol.* **2006**, *29* (6), 305–311.
(64) Helane Doherty, G. *J. Neurol. Disord.* **2013**, *1* (1), 1–9.

CHAPTER 2

Benzoyl chloride derivatization of proteinaceous samples

Reproduced in part from Flak, Patterson *et al*, *Nat. Neurosci*. **2014**, *17*, 1744-1750, where Malec contributed plasma catecholamine measurements, and Ro *et al*, *eLife*, **2016**, *5*, e16843, where Malec contributed serotonin measurements.

Introduction

Reliable, quantitative methods for metabolomics are desirable in neuroscience to relate neurochemical changes to behaviors, disease states, or stimuli. Microdialysis allows direct sampling from the brain and is compatible with a variety of analytical techniques for neurochemical detection.[1–3] Liquid chromatography - mass spectrometry (LC-MS) is sensitive and selective, which is ideal for neurochemical analysis; however, small polar neurochemicals are poorly retained in reversed phase chromatography, so benzoyl chloride (BzCl) derivatization has been previously described as a way to overcome these limitations while providing additional advantages for sensitivity and quantification.[1,3–5]

BzCl derivatization has been proven compatible with microdialysis experiments where the samples are filtered during collection and relatively free of large matrix interferents such as protein. In addition to microdialysis, analysis of biofluids and tissue can also provide important neurochemical information. In this work, we sought to extend the BzCl LC-MS/MS method to more complex sample such as serum and brain tissue. To prevent ion suppression and instrument contamination, these proteinaceous samples require extraction or clean-up steps prior to LC-MS analysis.

A variety of techniques have been used for metabolite extraction, including filtration, solid phase extraction (SPE), and solvent precipitation.[6–8] For our work, we were interested in developing a fast, inexpensive method which was compatible with small samples (i.e. less than 20 μL) and BzCl derivatization. Filtration with syringe filters or spin column filters is fast and does not dilute the sample, but requires consumables, which can be expensive, and requires large volumes (i.e. more than 50 μL). Thus, filtration was determined to not be generally applicable, but could be an option when large samples were available.

Like filtration, SPE requires expensive consumables and requires relatively large sample volumes, but samples can be preconcentrated when larger volumes are available. SPE can be rather slow, and due to high cost, we chose to investigate other options. Solvent precipitation is fast, inexpensive, and compatible with any sample volume. Solvent precipitation does result in sample dilution which can lower sensitivity but we chose to investigate solvent precipitation despite this due to its simplicity and low volume compatibility.

A variety of organic solvent and solvent mixes have been previously used for protein precipitation from biological fluids as well as metabolite extraction from homogenized tissue, although there is generally no consensus as to which solvent is optimal.[7,9,10] In this chapter, we evaluate three commonly used extraction solvents on basis of recovery and repeatability. Additionally, we explore two biological applications of the final method using solvent precipitation followed by BzCl derivatization in biofluids and tissue. These applications focused on single metabolites, but related metabolites were monitored in each study. Subsequent chapters discuss in greater depth the application of the sample preparation techniques developed here to wider ranges of metabolites.

The first application is related to the counter-regulatory response (CRR) to hypoglycemia. When blood glucose rises, such as after a meal, insulin is produced, which acts to reduce glucose to normal levels. If glucose drops too low, CRR hormones are released to suppress insulin release and to promote the breakdown of glycogen into glucose. Epinephrine is one of the CRR hormones which is released when blood glucose drops too low. Epinephrine promotes gluconeogenesis and ketogenesis, increasing blood glucose.[11] In diabetes, insulin-induced hypoglycemia can be quite common from insulin injections. Thus, the CRR is particularly important for diabetics to maintain normal blood glucose. Understanding the mechanism of the CRR could uncover drug targets which may help prevent insulin-induced hypoglycemia.

A population of leptin receptor (LepRb) containing neurons was identified in the parabrachial nucleus (PBN) which are activated by hypoglycemia. It was hypothesized that these neurons may be involved in the CRR. These neurons coexpress cholecystokinin (CCK), while hypothalamus LepRb neurons do not, allowing selective knockout of LepRb in the PBN neurons. Wild type and $LepRb^{CCK}$ knockout (KO) mice were challenged with 2-deoxyglucose (2DG), which mimics hypoglycemia. We monitored plasma concentrations of epinephrine, a CRR hormone, following 2DG challenge to determine if CRR differences exist between the WT and $LepRB^{CCK}$ KO mice.

The second application investigates the link between dietary protein and longevity in *Drosophila*. Calorie restriction has been shown to increase lifespan in many animals, including flies[12], and has been shown to have health benefits in humans as well.[13] Interestingly, this effect is not simply a direct effect of reduced calories in flies. Sensory perception is involved, as flies exposed to food odors will not experience the same benefits from a low calorie diet.[14]

Additionally, the effect seems to result from a low protein diet as opposed to a low calorie diet.[15] A low protein diet has also been shown to be beneficial to humans.[16] There is some evidence that serotonin is involved in macronutrient selection.[17,18] Here we investigate the role of serotonin in protein preference and aging in *Drosophila* by measuring serotonin in fly heads.

Experimental

Chemicals and reagents

All chemicals were from Sigma Aldrich (St. Louis, MO) unless otherwise noted. Water, acetonitrile, and methanol were Burdick & Jackson HPLC grade from VWR (Radnor, PA). Stock solutions of 20 mM GABA, Glu, 5HT, E, and DA were prepared in water and stored at -80 °C. $^{13}C_5$-Glu, d6-GABA, d4-5HT, d6-E, and $^{13}C_6$-DA were purchased from C/D/N Isoptopes (Pointe-Claire, Canada) and were used to prepare stock solutions at 20 mM in water. Calibration standards and internal standards were prepared as previously described[1] and stored in single use aliquots at -80 °C. On each day, an internal standard aliquot was thawed, diluted 100 fold in 20% (v/v) acetonitrile with 1% (v/v) sulfuric acid. This is referred to as the "internal standard solution." A fresh BzCl solution was prepared daily. Pooled human serum from the American Red Cross Detroit National Testing Lab was provided by the Michigan Regional Comprehensive Metabolomics Resource Core (MRC^2).

Metabolite analysis by LC-MS/MS

Separation of benzoylated metabolites was performed using a Waters nanoAcquity UPLC. The column was an Acquity HSS T3 C18 (1 mm x 100 mm, 1.8 μm, 100 Å pore size). The column was kept at 27 °C and the autosampler was at ambient temperature. Mobile phase A

was 10 mM ammonium formate with 0.15% (v/v) formic acid, and mobile phase B was acetonitrile. The flow rate was 100 µL/min, and unless specified otherwise, the gradient was: initial, 0% B; 0.01 min, 17% B; 0.5 min, 17% B; 3 min, 25% B; 3.3 min, 56% B; 4.99 min, 70% B; 5 min, 100% B; 6 min, 100% B; 6.1 min, 0% B; 8 min, 0% B. Partial loop injection mode was used for 5 µL injections.

Detection was performed using an Agilent G6410B triple quadrupole mass spectrometer operating in dynamic multiple reaction monitoring (dMRM) mode. Positive electrospray ionization mode was used at 4 kV. The gas temperature was 350 °C, gas flow was 11 L/min, and the nebulizer was at 15 psi. MRM conditions are listed in Table 2-1. Peak integration was performed using Agilent MassHunter Quantitative Analysis for QQQ, version B.05.00. All peaks were visually inspected to ensure proper integration.

Analyte	Precursor (m/z)	Product (m/z)	Fragmentor (V)	Collision Energy (V)
Bz-GABA	208	105	120	10
Bz-d6-GABA	214	105	120	10
$^{13}C_6$-Bz-GABA	214	111	120	10
Bz-Glu	252	105	120	20
Bz-$^{13}C_5$-Glu	257	105	120	20
$^{13}C_6$-Bz-Glu	258	111	120	20
Bz-5HT	385	264	140	20
Bz-d4-5HT	389	268	140	20
$^{13}C_6$-Bz-5HT	391	270	140	20
Bz-E	496	105	120	15
Bz-d6-E	502	105	120	15
$^{13}C_6$-Bz -E	514	111	120	15
$^{13}C_6$-Bz-d6-E	520	111	120	15
Bz-DA	466	105	140	20
Bz-$^{13}C_6$-DA	472	105	140	20
$^{13}C_6$-Bz-DA	484	111	140	20

Table 2-1: MRM conditions for benzoylated metabolites. Cell accelerator voltage was 4 V for all analytes.

Serum extraction with organic solvents

Acetonitrile, methanol, and a 1:1:1 mixture of methanol, acetonitrile, and acetone (MAA) were selected as common extraction solvents for comparison. Each solvent was kept at -20 °C. A mixture of 25 µM $^{13}C_5$-Glu and 2.5 µM d6-GABA, d4-5HT, and $^{13}C_6$-DA was prepared in water,

and 1 μL was spiked into nine aliquots of 50 μL of pooled human serum. The spiked serum was vortexed and three aliquots each were diluted with 200 μL cold acetonitrile, methanol, or MAA. These were vortexed briefly then centrifuged for 10 min at 12,100g, after which 20 μL of supernatant were derivatized by sequential addition of 10 μL 100 mM sodium carbonate, 10 μL 2% (v/v) BzCl in acetonitrile, and 10 μL internal standard solution. An additional 50 μL of water were added to reduce the organic content of the samples. Each sample was analyzed in triplicate by UPLC-MS/MS. Calibration standards were prepared in water, diluted with four volumes of each of the solvents, and derivatized in the same manner as the serum supernatant.

Comparison of extraction solvents

Extraction recovery was determined by comparing the calculated concentration of the spiked samples to the expected concentration. The relative standard deviation of the recovery was used to compare extraction repeatability. Matrix factor, a measure of ion suppression or enhancement from matrix components, is the ratio of analyte signal in matrix to the same concentration in matrix free standards. Matrix factors were calculated using the internal standard signal, as this is constant in all samples.

Mouse plasma collection

All of the procedures listed in this chapter were approved by the University of Michigan (UM) Committee on the Use and Care of Animals. C57BL/6 males were from Jackson Laboratories. *LepRb*^{Cck} KO study animals (along with *Cck*^{cre}, *Lepr*$^{flox/flox}$ and wild-type controls) were generated in our colony by crossing *Cck*^{cre}; *Lepr*$^{flox/+}$ and *Lepr*$^{flox/+}$ animals; these animals were on the segregating C57BL/6; 129Sv background. Mice were kept in a temperature-

controlled room on a 12-h light, 12-h dark cycle and provided with *ad libitum* food and water unless otherwise noted. Samples for the determination of epinephrine concentrations were obtained from animals with an arterial catheter (placed by the U M Animal Phenotyping Core (APC)). Data reported are from single-housed male animals studied during the light cycle. Investigators were blinded to genotype and treatment.

Mouse plasma analysis

Individual plasma samples were thawed, and 5 μL were spiked with 1.25 μL of d6-epinephrine (final concentration 50 nM) as an internal standard. Proteins were removed by the addition of 25 μL of ice-cold acetonitrile, followed by centrifugation for 10 min at 12,100g. The supernatant was removed and 20 μL were derivatized by sequential addition of 10 μL of 100 mM sodium tetraborate, 10 μL of 2% (v/v) BzCl in acetonitrile and 10 μL of 1% (v/v) sulfuric acid in dimethylsulfoxide.

Standard solutions of epinephrine were prepared in aCSF to create a calibration range of 0.1–20 nM. Standards were spiked with the internal standard, diluted with acetonitrile and derivatized as described above. Calibration curves were prepared based on the peak area ratio of the standard to the internal standard by linear regression. All samples and standards were analyzed by UPLC-MS/MS in triplicate. The gradient used was as follows: initial, 0% B; 0.01 min, 23% B; 2.51 min, 23% B, 3 min, 50% B; 5.3 min, 60% B; 6.46 min, 65% B; 6.47 min, 100% B; 7.49 min, 100% B; 7.5 min, 0% B; 8.5 min, 0% B. Example chromatograms are shown in Figure 2-1.

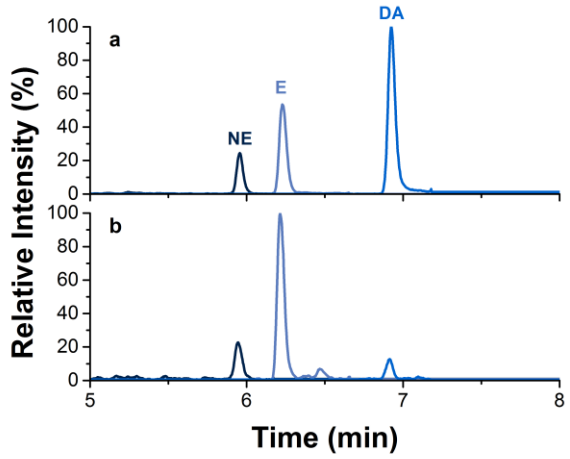

Figure 2-1: Extracted ion chromatograms from a. calibration standards and b. mouse plasma.

Fly stocks

The following stocks were obtained from Bloomington Stock center; Canton S. (RRID:FlyBase_FBst1000081), w1118, Trh^{c1440} (RRID:BDSC_10531),[19] $5HT2a^{PL00052}$ (RRID:BDSC_19367),[20] $JhI\text{-}21^{GE15185}$ (RRID:BDSC_26889).[21] UAS-dTrpA1,[22] UAS-shi^{ts1} (RRID:BDSC_44222),[23] Trh-GAL4[24] were gifts from P. Garrity (Brandeis University, Waltham, MA), T. Kitamoto (U of Iowa, Iowa city, IA), and B.G. Condron (U of Virginia, Charlottville, VA), respectively. Trh^{c1440}, $5HT2a^{PL00052}$, and $JhI\text{-}21^{GE15185}$ mutants were backcrossed at least 8 generations to w1118 prior to any followed up experiments after the candidate screens.

Fly husbandry

All fly stocks were maintained on a standard cornmeal-based larval growth medium and in a controlled environment (25 °C, 60% humidity) with a 12 Light: 12 dark cycles. If flies contained temperature-sensitive transgenes, they were reared in 23 °C and maintained at this temperature as adults until the experiments. Developmental larval density was controlled by manually aliquoting 32 μL of collected eggs into individual bottles containing 25 ml of food.[25] Following eclosion, mixed sex flies were kept on SY10% medium for 4–10 days until they were used for experiments. Unless otherwise noted, mated female flies that were between 5–14 days old were used for the choice experiments. When starvation was required for the feeding assay, 1% agar medium was used to deprive food but prevent dehydration.

Fly tissue analysis

Female flies were snap frozen in liquid nitrogen and vigorously vortexed to remove heads. The heads were homogenized with three volumes of ice cold acetonitrile (a single head was assumed to be 1 µL) using a pestle grinder. The homogenates were centrifuged at 18,000g for 5 min and the supernatant was collected as a tissue extract. To derivatize the samples prior to the UPLC-MS/MS analysis, 12 µL of each sample were benzoylated by the sequential addition of 6 µL of 100 mM sodium carbonate, 6 µL of 2% (v/v) BzCl in acetonitrile, and 6 µL of the internal standard solution.

Standards were prepared in aCSF and diluted with three volumes of acetonitrile. The diluted standards were derivatized in the same manner as the tissue extract samples. Samples and standards were analyzed by UPLC-MS/MS. The gradient used was: initial, 0% B; 0.01 min, 17% B; 0.5 min, 17% B; 3 min, 25% B; 3.3 min, 56% B; 4.99 min, 70% B; 5 min, 100% B; 6.5 min; 100% B; 6.51 min, 0% B; 8.5 min, 0% B. Example chromatograms are shown in Figure 2-2.

Results and siscussion

Comparison of extraction solvents

Recovery, repeatability, and matrix factors for the stable isotope labeled metabolites spiked into serum are compared in Figure 2-3. Recovery across the solvents and metabolites ranged from 25% to 85%. Recovery was lowest for glutamate and GABA with acetonitrile extraction, while

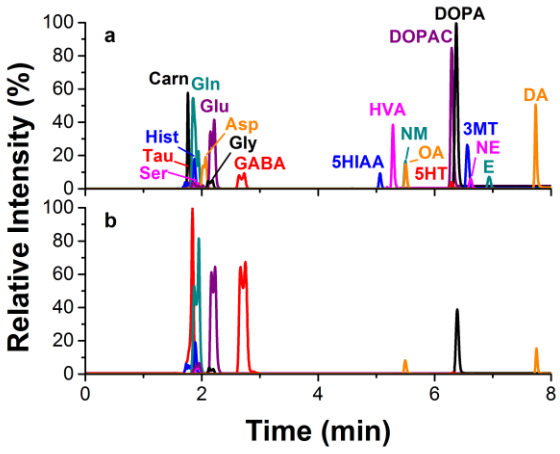

Figure 2-2: Extracted ion chromatograms from a. calibration standards and b. fly tissue homogenate.

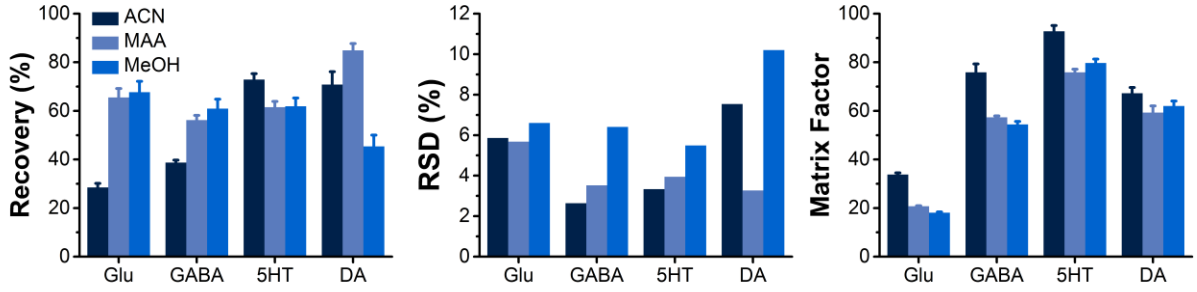

Figure 2-3: Comparison of extraction solvents. Recovery was determined by spiking pooled human serum with stable isotope labeled metabolites. Repeatability was calculated as the relative standard deviation of three spiked serum samples. Matrix factor was calculated by comparing the internal standard signal in serum samples to the internal standard signal in matrix-free standard solutions.

MAA had the highest average recovery. RSDs were below 10%, with the exception of dopamine following extraction with MeOH. MeOH had the highest RSDs, while acetonitrile and MAA were comparable. Matrix factors were highest for all metabolites with acetonitrile extraction, while methanol and MAA were similar. Although recovery was low for some metabolites, acetonitrile was selected as the optimal extraction solvent for its high repeatability and low matrix effects.

Importantly, the recovery and matrix effects varied between metabolites. For the neurochemicals tested, acetonitrile performed the best on average; but, it is possible that a different solvent would be more suitable when other metabolites are targeted. Thus, extraction solvent optimization is something that should be considered when designing a sample preparation method for targeted metabolomics. Additionally, the metabolite to metabolite variability in matrix effects further demonstrates the need for internal standards for each targeted metabolite. While it is common in metabolomics to use a single internal standard for all targeted metabolomics, this approach can lead to inaccurate quantification. For example, based on the data shown, using only $^{13}C_6$-Bz-GABA as an internal standard would underestimate the concentration of glutamate and dopamine by 54% and 12% respectively, while overestimating the concentration of serotonin by 16%. The simple creation of internal standards for all

metabolites with $^{13}C_6$-BzCl is thus a substantial advantage of derivatization for accurate quantification.

Comparison to existing methods

A number of methods exist for LC-MS/MS analysis of neurochemicals in proteinaceous biological samples.[26–30] Solvent precipitation is widely used for removal of proteins from biological fluids, though solvent compositions varied. Supernatants are often dried down and reconstituted prior to analysis. In this work, samples were not dried down prior to derivatization with BzCl as the extract was compatible with the derivatization procedure. This step could be added if preconcentration is desired, though it adds additional preparation time and could lead to degradation of thermally unstable metabolites. For metabolite extraction from tissue, organic solvents or perchloric acid are commonly added during homogenization.[10,31] BzCl requires basic samples, so we chose to use ACN for extraction when moving from biological fluids to tissue.

Because many neurochemicals are polar, HILIC is commonly used. While HILIC allows for good retention, chemical derivatization generally allows for greater sensitivity. A recently published method allows for analysis of 20 neurochemicals and metabolites with HILIC-MS/MS.[26] This method features lower limits of detection (LOD) than previously published HILIC methods. A comparison between this method and the BzCl method described here is summarized in Table 2-2.

Metabolite	LOD (nM)		Repeatability (%)		Injection Volume (µL)		Gradient Time (min)	
	HILIC	BzCl	HILIC	BzCl	HILIC	BzCl	HILIC	BzCl
Glu	17	30	18	5.9	5	5	20	8
GABA	190	4	4.2	2.6				
5HT	0.6	3	1.6	3.3				
DA	36	2	2.7	7.5				

Table 2-2: Comparison of LC-MS/MS methods for neurochemicals with HILIC or BzCl derivatization with RPLC.

While LODs for this HILIC method are better than previous HILIC methods, LODs are similar or better with BzCl. The HILIC LODs for glutamate and serotonin were approximately 2- and 6-fold better respectively, while BzCl LODs for dopamine and GABA were roughly 20- and 50-fold better. Repeatability between methods were similar. Analysis time with the BzCl method is less than half that of the HILIC method. Stable isotope labeled internal standards were used for nearly all analytes in the HILIC method, but BzCl derivatization allows for production of stable isotope labeled internal standards for all analytes. All BzCl work throughout this dissertation employs internal standards for each analyte.

Determination of epinephrine in mouse plasma

For this work, we monitored plasma epinephrine from wild type and knockout mice following 2DG challenge. Measuring epinephrine in plasma is challenging, as it is a stress hormone in addition to a counter-regulatory hormone. Common blood sampling techniques for mice such as decapitation or tail vein incision are stressful to the mice, leading to increased epinephrine which may obscure trends.[32] A lower stress technique, arterial catheterization, was chosen, but this leads to its own challenges. Since multiple time points were being taken from living mice, a limited volume of blood could be taken for each sample. An advantage of solvent precipitation is that it does not have a minimum volume requirement. In comparison, filtration requires enough sample volume to pass through the filter.

Plasma was sampled from mice via arterial catheterization every 30 min for 120 min following 2DG challenge. The resulting plasma was derivatized with BzCl and epinephrine concentrations were determine. All mice, regardless of genotype, showed an increase in epinephrine after 2DG challenge (Figure 2-4). Basal epinephrine levels were similar for all mice

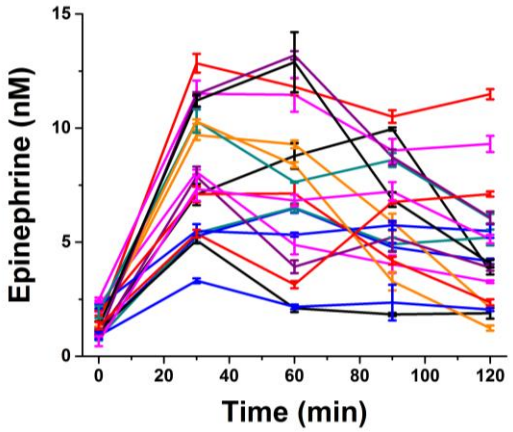

Figure 2-4: Plasma epinephrine over time following 2DG challenge (t = 0). Each line corresponds to an individual mouse. Data shown is average ± standard deviation of triplicate analysis at each time point. For all mice tested, epinephrine increases in response to hypoglycemia.

and were around 1-2 nM,which is consistent with previous findings from catheterized mice.[32] It was found that plasma epinephrine was significantly higher in the LepRb^{CCK} knockout mice compared to wild type mice following 2DG challenge (Figure 2-5a).

Glucagon and corticosterone, other CRR hormones, were also increased in LepRb^{CCK} KO mice relative to wild type (Figure 2-5b-c). These results suggest a more robust CRR in the LepRB^{CCK} KO mice and indeed, increased blood glucose was observed in the KO mice relative to the wild type (Figure 2-5d). Additional work revealed that selective inhibition of these neurons blunted the CRR, while selective activation enhanced the CRR. Together, this work shows that these LepRb^{CCK} neurons are involved in the CRR and are inhibited by leptin. The results lead to a greater understanding of the role of the central nervous system in the CRR, which may be beneficial in the treatment of diseases such as diabetes where inadequate responses to hypoglycemia can be lethal.

Role of serotonin in Drosophila protein preference and aging

In wild type flies, no preference was observed between a sugar-only food source and a protein-containing food source. However, when starved for 24 h prior to the food choice experiment, a preference for the protein-containing food was observed (Figure 2-6). In mutants where tryptophan hydroxylase (*Trh*), the rate limiting enzyme in serotonin production, was reduced, this protein preference following starvation was abolished (Figure 2-7).

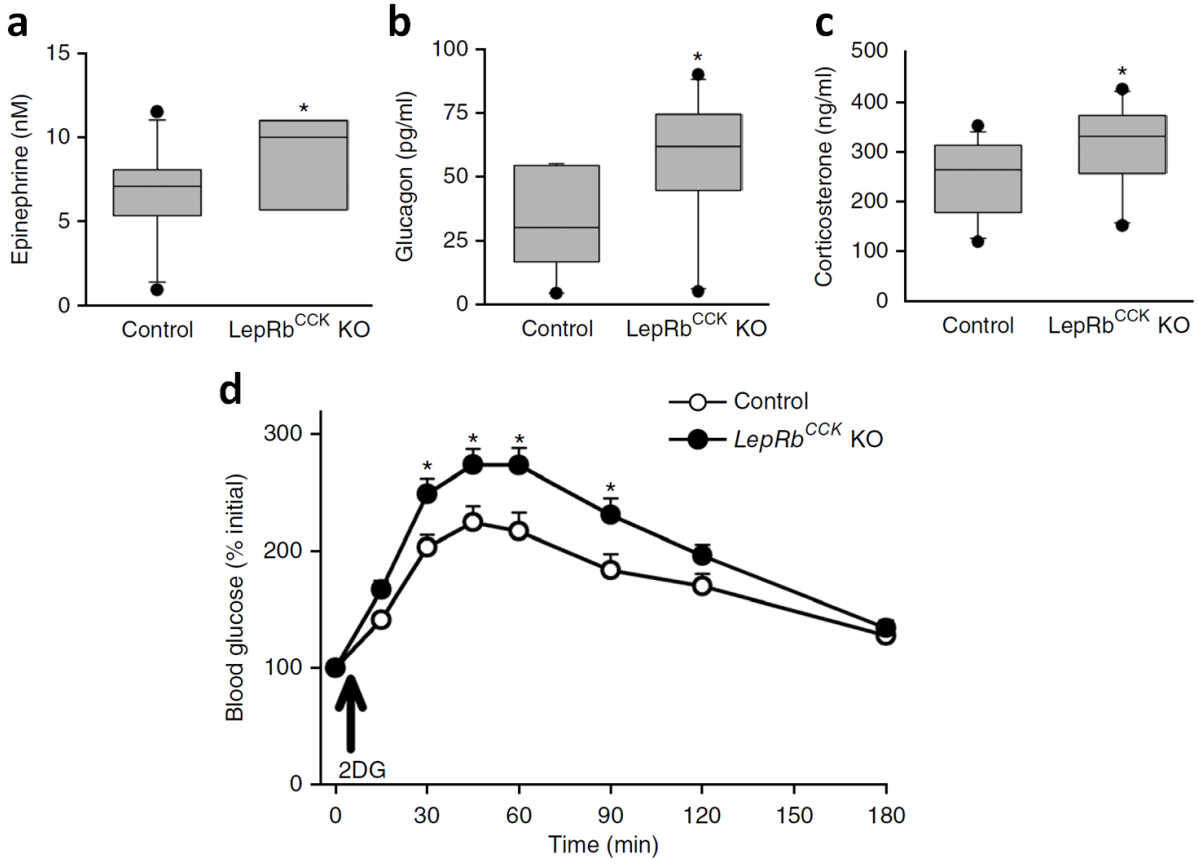

Figure 2-5: Counterregulatory response in LepRb^{CCK} KO mice 90 min following 2DG challenge. a. Epinephrine (n = 11 (control) and 8 (KO)); b. glucagon (n = 11 per condition); c. corticosterone (n = 11 per condition) were all increased in LepRb^{CCK} KO mice relative to controls. d. A greater increase in blood glucose was observed in LepRb^{CCK} KO mice (n = 13) relative to controls (n = 11).

This loss of preference suggests a role for serotonin in protein preference following starvation.

To determine if serotonin is involved in protein choice or post-ingestive reward, serotonin levels were measured in fly heads at varying points of the experiment. Serotonin does not change between fully fed flies and starved flies, but increases upon refeeding with protein containing food sources (Figure 2-8). Since serotonin does not increase prior to protein consumption, it is assumed that serotonin is involved in protein reward following starvation.

Protein consumption has been shown to impact longevity so lifespan of wild type control and mutant flies were compared. On a diet containing a fixed ratio of macronutrients, *Trh*

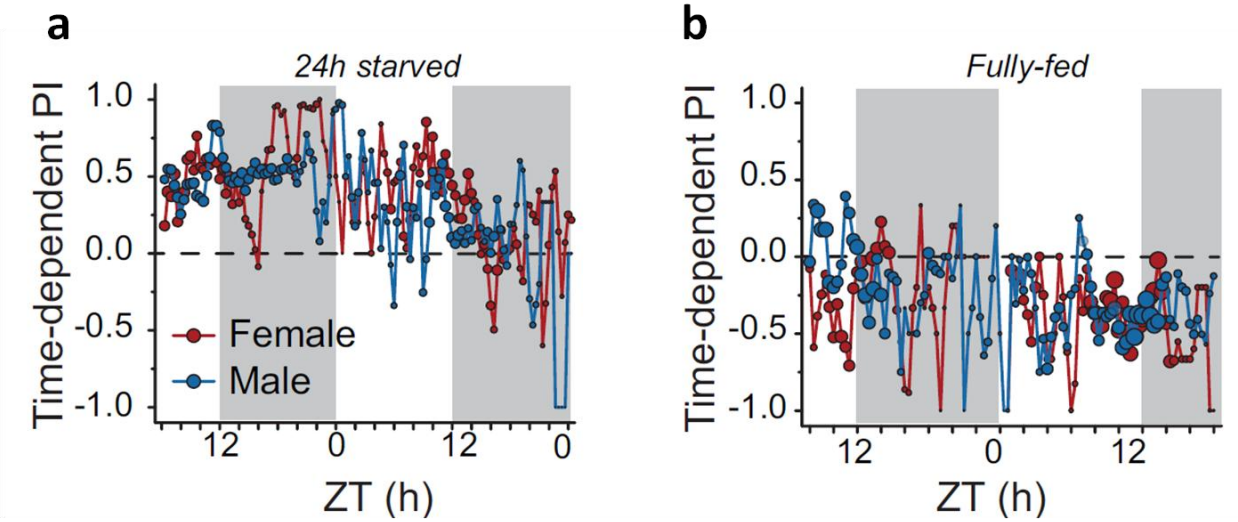

Figure 2-6: Preference index (PI) of WT flies presented the choice between sugar-containing or protein-containing food. A PI of 1 represents a complete preference for protein, while -1 represents a complete preference for sugar. White and gray periods indicate light and dark periods respectively. a. A preference for protein is observed when starved 24 h prior to the choice experiment. b. This preference is abolished when flies are fully fed prior to the experiment.

mutant flies showed increased lifespan compared to control flies. The serotonin receptor *5HT2a* was shown to be involved in protein reward, but mutants which do not express this receptor did not show increased lifespan relative to controls. However, when presented with a complex dietary environment where flies could choose between carbohydrate or protein containing foods, both the *Trh* and *5HT2a* mutants had longer lifespans than the control flies, and this increase was larger relative to that in a fixed diet (Figure 2-9). There was no difference in macronutrient consumption between control and mutant flies, so this evidence suggests the process of protein valuation impacts longevity independent of actual dietary consumption.

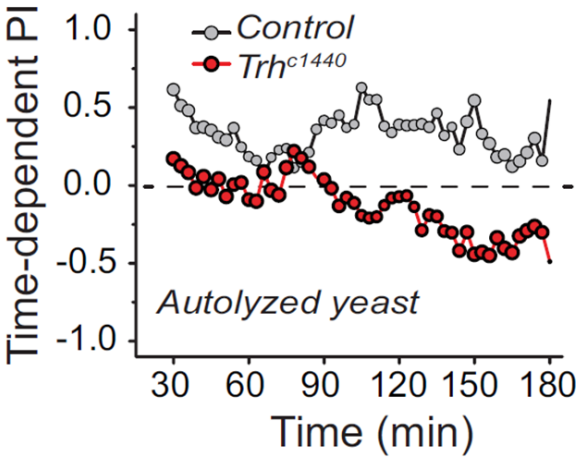

Figure 2-7: Preference index (PI) of control and tryptophan hydroxylase knockdown (Trh^{c1440}) flies following 24 h of starvation. A PI of 1 corresponds to a complete preference for the protein containing food, autolyzed yeast. The Trh^{c1440} flies showed no preference for protein.

To further understand the mechanism, mutations upstream of serotonin signaling

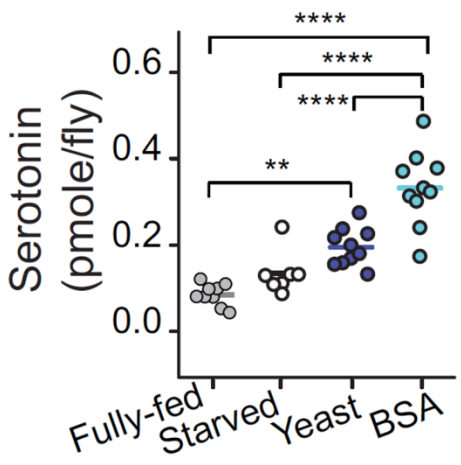

Figure 2-8: Serotonin concentrations in control fly heads at experimental timepoints. Serotonin does not increase during starvation, showing it is not involved in the protein choice stage. Serotonin does increase upon refeeding with protein containing foods, yeast or BSA, suggesting serotonin is involved in post-ingestive reward.

were tested and it was found that mutations in the amino acid transporter gene juvenile hormone inducible 21 (*JhI-21*) also abolished protein preference following starvation (Figure 2-10a). An increase in serotonin was not observed in these flies upon protein refeeding, confirming that *JhI-21* acts upstream of serotonin production (Figure 2-10b). Similarly to *Trh* and *5HT2a* mutants, *JhI-21* mutants showed an increase in lifespan in a choice food environment relative to controls (Figure 2-10c). We can conclude from this data that *JhI-21* acts together with serotonin signaling in this protein valuation and reward process. *JhI-21* is homologous to the SLC7 family of amino acid transporters in vertebrates, so it is possible this family may be implicated in other species.

Many factors make dietary research difficult. Mammalian models require relatively large housing and resources, and long lifespans make research slow. *Drosophila* and other insect models are attractive due to their small size and short lifespans, while maintaining many analogous systems to humans. *Drosophila* are genetically tractable so multiple genetic manipulations were used in this work to elucidate roles of specific enzymes and metabolites. Additionally, a number of fixed and choice dietary environments were used to determine if observed results are a product of protein consumption or the dietary choice process itself. The results here identify a role for serotonin signaling and protein valuation in the modulation of lifespan. The combination of BzCl derivatization with the *Drosophila* model is demonstrated as a powerful tool for dietary and metabolomic research.

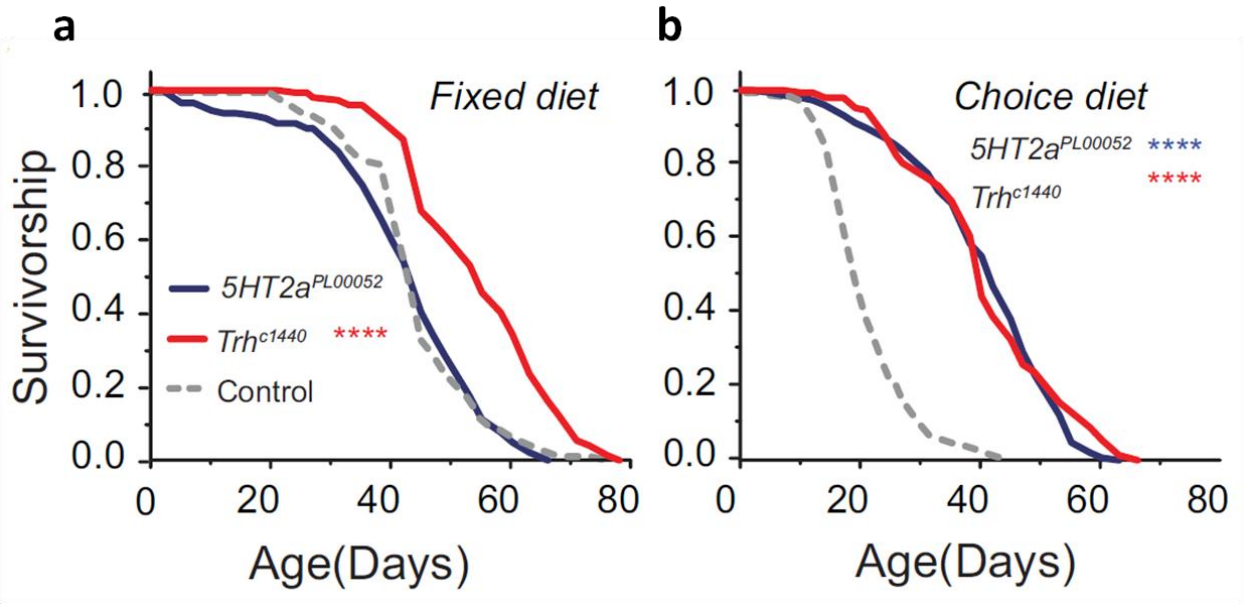

Figure 2-9: Lifespan of control flies and mutants for serotonin production and signaling. a. In a fixed diet environment, only the *Trh*^{c1440} flies showed an increased lifespan relative to controls. b. When allowed to choose between carbohydrate and protein containing foods, both Trh^{c1440} and 5HT2a^{PL00052} flies had longer lifespans than control flies, though no difference in macronutrient consumption was observed. These data suggest the protein valuation process has an impact on longevity independent of dietary consumption.

Conclusions

BzCl derivatization is a simple, rapid reaction which allows for greater retention and ionization efficiency of amines and phenols in RPLC-MS. While this method has been established in the filtered samples which result from microdialysis, additional sample preparation is required for proteinaceous samples such as plasma or tissue. Solvent precipitation was chosen as a method for protein removal, as it is fast, inexpensive, and compatible with large or small samples. In this chapter, multiple solvents were compared to determine the best choice for protein precipitation prior to BzCl derivatization. Acetonitrile was chosen as the optimal solvent for its high repeatability and limited matrix effects. Developing sample preparation for proteinaceous samples greatly expands the versatility of BzCl derivatization, which was demonstrated through applications using plasma and tissue as sample matrices.

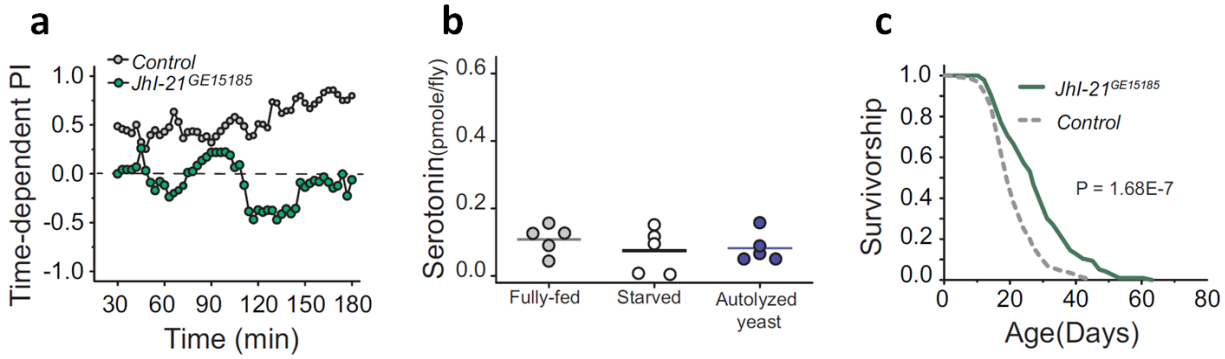

Figure 2-10: Behavior of amino acid transport mutants *JhI-21*^{GE15185} compared to control flies. a. Like *Trh* mutants, no protein preference was observed in *JhI-21*^{GE15185} flies following starvation. b. Unlike control flies, no increase in serotonin was observed following protein refeeding. This suggests that *JhI-21* is involved upstream of serotonin production in the protein valuation process. c. In a choice food environment, *JhI-21* mutants show an increased lifespan relative to control flies.

Two applications were explored using this optimized sample preparation. Epinephrine was measured in plasma from mice to confirm the role of PBN LepRb neurons in the CRR. These neurons were found to be inhibited by leptin and knocking out LepRb in these neurons produced an enhanced CRR relative to wild type mice. Epinephrine was increased, as well as other CRR hormones following 2DG challenge. This increase suggests that these neurons act to ensure an adequate blood glucose level through a robust CRR even during hypoglycemia, when normal endocrine signaling is reduced. The CRR is especially important in diabetic patients who are prone to insulin-induced hypoglycemia. Finding potential drug targets, such as these neurons, may help prevent insulin-induced hypoglycemia in diabetic patients.

We also investigated the role of serotonin in protein preference and aging in *Drosophila*. Flies were found to have a preference for protein-containing food following modest starvation. This preference was lost in *Trh* mutants, which are defective in serotonin production. The role of serotonin in this preference was further established as serotonin was found to increase in the heads of flies following refeeding on protein-containing food. The protein valuation process was found to be implicated in longevity, as *Trh* and *5HT2a* mutants had longer lifespans than control flies independent of diet.

Additionally, an amino acid transporter, *JhI-21*, was identified which acts upstream of serotonin signaling in this process. *JhI-21* mutant flies, like the serotonin mutants, were found to have no protein preference following starvation and did not produce an increase in serotonin upon protein refeeding. These flies also exhibited longer lifespans than control flies. These results demonstrate that the lifespan increasing properties observed from a low protein diet in flies are not exclusively a product of reduced protein consumption, and start to elucidate the mechanism for this. While this study was performed in flies, similar effects from calorie or protein restriction have been observed in other species, so the results could provide insight for other species as well.

References

(1) Song, P.; Mabrouk, O. S.; Hershey, N. D.; Kennedy, R. T. *Anal. Chem.* **2012**, *84*, 412–419.

(2) Ferry, B.; Gifu, E. P.; Sandu, I.; Denoroy, L.; Parrot, S. *J. Chromatogr. B* **2014**, *951–952* (1), 52–57.

(3) Vollbrecht, P. J.; Mabrouk, O. S.; Nelson, A. D.; Kennedy, R. T.; Ferrario, C. R. *Obesity* **2016**, *24* (3), 670–677.

(4) Zheng, X.; Kang, A.; Dai, C.; Liang, Y.; Xie, T.; Xie, L.; Peng, Y.; Wang, G.; Hao, H. *Anal. Chem.* **2012**, *84* (22), 10044–10051.

(5) Hamid, A. A.; Pettibone, J. R.; Mabrouk, O. S.; Hetrick, V. L.; Schmidt, R.; Vander Weele, C. M.; Kennedy, R. T.; Aragona, B. J.; Berke, J. D. *Nat. Neurosci.* **2015**, *19* (1), 117–126.

(6) Michopoulos, F.; Lai, L.; Gika, H.; Theodoridis, G.; Wilson, I. *J. Proteome Res.* **2009**, *8* (4), 2114–2121.

(7) Dietmair, S.; Timmins, N. E.; Gray, P. P.; Nielsen, L. K.; Krömer, J. O. *Anal. Biochem.* **2010**, *404* (2), 155–164.

(8) Barri, T.; Holmer-Jensen, J.; Hermansen, K.; Dragsted, L. O. *Anal. Chim. Acta* **2012**, *718*, 47–57.

(9) Sitnikov, D. G.; Monnin, C. S.; Vuckovic, D. *Sci. Rep.* **2016**, *6* (1), 38885.

(10) Lin, C. Y.; Wu, H.; Tjeerdema, R. S.; Viant, M. R. *Metabolomics* **2007**, *3* (1), 55–67.

(11) Beall, C.; Ashford, M. L.; McCrimmon, R. J. *Am. J. Physiol. Regul. Integr. Comp. Physiol.* **2012**, *302* (2), R215-23.

(12) Pletcher, S. D.; Macdonald, S. J.; Marguerie, R.; Certa, U.; Stearns, S. C.; Goldstein, D. B.; Partridge, L. *Curr. Biol.* **2002**, *12* (9), 712–723.
(13) Fontana, L.; Meyer, T. E.; Klein, S.; Holloszy, J. O. *Proc. Natl. Acad. Sci. U. S. A.* **2004**, *101* (17), 6659–6663.
(14) Linford, N. J.; Kuo, T.-H.; Chan, T. P.; Pletcher, S. D. *Annu. Rev. Cell Dev. Biol.* **2011**, *27* (1), 759–785.
(15) Mair, W.; Piper, M. D. W.; Partridge, L. *PLoS Biol.* **2005**, *3* (7), 1305–1311.
(16) Levine, M. E.; Suarez, J. A.; Brandhorst, S.; Balasubramanian, P.; Cheng, C. W.; Madia, F.; Fontana, L.; Mirisola, M. G.; Guevara-Aguirre, J.; Wan, J.; Passarino, G.; Kennedy, B. K.; Wei, M.; Cohen, P.; Crimmins, E. M.; Longo, V. D. *Cell Metab.* **2014**, *19* (3), 407–417.
(17) Leibowitz, S. F.; Alexander, J. T.; Cheung, W. K.; Weiss, G. F. *Pharmacol. Biochem. Behav.* **1993**, *45* (1), 185–194.
(18) Leibowitz, S. F.; Alexander, J. T. *Biological Psychiatry*. 1998, pp 851–864.
(19) Neckameyer, W. S.; Coleman, C. M.; Eadie, S.; Goodwin, S. F. *Genes, Brain Behav.* **2007**, *6* (8), 756–769.
(20) Nichols, C. D. *Dev. Neurobiol.* **2007**, *67* (6), 752–763.
(21) Jin, L. H.; Shim, J.; Yoon, J. S.; Kim, B.; Kim, J.; Kim-Ha, J.; Kim, Y. J. *PLoS Pathog.* **2008**, *4* (10), e1000168.
(22) Hamada, F. N.; Rosenzweig, M.; Kang, K.; Pulver, S. R.; Ghezzi, A.; Jegla, T. J.; Garrity, P. A. *Nature* **2008**, *454* (7201), 217–220.
(23) Kitamoto, T. *Dev. Neurobiol.* **2001**, *47* (2), 81–92.
(24) Daubert, E. A.; Heffron, D. S.; Mandell, J. W.; Condron, B. G. *Mol. Cell. Neurosci.* **2010**, *44* (3), 297–306.
(25) Linford, N. J.; Bilgir, C.; Ro, J.; Pletcher, S. D. *J. Vis. Exp.* **2013**, No. 71, e50068–e50068.
(26) Tufi, S.; Lamoree, M.; de Boer, J.; Leonards, P. *J. Chromatogr. A* **2015**, *1395*, 79–87.
(27) Cai, H. L.; Zhu, R. H.; Li, H. D. *Anal Biochem* **2010**, *396* (1), 103–111.
(28) Wei, B.; Li, Q.; Fan, R.; Su, D.; Chen, X.; Jia, Y.; Bi, K. *J. Pharm. Biomed. Anal.* **2014**, *88*, 416–422.
(29) Fuertig, R.; Ceci, A.; Camus, S. M.; Bezard, E.; Luippold, A. H.; Hengerer, B. *Bioanalysis* **2016**, *8*, 1903–1917.
(30) González, R. R.; Fernández, R. F.; Vidal, J. L. M.; Frenich, A. G.; Pérez, M. L. G. *J. Neurosci. Methods* **2011**, *198* (2), 187–194.
(31) Want, E. J.; Masson, P.; Michopoulos, F.; Wilson, I. D.; Theodoridis, G.; Plumb, R. S.; Shockcor, J.; Loftus, N.; Holmes, E.; Nicholson, J. K. *Nat. Protoc.* **2013**, *8* (1), 17–32.
(32) Grouzmann, E.; Cavadas, C.; Grand, D.; Moratel, M.; Aubert, J. F.; Brunner, H. R.; Mazzolai, L. *Pflugers Arch. Eur. J. Physiol.* **2003**, *447* (2), 254–258.

CHAPTER 3

Benzoyl chloride derivatization with liquid chromatography - mass spectrometry for targeted metabolomics of neurochemicals in biological samples

 Equal authorship was awarded to Wong and Malec. Malec contributed selection of compounds assayed, extraction optimization and applications in human serum and *Drosophila* tissue.

Introduction

Metabolomics is a valuable approach for studying physiological mechanisms and identifying biomarkers. Both untargeted and targeted assays, also called metabolite profiling, are used in such studies. Targeted assays measuring a limited number of metabolites allow focus on important known compounds or pathways and offer better quantification, but they provide lower metabolome coverage compared to untargeted methods. Targeted assays that measure relatively large numbers of compounds (i.e., over 50) help mitigate the disadvantage of limited metabolome coverage. Gas chromatography-mass spectrometry (MS) and high performance liquid chromatography (HPLC)-MS are well-suited platforms for developing such widely targeted assays. Several methods for measuring over 100 known metabolites in a single assay using these techniques have been reported.[1–6] These widely targeted assays are powerful, but they rarely use more than a few internal standards, and for HPLC often make use of ion-pairing reagents[3,6] or multiple LC pumps[4,5] to account for the wide polarity range of the metabolites. Here we report a targeted method for 70 neurochemicals that uses HPLC-MS/MS with benzoyl chloride (BzCl) as a derivatizing agent and avoids these limitations.

HPLC-tandem mass spectrometry (MS/MS) using a triple quadrupole mass spectrometer is well established as a sensitive, quantitative, and selective technique for metabolite profiling.[7,8] Although compounds can be detected by MS/MS without labeling, the use of BzCl provides numerous advantages with only minor drawbacks. In particular, addition of a phenyl group to the polar analytes increases retention on reversed phase columns, which aids resolution and decreases ion suppression. Many compounds are detected with greater sensitivity after labeling, e.g. 1,000-fold increases in sensitivity have been reported for BzCl labeling.[9] The labeling step allows rapid creation of stable-isotope labeled internal standards by using ^{13}C-BzCl for labeling standards, thereby improving quantification for every analyte. BzCl is widely applicable because it derivatizes primary and secondary amines, phenols, thiols, and some alcohols (e.g., ribose hydroxyls and glucose). Indeed, it has previously been used with MS or ultraviolet absorption detection for monitoring neurochemicals in dialysate,[9,10] plasma,[10] and human cerebrospinal fluid (CSF).[11] It has also been used for other amine[12,13] and alcohol[14,15] containing compounds. These previous assays targeted a relatively narrow group of compounds.

Although we focus on BzCl, other reagents such as dansyl chloride may provide similar utility for metabolomics.[16–19] We favor BzCl because it reacts faster (seconds at room temperature compared to 20 min at elevated temperature), has a wider pH range for reaction, is less prone to photodegradation, and is commercially available in ^{13}C-labeled form. Additionally benzoylated products are stable for a week at room temperature,[9] and standards and internal standards are stable for six months at -80 °C (data not shown).

The 70 compound assay described here targets neurochemicals. Neurons specialize in storing and transmitting information using neurotransmitters and neuromodulators. Low molecular weight polar compounds represent an important class of neurotransmitters including

acetylcholine, adenosine, catecholamines, indoleamines, amino acids, trace amines, and dipeptides. A variety of other compounds, such as energy metabolites, antioxidants, and polyamines that affect neuronal function or have been linked to neurological disease are also included in the assay. This assay focuses on these compounds and their precursors and degradation products, as their measurement can provide insights into neuronal function to better understand the neurochemical changes in brain diseases. Although this is not a comprehensive assay for all neurochemicals, it demonstrates the wide applicability of BzCl derivatization. The method is an improvement over previous neurochemical assays which were limited to even smaller subsets of neurochemicals,[10,20–26] including our previously described 17 compound method based on similar technology.[9]

This report demonstrates the utility of BzCl with HPLC-MS for targeted metabolomics on several sample types including tissue, serum, CSF, and microdialysate. Tissue samples are used to characterize concentrations at fixed time points and are best used for determining the overall production and metabolism of neurochemicals. We demonstrate the assay for *Drosophila melanogaster* tissue and hemolymph, an important neurochemical model system. Serum and CSF assays are useful for biomarker studies and assessment of overall physiological state. Microdialysis samples the brain extracellular space and enables the measurement of released neurochemicals over time, making it valuable for correlating neurochemical dynamics to behavior, monitoring drug effects, and assessing the effect of disease states on neurochemical concentrations. However, the low samples volumes of microdialysate in our studies (typically 1 µL) make analysis challenging.

Although BzCl labeling with HPLC-MS/MS has been used for neurochemicals before, the current work increases the number of analyzed compounds by 4-fold, streamlines reagent

addition, and improves labeling conditions to give better sensitivity and reproducibility for some compounds. Finally, the assay is shown to be useful for a wider range of sample types.

Experimental

Chemicals and reagents

All chemicals were purchased from Sigma Aldrich (St. Louis, MO) unless otherwise noted. Water, methanol, and acetonitrile for mobile phases are Burdick & Jackson HPLC grade purchased from VWR (Radnor, PA). Stock solutions of 500 mM Glc; 10 mM DOMA, DOPAC (Acros Organics, Geel, Belgium), MOPEG, GABA, 5HIAA, 5HTP, Agm, Ala, Ans, Arg, Asn, Asp, βAla, Carn, Cit, CA, Cys, DA, E, ETA, Glu, Gln, GSH, Gly, Hist, His, HCA, HCY, HSer, HVA (Tocris, Bristol, UK), HTau, Kyo (MP Biomedicals, Santa Ana, CA), Leu, Lys, Met, NAP, NAS, NE, NM, OA, Orn (Acros Organics, Geel, Belgium), PhEt (MP Biomedicals, Santa Ana, CA), Pro, Put, Ser, 5HT, Spd, Spm, Syn, Tau, Thr, Val, and VMA; 5 mM ACh, 5HTOL (Cayman Chemical, Ann Arbor, MI), Ado, Kyn, LDOPA, Phe, and Trp; 2.5 mM 3HK; 2 mM Tyr; 1 mM DOPEG, 3HAA, 3MT, KA, and TyrA; 0.25 mM TrpA; and 20 mM isotopically labeled d4-ACh and d4-Ch (C/D/N isotopes, Pointe-Claire, Canada); were made in HPLC water and kept at -80 °C. A standard mixture was diluted from stocks with artificial cerebrospinal fluid (aCSF) consisting of 145 mM NaCl, 2.68 mM KCl, 1.4 mM $CaCl_2$, 1.0 mM $MgSO_4$, 1.55 mM Na_2HPO_4, and 0.45 mM NaH_2PO_4 adjusted pH to 7.4 with NaOH. Calibration curves were made using standards at 0.1, 0.5, 1, 5, 10, 25, 50 μM for Glc; 10, 50, 100, 500, 1000, 250, 5000 nM for 3HK, Asn, Asp, CA, GSH, Gly, HTau, Ser, and Tau; 1, 5, 10, 50, 100, 250, 500 nM for Ch, 3HAA, MOPEG, 5HIAA, 5HTP, 5HTOL, Ado, Agm, Ala, Ans, βAla, Carn, Cit, Cys, ETA, Glu, Gln, His, HCA, HCY, HSer, HVA, KA, Kyn, Met, NAP, Orn, Phe, Pro, Thr, Trp, Val, and

VMA; 0.1, 0.5, 1, 5, 10, 25, 50 nM for ACh, DOMA, DOPAC, DOPEG, 3MT, GABA, Arg, DA, E, Hist, Kyo, LDOPA, Leu, Lys, NAS, NE, NM, OA, PhEt, Put, 5HT, Spd, Spm, Syn, TrpA, TyrA, and Tyr. An internal standard stock was prepared with 5 mM Glc; 500 μM 3HK, Asn, Asp, CA, GSH, Gly, HTau, Ser, and Tau; 50 μM 3HAA, MOPEG, 5HIAA, 5HTP, 5HTOL, Ado, Agm, Ala, Ans, βAla, Carn, Cit, Cys, ETA, Glu, Gln, His, HCA, HCY, HSer, HVA, KA, Kyn, Met, NAP, Orn, Phe, Pro, Thr, Trp, Val, and VMA; 5 μM DOMA, DOPAC, DOPEG, 3MT, GABA, Arg, DA, E, Hist, Kyo, LDOPA, Leu, Lys, NAS, NE, NM, OA, PhEt, Put, 5HT, Spd, Spm, Syn, TrpA, TyrA, and Tyr; and derivatized with $^{13}C_6$-BzCl using a similar procedure as ^{12}C reagents.

Calibration standard and internal standard stocks were frozen at -80 °C in aliquots to prevent multiple freeze/thaw cycles. A single internal standard stock aliquot was thawed the day of use, diluted 100-fold in 20% (v/v) acetonitrile containing 1% (v/v) sulfuric acid, and spiked with deuterated acetylcholine and choline (C/D/N isotopes, Pointe-Claire, Canada) to a final concentration of 20 nM. A fresh benzoyl chloride solution was made daily.

Microdialysis in anesthetized rat

Adult male Sprague-Dawley rats (Harlan, Indianapolis, IN) weighing 250-275 g were used for microdialysis collection. Rats were housed with access to food and water ad libitum in a temperature and humidity controlled room with 12 h light/dark cycles. All animals were treated as approved by the University Committee on Use and Care of Animals at the University of Michigan, the National Institute of Health Guidelines for the Care and Use of Laboratory Animals. All precautions were taken to prevent animal discomfort through the course of the

experiments. In addition, all animal experiments were conducted within the guidelines of Animal Research Reporting in vivo Experiments.

A custom-made concentric microdialysis probe (4 mm dialyzing membrane), made using regenerated cellulose (Spectrum Laboratories, Inc., Rancho Dominguez, CA, USA), was implanted into the striatum. Rats were anesthetized with 1-4% isoflurane and placed into a stereotaxic frame (David Kopf, Tujunga, CA). A burr hole was placed above the striatum using the anterior-posterior +1.0 mm and lateral ±3.0 mm coordinates from bregma. The microdialysis probe was flushed with artificial CSF (aCSF) at a flow rate of 2 μL/min using a Fusion 400 syringe pump (Chemyx, Stafford, TX) as it was lowered -6.15 mm from top of skull. Once the probe was positioned, the probe was flushed at 2 μL/min for 30 min followed by 30 min at 1.0 μL/min prior to collection. 10 μL dialysate was derivatized using the modified method reported: 5 μL of 100 mM sodium carbonate, 5 μL BzCl (2% (v/v) in acetonitrile), and 5 μL internal standard mixture were added sequentially, with vortex mixing after each addition. At the completion of the experiment, animals were euthanized, brains were extracted and stored at 4 °C in 4% paraformaldehyde. Probe placement was confirmed with histology.

Human CSF

Pooled human CSF from healthy patients was obtained from the Batemen lab at Washington University School of Medicine, St. Louis, MO.[27] Samples were diluted 100-fold in water, and a 10 μL aliquot was derivatized using 5 μL of 100 mM sodium carbonate, 5 μL BzCl (2% (v/v) in acetonitrile), and 5 μL internal standard mixture before LC-MS analysis.

Human serum

Pooled human serum from the American Red Cross Detroit National Testing Lab was provided by the Michigan Regional Comprehensive Metabolomics Resource Core. To remove proteins, 20 µL of serum were diluted with 80 µL of ice-cold acetonitrile. The samples were vortexed briefly, then centrifuged for 10 min at 12,100 × g. 20 µL of the supernatant was derivatized by sequential addition of 10 µL of 100 mM sodium carbonate, 10 µL of BzCl (2% (v/v) in acetonitrile), and 10 µL of the internal standard mixture. 50 µL of water were added to reduce the organic content of the samples. Calibration standards were prepared in aCSF, which is similar in composition to serum without proteins.[28] Five µL aliquots of the standards were diluted with 20 µL acetonitrile to match the sample composition, and then derivatized in the same manner as the serum supernatant.

Fly tissue homogenate

Homogenized *Drosophila* samples were provided by the Pletcher lab at the University of Michigan, Ann Arbor. Female flies were treated with 250 µM 5HTP for four days prior to harvesting. The flies were snap frozen in liquid nitrogen and vortexed to remove heads. The heads were homogenized in 4 µL of ice cold acetonitrile per head, and 20 µL ice-cold acetonitrile per body, using a pestle grinder. The homogenate was centrifuged at 18,000 × g for 5 min and the supernatant was removed and stored at -80 °C until derivatization. 20 µL of the supernatant was derivatized by sequential addition of 10 µL of 100 mM sodium carbonate, 10 µL of BzCl (2% (v/v) in acetonitrile), and 10 µL of the internal standard mixture. Finally, 50 µL of water were added to reduce the organic content of the samples. Calibration standards were prepared in aCSF. Five µL aliquots of the standards were diluted with 20 µL acetonitrile to match the sample composition, and then derivatized in the same manner as the tissue homogenate supernatant.

Fly hemolymph

Hemolymph from *Drosophila* was provided by the Dus lab at the University of Michigan. Flies were reared in standard cornmeal-glucose medium at 25 °C in a 12:12 light/dark cycle. After eclosion groups of 100 $w1118^{CS}$ (*w1118* backcrossed to *CS* for 10 generations) males were placed in bottles and aged for 7-10 days until the time of hemolymph collection. Fresh food was provided every 2 days.

Hemolymph collection was performed as previously described, with modifications to the sated condition.[29] $w118^{CS}$ males in groups of 100 were moved into bottles containing agar and fasted for 24 h. For the starved condition, males were collected directly from the starvation bottles; for the sated condition, males were moved to bottles containing 5% sucrose agar and red food dye for 1 h, and then gathered for hemolymph collection. To generate a sufficient sample volume, multiple collections of hemolymph each from 100 males were pooled together. Hemolymph was stored at -80 °C until derivatization.

20 µL of hemolymph were diluted with 80 µL of ice cold acetonitrile. The samples were vortexed, then centrifuged for 10 min at 12,100g. 20 µL of the supernatant was derivatized by sequential addition of 10 µL of 100 mM sodium carbonate, 10 µL of BzCl (2% (v/v) in acetonitrile), and 10 µL of the internal standard mixture. 50 µL of water were added. Calibration standards were prepared in aCSF. 5 µL aliquots of the standards were diluted with 20 µL acetonitrile to match the sample composition, and then derivatized in the same manner as the hemolymph supernatant.

Protein precipitation method validation

To validate the method and test recovery of the solvent precipitation, we spiked a mixture of stable isotope labeled metabolites (500 nM $^{13}C_5$-glutamate, 50 nM d6-GABA, 50 nM d4-serotonin, and 50 nM $^{13}C_6$-dopamine) into 50 µL of pooled human serum. The spiked serum was diluted with 200 µL ice cold acetonitrile, followed by centrifugation for 10 minutes at 12,100g. 20 µL of supernatant was derivatized by sequential addition of 10 µL of 100 mM sodium carbonate, 10 µL of BzCl (2% (v/v) in acetonitrile), and 10 µL of the internal standard mixture. Three spiked serum samples were extracted and derivatized in parallel for triplicate analysis. Calibration standards were prepared in aCSF, and 5 µL aliquots of the standards were diluted with 20 µL acetonitrile to match the sample composition, and then derivatized in the same manner as the serum supernatant.

Small molecule neurochemical analysis using QQQ MS/MS

Derivatized samples were analyzed by LC-MS (as further described in the results section) using a Waters nanoAcquity UPLC (Milford, MA) coupled to an Agilent 6410 (Santa Clara, CA) triple quadrupole mass spectrometer operating in dynamic multiple reaction monitoring (dMRM) mode. Five µL were injected onto an Acquity HSS T3 C18 column (1 mm x 100 mm, 1.8 µm, 100 Å pore size) in partial loop injection mode. Samples were analyzed in triplicate. Mobile phase A was 10 mM ammonium formate with 0.15% formic acid, and mobile phase B was acetonitrile. The flow rate was 100 µL/min and the elution gradient was as follows: initial, 0% B; 0.01 min, 15% B; 0.5 min, 17% B; 14 min, 55% B; 14.5 min, 70% B; 18 min, 100% B; 19 min, 100% B; 19.1 min, 0% B; and 20 min, 0% B. An additional 10 min of column equilibration at 0% B were required to achieve reproducible chromatography. The required pressure over the gradient was from 2,500 - 8,000 psi. The autosampler was kept at ambient temperature and the

column was kept at 27 °C. Electrospray ionization was used in positive mode at 4 kV. The gas temperature was 350 °C, gas flow was 11 L/min, and the nebulizer was at 15 psi. Automated peak integration was performed using Agilent MassHunter Workstation Quantitative Analysis for QQQ, version B.05.00; all peaks were visually inspected to ensure proper integration.

Statistical analyses

All statistical analyses were performed in Prism 7 (GraphPad, La Jolla, CA). For statistical analysis unpaired Student's t test were applied. Differences were deemed significant if $p < 0.05$.

Results and discussion

BzCl labeling has been previously reported for the analysis of small molecule neurotransmitters, polyamines and steroids with HPLC-MS or ultraviolet-absorption detection.[9,10,30,31] Here we identify new reaction conditions that improve sensitivity for LC-MS/MS for many of the neurochemicals tested and demonstrate the wide applicability of BzCl derivatization for low molecular weight metabolites in a variety of complex sample matrices.

Effect of buffer and solvents on reaction conditions

The initial report of using BzCl with HPLC-MS/MS for neurochemicals utilized four reagent addition steps[9]: 1) sodium tetraborate buffer (100 mM) to the sample to achieve basic pH conditions required for BzCl labeling; 2) 2% (v/v) BzCl in acetonitrile; 3) internal standards diluted in dimethyl sulfoxide (DMSO) with 1% (v/v) formic acid, 4) d4-ACh in water to provide an internal standard for this neurotransmitter that does not react with BzCl. Tetraborate buffer

was originally selected because it forms a reversible complex with catechol groups to prevent oxidation under high pH conditions.[9,32] Our present work first focused on modifying reaction conditions to improve sensitivity and reduce the number of steps. These initial studies used 17 neurochemicals as test analytes (Figure 3-1, Table 3-1)

We found that sodium carbonate instead of borate buffer significantly improved sensitivity (i.e. slope of the calibration curve; Figure 3-1) for compounds containing a 1,2 diol

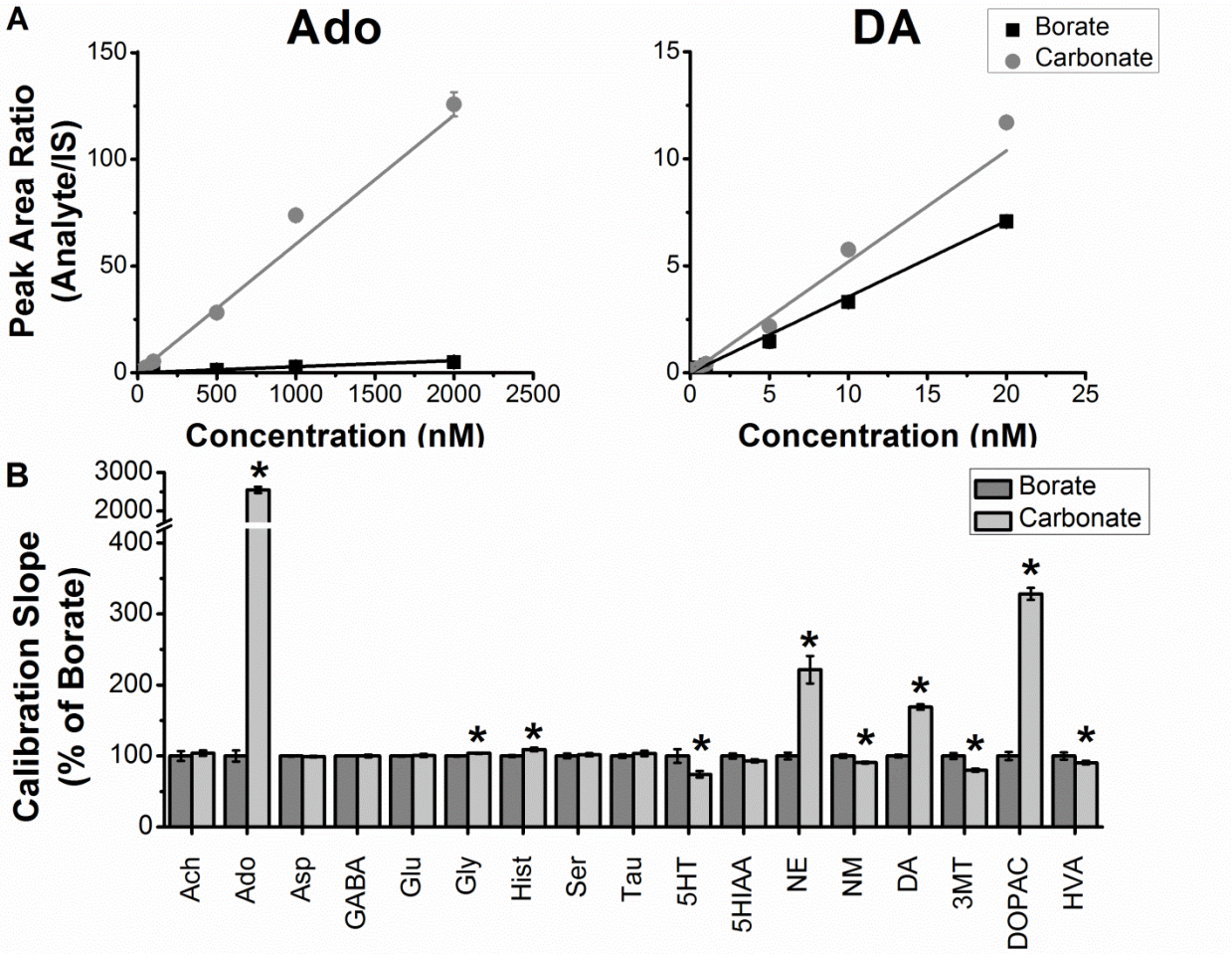

Figure 3-1: Normalized effect of sodium borate versus sodium carbonate buffer on calibration slope for select analytes. Standards made using sodium borate buffer and sodium carbonate buffer were analyzed with LC-MS in triplicate. A 6-point calibration curve for all analytes of interest was made to determine the average calibration slope for each analyte (n = 3 for each concentration tested). For the calibrations, the high concentrations were 20 nM for ACh, 5HT, NE, NM, DA and 3MT; 200 nM for Hist, GABA, 5HIAA, HVA, and DOPAC; and 2 µM for Tau, Ser, Asp, Ado, Gly, and Glu; followed by serial dilution. Analyte to internal standard ratios were plotted against known concentrations and a linear trend line was applied to determine slope (A). Sodium carbonate slopes were normalized to sodium borate slopes. Significant improvements to Ado, Gly, Hist, NE, DA, and DOPAC occurred when using 100 mM sodium carbonate as the buffer. Slopes were decreased for 5HT, NM, 3MT, and HVA. Unpaired two-tailed Students *t* test statistics were performed (B). Data expressed as percent borate ± SD. *$p < 0.05$, n = 3.

group, such as dopamine, norepinephrine, and DOPAC (Figure 3-2). Use of 100 mM carbonate buffer instead of 100 mM borate increased the slope of norepinephrine 221% ($t(4) = 19.6$, $p < 0.0001$), dopamine 170% ($t(4) = 27.7$, $p < 0.0001$), and DOPAC 330% ($t(4) = 39.5$, $p < 0.0001$). The slope was increased 2550% for adenosine ($t(4) = 52.0$, $p < 0.0001$), which is also a diol. The slope increased slightly for two compounds without diols: glycine 103% ($t(4) = 5.6$, $p < 0.01$) and histamine 110% ($t(4) = 5.4$, $p < 0.01$). Although these compounds improved, the calibration slope was reduced 25% for serotonin ($t(4) = 4.2$, $p < 0.05$), 10% for normetanephrine ($t(4) = 5.3$, $p < 0.01$), 20% for 3MT ($t(4) = 7.7$, $p < 0.01$), and 10% for HVA ($t(4) = 2.9$, $p < 0.05$). These small decreases in slope are a reasonable trade-off for the large gains for the diols.

Improved catechol detection sensitivity may relate to how the buffers interact with 1,2 diol groups. Both borate and carbonate can be used as protecting groups for 1,2 diols; however, cyclic borates are deprotected using dilute acid, while cyclic carbonates hydrolyze in water.[33–35] The protection of the carbonate group is more readily reversed than borate due to the high aqueous content of the sample, allowing for greater access of the diols for BzCl. The reason for the decreases in sensitivity of some compounds is unclear, but several of the compounds with decreased slopes have an ortho configuration of an alcohol and methoxy group (Figure 3-2a). A potential problem with the BzCl assay is that organic solvent in the injected sample could cause poor peak shape for the most polar analytes, particularly acetylcholine (Figure 3-3) However, some organic solvent is needed to maintain solubility of the hydrophobic internal standards that are added to the sample. Replacing DMSO in the internal standard mixture with 20% (v/v) acetonitrile improved peak shape and signal intensity for acetylcholine, while retaining sufficient organic content to maintain solubility of hydrophobic compounds. The peak area for acetylcholine standards treated with internal standards in 20% (v/v) acetonitrile increased 5-fold

relative to samples treated with internal standards in DMSO. This change in solvent reduces the final organic content of the samples, so band broadening is reduced for polar metabolites such as acetylcholine, as the sample composition is more closely matched in elution strength to the initial gradient conditions.

Analyte	Retention Time (min)	Concentration (nM)	Formic Acid Peak Area	Sulfuric Acid Peak Area	Increase with Sulfuric (%)
ACh	1.2	50	9409	8219	87
Tau	2.3	2000	17373	17723	102
Hist	2.3	200	78624	81494	104
Ser	2.6	5000	19108	20770	109
Asp	2.8	200	1118	1324	118
Gly	2.9	5000	4163	4695	113
Glu	3.1	2000	19442	23809	122
GABA	3.7	200	23076	30285	131
Ado	4.6	200	8894	12443	140
5HIAA	5.2	500	12758	16814	132
HVA	5.3	500	54869	69455	127
NM	5.5	20	13240	31391	237
DOPAC	5.9	500	158474	261578	165
5HT	5.9	20	2221	10703	482
NE	6.0	20	5974	28457	476
3MT	6.0	20	16229	71462	440
DA	6.4	20	21510	100588	468

Table 3-1: Improvements in sensitivity using sulfuric acid compared to formic acid additive to reagent mixture. Standards were derivatized with sodium carbonate (100 mM), BzCl (2% (v/v) in acetonitrile), and an internal mixture that contained 20% (v/v) acetonitrile with 1% (v/v) formic acid or sulfuric acid.

Substituting 1% (v/v) sulfuric acid for 1% (v/v) formic acid in the internal standard mixture improved signals of late eluting compounds by 237% for normetanephrine, 165% for DOPAC, 481% for serotonin, 476% for norepinephrine, 440% for 3MT, and 468% for dopamine (Table 3-1). While the explanation for this increased signal is unclear, we hypothesize that it is due to the decreased formation of formate adducts late in the gradient. The production of undetectable formate adducts limits the production of detectable proton adducts. Formic acid is

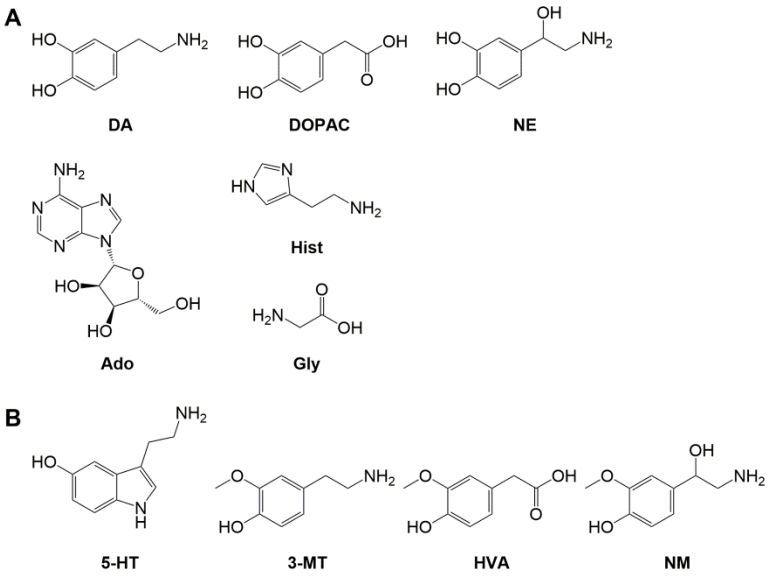

Figure 3-2: Chemical structures of neurochemicals enhanced by sodium carbonate buffer (A). Structures of neurochemical reduced with carbonate buffer (B).

used in our mobile phase A, so early eluting compounds may still form formate adducts; whereas later eluting compounds have less likelihood of formate adducts due to the lack of formic acid in sample and mobile phase B.

To reduce the number of reagent addition steps and the dilution associated with derivatization, we added the d4-acetylcholine internal standard to the ^{13}C-labeled internal standards and introduced all internal standards in one step. This modification had no effect on d4-acetylcholine or the ^{13}C-labeled compounds.

Addition of new compounds

To illustrate the potential for more comprehensive measurement of neurochemical pathways with this assay, 53 compounds were added to the original 17 compound assay. The selected 70 compounds include 19 proteinogenic amino acids and intermediates in the metabolism of phenylalanine, tyrosine,

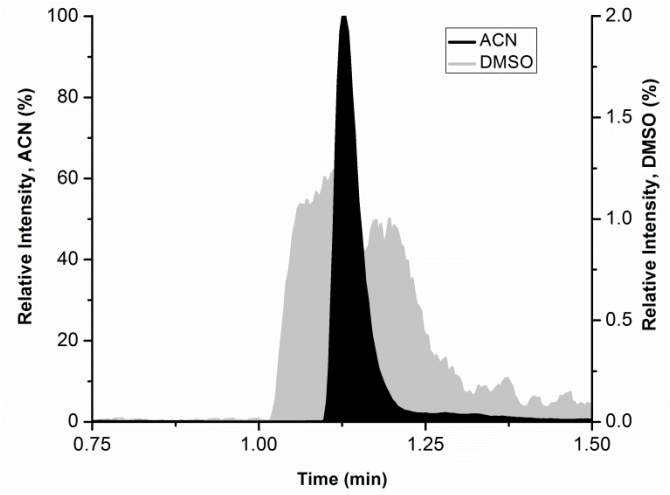

Figure 3-3: Replacement of DMSO with acetonitrile as solvent for internal standards improves the peak shape and area for early eluting metabolite ACh. Standards were derivatized with 2% BzCl (v/v in acetonitrile), 100 mM sodium carbonate, and an internal standard mixture diluted in either DMSO or 20% (v/v) acetonitrile. ACh ion chromatograms were extracted and normalized to the ACh peak in acetonitrile and overlaid.

tryptophan, and arginine. Phenylalanine and tyrosine are precursors to the catecholamines and several trace amines, so many metabolites in this pathway were added. These include several norepinephrine metabolites (e.g. VMA and MOPEG), as well as tyrosine derivatives such as tyramine and octopamine. Trace amines (tyramine, octopamine, tryptamine, and phenethylamine) play prominent roles in many invertebrate species,[36–40] and are present as metabolic by-products in the mammalian central nervous system, where they may neuromodulate biogenic amine signaling.[40,41] Serotonin is derived from tryptophan, so several intermediates in tryptophan metabolism were included (Figure 3-4). These include 5HTP, the direct precursor to serotonin, as well as serotonin metabolite N-acetylserotonin, which is particularly relevant in flies.[42,43] Monoamine oxidase (MAO) activity is limited in flies, so metabolites produced via MAO (e.g., 5HIAA) are not typically observed. Instead, monoamines are preferentially metabolized by N-acetylation, producing compounds such as N-acetylserotonin.[42–44] Tryptophan is also the precursor to kynurenine and its metabolites, which may have both neuroprotective and neurotoxic properties.[45]

Several intermediates in arginine metabolism were also included in the method. Arginine is involved in the urea cycle and nitric oxide production. Ornithine, another member of the urea cycle, serves as a precursor for many polyamines, ubiquitous small molecules with a broad array of functions,[46] whose dysfunction are associated with neurodegenerative disease.[47,48] Thiol-containing dipeptide glutathione, and histidine-containing dipeptides, carnosine and metabolite anserine, have antioxidative effects in the brain,[49–51] and decreased glutathione activity is associated with oxidative stress. Postmortem prefrontal-cortex tissue from human patients with psychiatric conditions such as bipolar, depression, and schizophrenia, show decreased levels of glutathione.[51] Carnosine may be neuroprotective by inhibiting the formation of β-amyloid

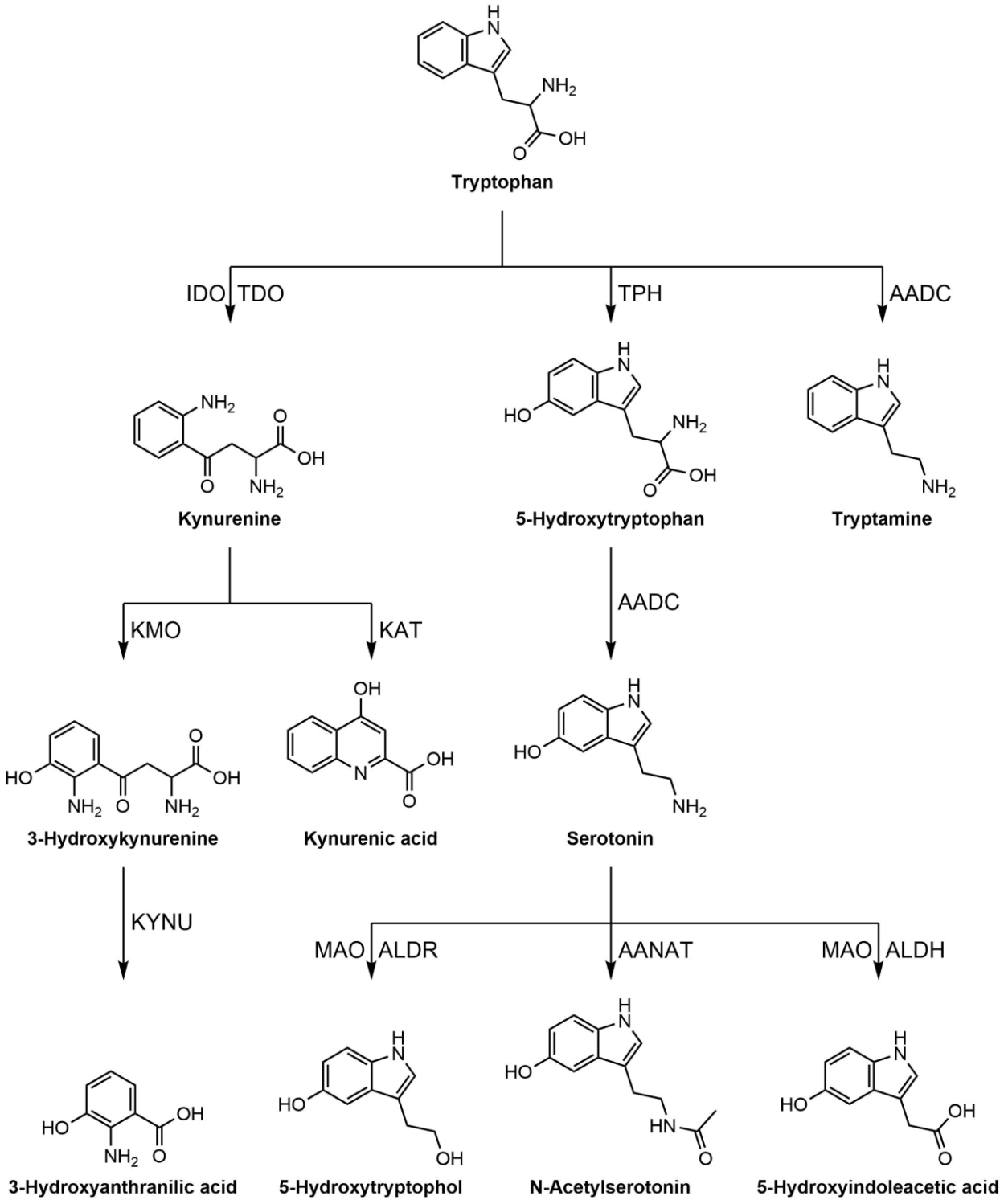

Figure 3-4: Tryptophan Metabolic Pathway. Abbreviations: aromatic amino acid decarboxylase (AADC), aralkylamine N-acetyltransferase (AANAT), aldehyde dehydrogenase (ALDH), aldehyde reductase (ALDR), indoleamine 2,3-dioxygenase (IDO), kynurenine aminotransferase (KAT), kynurenine 3-monooxygenase (KMO), kynureninase (KYNU), monoamine oxidase (MAO), tryptophan 2,3-dioxygenase (TDO), and tryptophan hydroxylase (TPH).

polymerization and α-synuclein oligomerization, toxic species in Alzheimer's and Parkinson's diseases.[50] Glucose indicates neuronal energy expenditure, and alterations of normal glucose metabolism can lead to synaptic dysfunction, including glucose hypometabolism in Alzheimer's disease and Parkinsonian patients with dementia.[52–55]

All 70 analytes of interest and their internal standards are benzoylated, except acetylcholine and choline, and detected by MS/MS (Table 3-2 and Table 3-3). Analytes were labeled 1-4 times with BzCl depending on the functional groups. In all cases, only the fully labeled compounds were observed, indicating quantitative (i.e., complete labeling) reactions. As an example, dopamine is triply labeled; singly and doubly labeled dopamine were not detectable. Protonated benzoylation products (MW + 1) were observed for most compounds with ESI in positive mode. A protonated water loss was observed for octopamine, normetanephrine, and synephrine (MW – 18 + 1), and the ammonium adduct (MW + 18) was detected for VMA, MOPEG, 5HIAA, HVA. DOMA, DOPEG, and DOPAC. A sodium adduct was observed for glucose (MW + 23). Other hexoses (e.g. fructose, mannose, and galactose) were resolved chromatographically or by MRM. For acetylcholine and choline, the unlabeled molecular ions were used for detection.

Analytes were detected by MS/MS under collision activated dissociation (CAD) conditions. The fragmentation of each analyte was examined to determine the best product ion to use for quantification (Table 3-2 and Table 3-3). For benzoylated analytes, the benzoyl fragment of 105 m/z was usually the most abundant product ion, and used for dMRM. Unique fragments for acetylcholine, choline, histidine, carnosine, phenylalanine, kynurenine, adenosine, tryptamine, 5HIAA, tryptophan, 5HTOL, spermidine, ornithine, kyotorphin, agmatine, N-acetylputrescine, VMA, glucose, lysine, 3HAA, 3HK, N-acetylserotonin, serotonin, 5HTP, and

Analyte	Precursor (*m/z*)	Product (*m/z*)	Fragmentor (V)	Collision Energy (V)	Retention Time (min)
ACh	146	87	120	15	1.30
Ch	104	60	120	20	1.30
Bz-CA	274	105	120	10	2.31
Bz-His	260	110	130	20	2.33
Bz-Ans	345	105	130	30	2.40
Bz-Carn	331	110	135	20	2.40
Bz-HTau	214	105	120	20	2.48
Bz-Tau	230	105	120	10	2.49
Bz-Arg	279	105	135	30	2.58
Bz-Hist	216	105	120	20	2.61
Bz-Asn	237	105	120	20	2.62
Bz-Ser	210	105	120	20	2.71
Bz-Gln	251	105	120	20	2.72
Bz-HSer	224	105	120	20	2.88
Bz-Cit	280	105	120	20	2.91
Bz-ETA	166	105	120	20	2.93
Bz-Asp	238	105	120	10	2.98
Bz-Agm	235	176	110	30	3.02
Bz-Glc	307	185	130	20	3.10
Bz-Gly	180	105	120	10	3.10
Bz-Glu	252	105	120	20	3.28
Bz-BAla	194	105	120	20	3.53
Bz-Ala	194	105	120	20	3.78
Bz-NAP	235	176	135	20	3.85
Bz-GABA	208	105	120	10	3.99
Bz-Pro	220	105	120	20	4.60
Bz-Ado	372	136	120	30	6.28
Bz-Val	222	105	120	30	6.63
Bz-Met	254	105	120	15	6.73
Bz-Orn	341	174	120	15	7.50
Bz-GSH	516	105	120	15	8.28
Bz-Lys	355	188	120	20	8.35
Bz-Put	297	105	120	30	8.79
Bz-Leu	236	105	120	30	9.30
Bz-Phe	270	120	120	10	9.67
Bz-Thr	224	105	140	20	9.67
Bz-VMA	320	181	120	10	9.77
Bz-Trp	309	159	120	10	9.96

Analyte	Precursor (*m/z*)	Product (*m/z*)	Fragmentor (V)	Collision Energy (V)	Retention Time (min)
Bz-MOPEG	306	105	120	20	10.08
Bz-Kyo	546	175	110	30	11.35
Bz-Cys	330	105	120	20	11.64
Bz-KA	294	105	120	30	11.78
Bz-Spd	458	162	120	30	12.00
Bz-PhEt	226	105	120	15	12.23
Bz-TrpA	265	144	130	30	12.38
Bz-NAS	323	264	120	15	12.39
Bz-5HIAA	313	146	120	15	12.60
Bz-5HTOL	282	160	130	20	12.73
Bz-HCY	344	105	120	20	13.00
Bz-3HAA	362	240	120	10	13.07
Bz-HCA	288	105	120	10	13.13
Bz-HVA	304	105	120	15	13.13
Bz-DOMA	410	105	130	20	13.35
Bz-Kyn	417	122	120	10	13.35
Bz-Spm	619.6	497	135	25	13.52
Bz-DOPEG	396	105	120	20	13.59
Bz-5HTP	429	279	120	15	13.82
Bz-OA	344	105	140	20	13.84
Bz-NM	374	105	140	15	13.88
Bz-Tyr	390	105	120	30	14.12
Bz-3HK	537	240	135	25	14.40
Bz-Syn	358	105	140	20	14.43
Bz-5HT	385	264	140	20	15.46
Bz-DOPAC	394	105	140	20	15.49
Bz-3MT	376	105	120	20	15.67
Bz-LDOPA	510	105	120	25	15.67
Bz-TyrA	346	105	135	25	15.73
Bz-NE	482	105	140	30	15.77
Bz-E	496	105	120	15	15.96
Bz-DA	466	105	140	20	16.40

Table 3-2: MRM conditions of 70 targeted metabolites.

spermine were identified. These correspond to immonium ions for histidine, phenylalanine, and tryptophan, y ions for kyotorphin and carnosine, and the adenine moiety for adenosine. Several

fragmentation patterns are shown in Figure 3-5. When possible, unique fragments were chosen for quantification to increase the selectivity of the assay for these compounds, reducing the likelihood of interferences from unknowns with similar precursor masses. The unique fragments have comparable or increased sensitivity relative to the 105 fragments for those compounds.

Analyte	Precursor (m/z)	Product (m/z)	Fragmentor (V)	Collision Energy (V)	Retention Time (min)
d_4-Ach	150	91	120	15	1.30
d_4-Ch	108	60	120	20	1.30
$^{13}C_6$Bz-CA	280	111	120	10	2.31
$^{13}C_6$Bz-His	266	110	130	20	2.33
$^{13}C_6$Bz-Ans	351	111	130	30	2.40
$^{13}C_6$Bz-Carn	337	110	135	20	2.40
$^{13}C_6$Bz-HTau	220	111	120	20	2.48
$^{13}C_6$Bz-Tau	236	111	120	10	2.49
$^{13}C_6$Bz-Arg	285	111	135	30	2.58
$^{13}C_6$Bz-Hist	222	111	120	20	2.61
$^{13}C_6$Bz-Asn	243	111	120	20	2.62
$^{13}C_6$Bz-Ser	216	111	120	20	2.71
$^{13}C_6$Bz-Gln	257	111	120	20	2.72
$^{13}C_6$Bz-HSer	230	111	120	20	2.88
$^{13}C_6$Bz-Cit	286	111	120	20	2.91
$^{13}C_6$Bz-ETA	172	111	120	20	2.93
$^{13}C_6$Bz-Asp	244	111	120	10	2.98
$^{13}C_6$Bz-Agm	241	182	110	30	3.02
$^{13}C_6$Bz-Glc	313	185	130	20	3.10
$^{13}C_6$Bz-Gly	186	111	120	10	3.10
$^{13}C_6$Bz-Glu	258	111	120	20	3.28
$^{13}C_6$Bz-BAla	200	111	120	20	3.53
$^{13}C_6$Bz-Ala	200	111	120	20	3.78
$^{13}C_6$Bz-NAP	241	182	135	20	3.85
$^{13}C_6$Bz-GABA	214	111	120	10	3.99
$^{13}C_6$Bz-Pro	226	111	120	20	4.60
$^{13}C_6$Bz-Ado	378	136	120	30	6.28
$^{13}C_6$Bz-Val	228	111	120	30	6.63
$^{13}C_6$Bz-Met	260	111	120	15	6.73
$^{13}C_6$Bz-Orn	353	180	120	15	7.50
$^{13}C_6$Bz-GSH	528	111	120	15	8.28
$^{13}C_6$Bz-Lys	367	194	120	20	8.35
$^{13}C_6$Bz-Put	309	111	120	30	8.79
$^{13}C_6$Bz-Leu	242	111	120	30	9.30
$^{13}C_6$Bz-Phe	276	120	120	10	9.67

Analyte	Precursor (m/z)	Product (m/z)	Fragmentor (V)	Collision Energy (V)	Retention Time (min)
$^{13}C_6$Bz-Thr	230	111	140	20	9.67
$^{13}C_6$Bz-VMA	326	181	120	10	9.77
$^{13}C_6$Bz-Trp	315	159	120	10	9.96
$^{13}C_6$Bz-MOPEG	312	111	120	20	10.08
$^{13}C_6$Bz-Kyo	558	175	110	30	11.35
$^{13}C_6$Bz-Cys	342	111	120	20	11.64
$^{13}C_6$Bz-KA	300	111	120	30	11.78
$^{13}C_6$Bz-Spd	476	168	120	30	12.00
$^{13}C_6$Bz-PhEt	232	111	120	15	12.23
$^{13}C_6$Bz-TrpA	271	144	130	30	12.38
$^{13}C_6$Bz-NAS	329	270	120	15	12.39
$^{13}C_6$Bz-5HIAA	319	146	120	15	12.60
$^{13}C_6$Bz-5HTOL	288	160	130	20	12.73
$^{13}C_6$Bz-HCY	356	111	120	20	13.00
$^{13}C_6$Bz-3HAA	374	246	120	10	13.07
$^{13}C_6$Bz-HCA	294	111	120	10	13.13
$^{13}C_6$Bz-HVA	310	111	120	15	13.13
$^{13}C_6$Bz-DOMA	422	111	130	20	13.35
$^{13}C_6$Bz-Kyn	429	128	120	10	13.35
$^{13}C_6$Bz-Spm	643.6	515.6	135	25	13.52
$^{13}C_6$Bz-DOPEG	408	111	120	20	13.59
$^{13}C_6$Bz-5HTP	441	285	120	15	13.82
$^{13}C_6$Bz-OA	356	111	140	20	13.84
$^{13}C_6$Bz-NM	386	111	140	15	13.88
$^{13}C_6$Bz-Tyr	402	111	120	30	14.12
$^{13}C_6$Bz-3HK	555	246	135	25	14.40
$^{13}C_6$Bz-Syn	370	111	140	20	14.43
$^{13}C_6$Bz-5HT	397	270	140	20	15.46
$^{13}C_6$Bz-DOPAC	406	111	140	20	15.49
$^{13}C_6$Bz-3MT	388	111	120	20	15.67
$^{13}C_6$Bz-LDOPA	528	111	120	25	15.67
$^{13}C_6$Bz-TyrA	358	111	135	25	15.73
$^{13}C_6$Bz-NE	500	111	140	30	15.77
$^{13}C_6$Bz-E	514	111	120	15	15.96
$^{13}C_6$Bz-DA	484	111	140	20	16.40

Table 3-3: Transitions for $^{13}C_6$-BzCl labeled internal standards.

After determining the MS/MS transitions, a gradient was developed to separate the analytes (Figure 3-6). The gradient was not designed to fully resolve all analytes but to spread

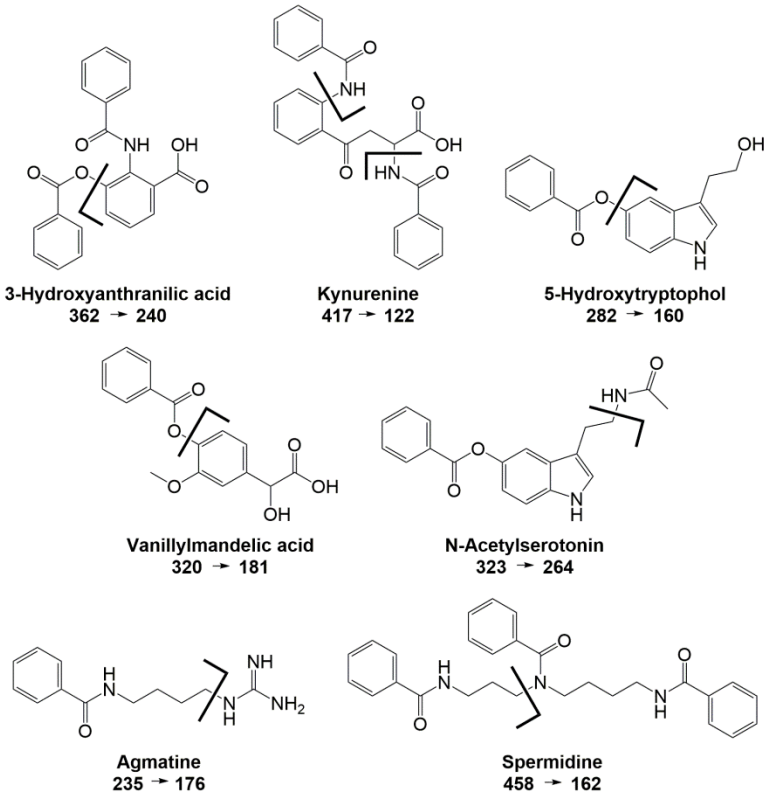

Figure 3-5: Fragmentation patterns for select benzoyl labeled compounds. Analytes were detected by MS/MS under collision activated dissociation (CAD) conditions. While the benzoyl fragment of 105 m/z was the most abundant product ion for most analytes detected, unique fragments were chosen for detection to increase the selectivity of the assay for these compounds.

the analytes out over the 20 min separation time and minimize the number of dMRMs at any given time. The gradient results show that even very polar compounds like dopamine can be well retained after benzoylation. Total analysis time for each sample is around 33 min including injection time, elution and column re-equilibration on the Waters nanoAcquity system. Higher throughput may be possible. In preliminary tests, the method was transferred to a higher flow rate HPLC with higher pressure limits and the separation time was reduced to 12 min, with a total analysis time around 14 min. Further reductions in the analysis time per sample can be achieved as LC pressure limits and MS scan rates continue to increase.

The method yields good detection limits, linearity, reproducibility and low carryover for all detected compounds (Table 3-4). All detection limits were better than 10 nM except for glutathione, alanine, citrulline, glycine, serine, and glucose.[56] While limits of detection (LOD) for these select compounds were higher than other reported compounds in the assay, these levels were below the observed concentrations in dialysate and CSF.

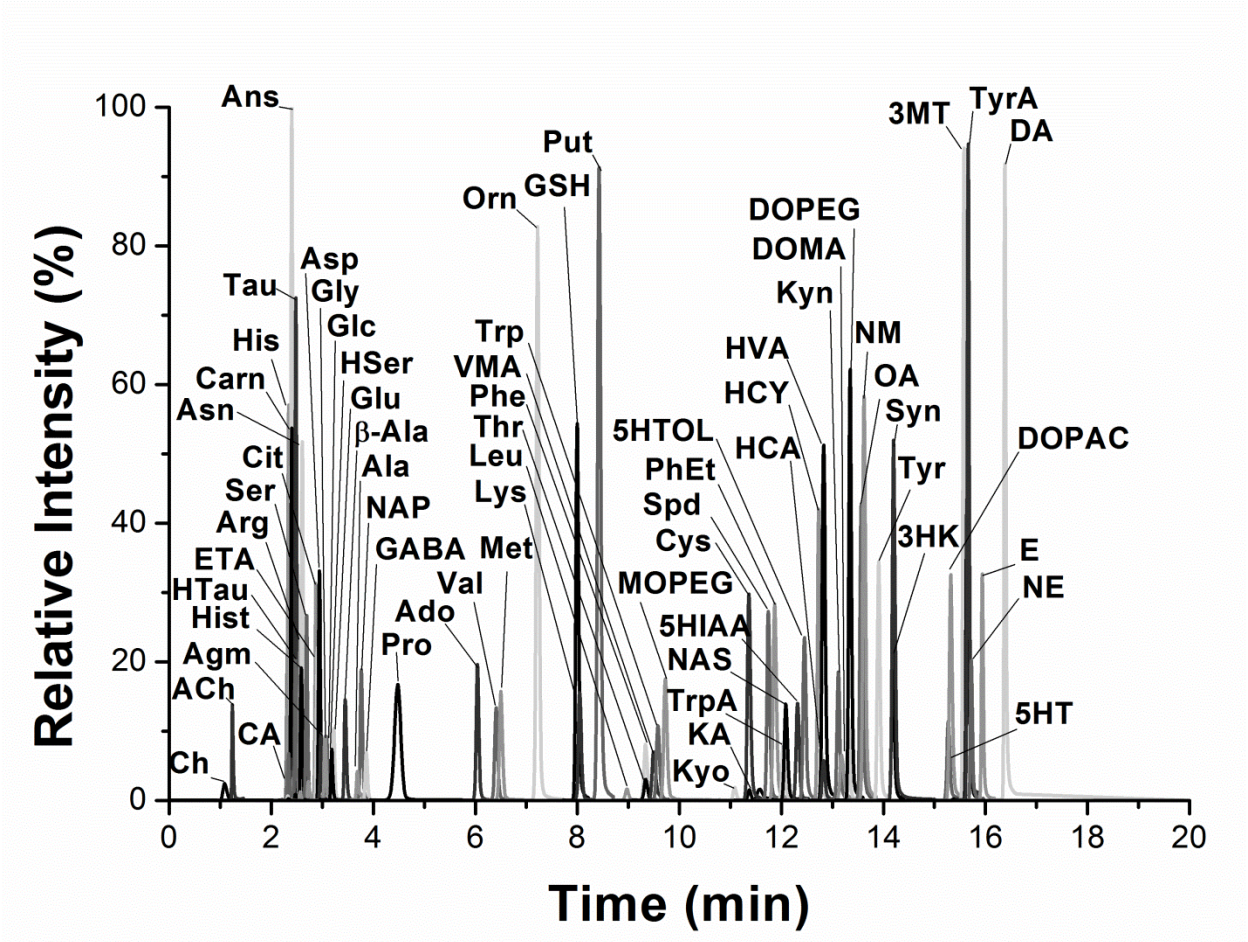

Figure 3-6: Reconstructed ion chromatogram of 70 compounds detected in 20 min. Extracted ion chromatograms for each compound at the highest concentration calibration standard run, were normalized to highest intensity and overlaid.

Application of 70 compound assay in various matrices

To test the versatility of the assay, we analyzed several types of biological samples, including rat striatal dialysate, human CSF, human serum, and *Drosophila* tissue homogenate (Table 3-5, Table 3-6, Table 3-7). 57 compounds were detected in dialysate samples, whereas 35 and 50 compounds were above the limits of detection in human CSF and serum samples, respectively. *Drosophila* heads and bodies were isolated and analyzed separately, with detection of 44 compounds in head and 42 compounds in bodies. 54 compounds were detected in hemolymph from *Drosophila*.

Analyte	LoD (nM)	Carryover (%)	RSD (%)	Fit (R^2)	Analyte	LoD (nM)	Carryover (%)	RSD (%)	Fit (R^2)
ACh	1	1	0.7	0.9996	Thr	5	0.3	1	0.9995
Ch	3	0.2	1	0.9997	VMA	1	0.1	1	0.9999
CA	4	0.02	2	1.0000	Trp	1	0.1	0.9	0.9997
His	2	0.1	2	0.9996	MOPEG	0.7	0.08	0.6	0.9999
Ans	0.4	0.03	2	0.9999	Kyo	0.2	0.2	2	0.9998
Carn	0.8	0.04	2	0.9999	Cys	1	0.1	5	0.9971
HTau	7	0.05	4	0.9977	KA	1	0.1	0.9	0.9997
Tau	3	0.02	1	0.9998	Spd	0.09	0.1	0.5	0.9994
Arg	1	0.5	3	0.9576	PhEt	0.08	0.09	2	0.9989
Hist	0.09	0.04	3	0.9996	TrpA	0.1	0.09	3	0.9993
Asn	2	0.1	2	0.9999	NAS	0.09	0.06	0.8	0.9997
Ser	70	0.6	1	0.9976	5HIAA	0.7	0.08	0.8	0.9999
Gln	4	0.2	3	0.9998	5HTOL	0.9	0.07	1	0.9997
HSer	11	0.5	3	0.9994	HCY	0.9	0.08	1	0.9968
Cit	20	2	2	0.9965	3HAA	1	0.1	0.9	0.9996
ETA	6	0.4	2	0.9997	HCA	1	0.09	2	0.9998
Asp	8	0.05	1	0.9999	HVA	0.6	0.07	0.4	1.0000
Agm	1	0.03	4	0.9997	DOMA	0.3	0.2	3	0.9998
Glc	160	0.06	6	0.9997	Kyn	1	0.1	3	0.9994
Gly	30	0.09	7	0.9997	Spm	0.1	0.1	2	0.9984
Glu	0.3	0.2	1	1.0000	DOPEG	0.1	0.1	1	0.9992
BAla	5	0.09	1	1.0000	5HTP	2	0.2	3	0.9996
Ala	20	2	2	0.9994	OA	0.2	0.2	1	0.9983
NAP	0.5	0.05	1	0.9999	NM	0.08	0.09	2	0.9988
GABA	0.5	0.4	2	0.9997	Tyr	4	2	3	0.9950
Pro	5	0.5	0.4	0.9996	3HK	8	0.06	2	0.9941
Ado	1	0.1	0.2	0.9956	Syn	0.2	0.2	0.1	0.9982
Val	7	0.6	3	0.9998	5HT	0.4	0.4	1	0.9970
Met	0.7	0.09	1	0.9998	DOPAC	0.2	0.2	2	0.9999
Orn	7	0.4	0.2	0.9963	3MT	0.2	0.2	2	0.9987
GSH	10	0.1	2	0.9999	LDOPA	1	0.9	2	0.9999
Lys	4	2	0.7	0.9867	TyrA	0.2	0.3	1	0.9964
Put	0.1	0.1	1	0.9999	NE	0.3	0.2	2	0.9970
Leu	5	4	2	0.9894	E	0.3	0.2	1	0.9964
Phe	3	0.2	0.8	0.9999	DA	0.3	0.3	3	0.9965

Table 3-4: Summary of limits of detection (LOD), carryover, relative standard deviation (n = 3), and R^2 value of a six-point calibration for aqueous standards.

All commonly studied neurotransmitters (i.e. GABA, glutamate, and monoamines) were within expected ranges in rat striatal dialysate (Table 3-5). Several detectable compounds were

not previously reported in rat dialysate or tissue homogenate studies, and include homoserine, a precursor to amino acids threonine and methionine; N-acetylputrescine, a metabolite of polyamine putrescine; and DOMA, a norepinephrine metabolite. Polyamines putrescine, spermidine, and spermine were also detected in the dialysate sample. The norepinephrine and normetanephrine metabolites MOPEG, DOPEG, and DOMA (but not epinephrine or VMA) were detected in rat dialysate, demonstrating the potential for analysis of metabolic pathways.

Analysis of human serum, derivatized after protein precipitation, revealed kyotorphin at 31 nM concentration. Kyotorphin is an endogenous analgesic dipeptide with potential neuroprotective properties. It has previously been found in rat brain tissue and human CSF samples.[57,58] This is the first report of quantitative detection of kyotorphin in human serum. Kyotorphin is proposed to have indirect opioid-like actions by modulating enkephalin release.[59] Kyotorphin does not cross the blood brain barrier, and is a candidate biomarker for neurodegenerative diseases such as Alzheimer's disease.[57] While previous studies detected kyotorphin in CSF samples obtained from lumbar puncture, less invasive blood sample collection would be beneficial for patients, with subsequent detection as reported here. Interestingly, kyotorphin was not detected in our analysis of pooled human CSF from healthy patients, which did not undergo a protein precipitation step prior to analysis.

Fly tissue homogenate contained detectable levels of tyramine and octopamine, which was expected as they are the fly analogs of epinephrine and norepinephrine, respectively. 5HTP pretreatment of the flies resulted in high levels of 5HTP in both bodies and heads. 5HTP metabolites serotonin and N-acetylserotonin were also elevated, though the effect was more pronounced in the bodies. Interestingly, 5HIAA was observed in both bodies and heads, despite the expected lack of MAO activity in flies, likely due to the excess of 5HTP.[44]

Analyte	Concentration (nM)						Analyte	Concentration (nM)					
	Rat Dialysate			Human CSF				Rat Dialysate			Human CSF		
ACh	12.2	±	0.1	1.19	±	0.04	Thr	691	±	7	65	±	2
Ch	1212	±	5	14	±	2	VMA						
CA	2170	±	90	300	±	30	Trp	141	±	4	20.9	±	0.2
His	930	±	10	91.4	±	0.8	MOPEG	4.3	±	0.3			
Ans							Kyo						
Carn	14.0	±	0.4				Cys	503	±	9			
HTau							KA						
Tau	1820	±	70	33	±	2	Spd	2.38	±	0.08	0.19	±	0.02
Arg	1380	±	70	211	±	6	PhEt	0.53	±	0.02			
Hist	0.76	±	0.08	0.20	±	0.03	TrpA						
Asn	40	±	1	6.6	±	0.3	NAS	0.23	±	0.02			
Ser	4100	±	250	570	±	40	5HIAA	390	±	6	2.4	±	0.2
Gln	37300	±	1300	4080	±	60	5HTOL	1.9	±	0.1			
HSer	2920	±	20	266	±	7	HCY	4.91	±	0.03			
Cit	390	±	10				3HAA						
ETA	6980	±	310	124	±	4	HCA	1050	±	30	4.7	±	0.3
Asp	108	±	7	15	±	2	HVA	1130	±	40	4.4	±	0.4
Agm							DOMA	0.47	±	0.02			
Glc	633000	±	85000	55400	±	840	Kyn	7.1	±	0.3			
Gly	690	±	10	52	±	5	Spm	2.9	±	0.1			
Glu	21	±	1	4.9	±	0.1	DOPEG	1.26	±	0.03			
BAla	5.8	±	0.9				5HTP						
Ala	5260	±	160	306	±	8	OA						
NAP	1.0	±	0.1	0.74	±	0.02	NM	0.30	±	0.01			
GABA	40.5	±	0.6	3.3	±	0.2	Tyr	350	±	20	76.6	±	0.3
Pro	1326	±	8	13.8	±	0.2	3HK						
Ado	112.8	±	0.6				Syn						
Val	1760	±	20	104	±	2	5HT	0.89	±	0.02			
Met	855	±	6	26.2	±	0.5	DOPAC	598	±	5	0.6	±	0.1
Orn	196	±	3	54.9	±	0.8	3MT	8.5	±	0.2			
GSH	74	±	2				LDOPA	4.00	±	0.04			
Lys	4030	±	170	249	±	7	TyrA	0.21	±	0.02			
Put	0.83	±	0.03	0.41	±	0.03	NE	1.00	±	0.08			
Leu	2200	±	140	102	±	4	E						
Phe	710	±	5	66.9	±	0.8	DA	29.4	±	0.8			

Table 3-5: Application of 70 compound method to analyze rat dialysate and human CSF. The average of 3 repeated injections with standard deviation is reported below. Values for analytes were reported only if they were above the limit of detection.

Analyte	LoD (nM)	Concentration (nM) Human Serum	Analyte	LoD (nM)	Concentration (nM) Human Serum
ACh	4	380 ± 10	Thr	30	62000 ± 5000
Ch	50	15200 ± 200	VMA	20	
CA	50		Trp	30	51000 ± 3000
His	30	37000 ± 1000	MOPEG	5	20 ± 5
Ans	3	160 ± 20	Kyo	5	31 ± 3
Carn	6	14 ± 3	Cys	30	1600 ± 100
HTau	500	160000 ± 10000	KA	40	220 ± 30
Tau	60	115000 ± 2000	Spd	2	41 ± 0.6
Arg	10	7100 ± 300	PhEt	1	
Hist	2	41 ± 2	TrpA	2	
Asn	70	20900 ± 800	NAS	2	5 ± 4
Ser	700	45000 ± 4000	5HIAA	5	67 ± 4
Gln	10	180000 ± 10000	5HTOL	10	16 ± 2
HSer	100	65000 ± 2000	HCY	30	
Cit	20	9400 ± 200	3HAA	20	76 ± 6
ETA	10	6300 ± 100	HCA	10	56 ± 7
Asp	200	2300 ± 200	HVA	20	57 ± 1
Agm	20		DOMA	6	
Glc	500	1050000 ± 90000	Kyn	40	2380 ± 50
Gly	200	102000 ± 4000	Spm	2	39 ± 3
Glu	30	21800 ± 700	DOPEG	2	
BAla	20	2300 ± 400	5HTP	30	
Ala	70	254000 ± 8000	OA	2	
NAP	7	24 ± 2	NM	2	
GABA	4	115 ± 4	Tyr	40	56000 ± 1000
Pro	30	24300 ± 3000	3HK	200	
Ado	3		Syn	4	
Val	40	160000 ± 10000	5HT	3	300 ± 40
Met	8	21800 ± 300	DOPAC	5	
Orn	200	27400 ± 300	3MT	4	
GSH	90		LDOPA	2	390 ± 20
Lys	40	37000 ± 1000	TyrA	8	
Put	0.4	13 ± 1	NE	3	3.2 ± 0.7
Leu	40	139000 ± 3000	E	4	
Phe	30	63000 ± 3000	DA	2	

Table 3-6: Application of 70 compound method after protein precipitation for human serum. The average of 3 repeated injections with standard deviation is reported below. Values for analytes were reported only if they were above the limit of detection (LOD).

Analyte	Amount (pmol/fly)						Analyte	Amount (pmol/fly)					
	Fly Bodies			Fly Heads				Fly Bodies			Fly Heads		
ACh	2.64	±	0.08	0.212	±	0.011	Thr	18.4	±	1.8	0.98	±	0.04
Ch	312	±	8.8	66.36	±	1.14	VMA						
CA							Trp	17.1	±	0.9	0.44	±	0.02
His	2.7	±	0.1	0.27	±	0.04	MOPEG						
Ans							Kyo						
Carn							Cys						
HTau	21	±	6				KA	1.9	±	0.1	0.4	±	0.04
Tau	278.5	±	4.1	88.81	±	3.19	Spd	0.03	±	0.002	0.01	±	0.0003
Arg	0.45	±	0.01	0.06	±	0.004	PhEt	0.336	±	0.015	0.005	±	0.0004
Hist	1.92	±	0.13	0.772	±	0.011	TrpA	1.85	±	0.09	0.024	±	0.002
Asn	6.5	±	0.7	0.74	±	0.04	NAS	29.61	±	0.7	4.24	±	0.242
Ser				0.8	±	0.4	5HIAA	0.47	±	0.07	0.025	±	0.001
Gln	54.99	±	0.59	5.61	±	0.14	5HTOL						
HSer	4.5	±	1.1	0.4	±	0.01	HCY						
Cit							3HAA						
ETA	44.03	±	0.92	5.56	±	0.27	HCA	0.07	±	0.01			
Asp							HVA						
Agm							DOMA						
Glc	3170	±	295	1111.5	±	0.2	Kyn	8	±	0.7			
Gly	8	±	1	0.8	±	0.004	Spm						
Glu	1.1	±	0.2	0.21	±	0.03	DOPEG						
BAla	83.5	±	0.7	3.04	±	0.13	5HTP	184.1	±	3.6	1.83	±	0.04
Ala	90.4	±	5.4	22.84	±	2.69	OA				0.003	±	0.0002
NAP	0.16	±	0.01	0.009	±	0.0001	NM						
GABA	6.25	±	0.18	1.661	±	0.055	Tyr	8.4	±	0.2	0.35	±	0.007
Pro	614.3	±	2.8	100.46	±	2.2	3HK	36	±	3	1.7	±	0.1
Ado	31.1	±	0.12	2.599	±	0.038	Syn						
Val	22.3	±	0.3	2.17	±	0.1	5HT	81.66	±	10.34	5.98	±	0.666
Met	16.17	±	0.58	1.186	±	0.025	DOPAC	0.09	±	0.003	0.013	±	0.001
Orn							3MT						
GSH							LDOPA	1.5	±	0.13	0.541	±	0.026
Lys	0.2	±	0.02				TyrA	11.89	±	0.64	0.062	±	0.001
Put	0.08	±	0.001	0.0074	±	0.0003	NE						
Leu	53.6	±	1.9	3.84	±	0.04	E						
Phe	18.4	±	0.3	1.02	±	0.03	DA	0.22	±	0.01	0.005	±	0.0001

Table 3-7: Application of 70 compound method with a protein precipitation step for fly bodies and heads. The average of 3 repeated injections with standard deviation is reported below. Values for analytes were reported only if they were above the limit of detection.

Of the 54 compounds detected in fly hemolymph, 10 showed significant ($p < 0.05$) changes between starved and sated states (Figure 3-7). These compounds were Ch ($t(4) = 9.7$, p

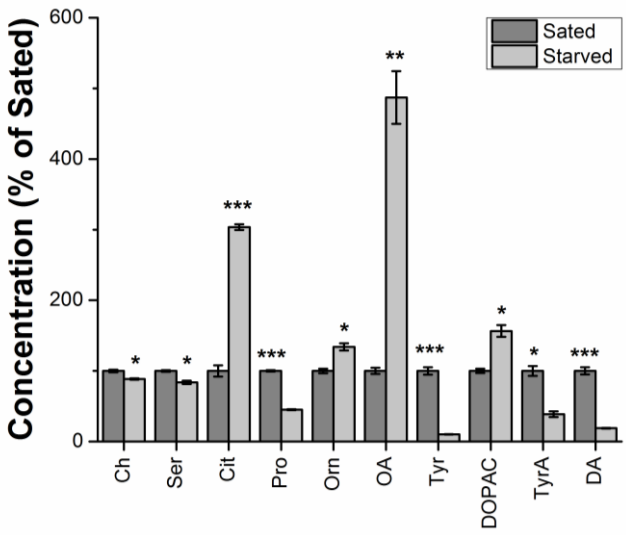

Figure 3-7: Metabolites showing significant differences between sated and starved states in fly hemolymph. Metabolite concentrations were normalized to total protein content, and then normalized to the sated sample. Each sample was run in triplicate. Unpaired two-tailed Students *t* tests were performed, and the Holm-Bonferroni correction was used. Data expressed as average ± SD. *p < 0.05; **p < 0.01; ***p < 0.001.

< 0.0001); Ser ($t(4) = 10.5$, $p < 0.0001$), Cit ($t(4) = 39.3$, $p < 0.0001$), Pro ($t(4) = 80.2$, $p < 0.0001$), Orn ($t(4) = 9.8$, $p < 0.0001$), OA ($t(4) = 17.9$, $p < 0.0001$), Tyr ($t(4) = 29.5$, $p < 0.0001$), DOPAC ($t(4) = 11.0$, $p < 0.0001$), TyrA ($t(4) = 13.1$, $p < 0.0001$), DA ($t(4) = 27.2$, $p < 0.0001$). Of particular note was a nearly 5 fold increase of octopamine in starved flies relative to sated flies. Increased octopamine activity has been reported in flies upon starvation, and has been linked to foraging-like behaviors as the flies presumably try to locate food.[60,61] The roles of other implicated metabolites are currently undergoing further investigation.

Protein removal prior to analysis of bodily fluids and tissue homogenate prevents column contamination and exposure of the HPLC-MS to high protein concentrations. Many extraction techniques are used in metabolomics.[62–64] These methods vary in effectiveness based on the sample type and target metabolites, and require optimization for each assay. Solvent precipitation with cold acetonitrile was selected for its simplicity and reproducibility. To evaluate the effect of protein precipitation on recovery and reproducibility we spiked known amounts of isotopically labeled glutamate, GABA, serotonin, and dopamine into serum prior to solvent precipitation. We then measured concentrations of the isotopically labeled compounds after solvent precipitation and derivatization, and compared these measured concentrations to the known amount spiked

into serum to determine the relative recovery (Figure 3-8). The recovery varied for each tested metabolite, but was reproducible (RSD < 8%). As such, we concluded that fair comparison could be made between samples analyzed using this method, though comparisons to other methods would require correction for recovery.

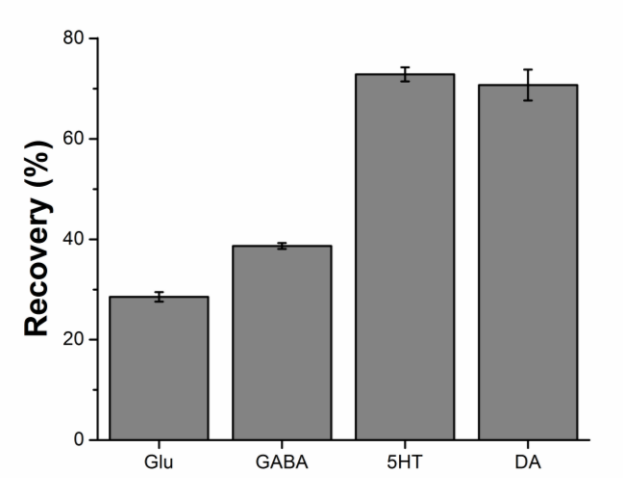

Figure 3-8: Recovery of four isotopically labeled metabolites spiked into plasma prior to solvent precipitation and derivatization. Percent recovery calculated as measured concentration after precipitation, relative to concentration spiked into serum. The average of three extraction replicates is shown. Error bars represent the standard error of the mean.

Conclusions

These results demonstrate the utility of BzCl derivatization with HPLC-MS/MS for targeted neurochemical metabolomics. Improvements to the benzoylation of small neurochemicals resulted in a comprehensive, robust, and quantitative method to monitor 70 neurochemicals. This modified method improves sensitivity for compounds containing 1,2-diols and early eluting peaks such as acetylcholine, and was expanded to 4-fold more neurochemicals compared to prior studies. The method is suitable for multiple samples types, including CSF, serum, and tissue homogenate.

The results also indicate considerable potential for even wider use of BzCl as a MS labeling reagent. For example, the Michigan Regional Comprehensive Metabolomics Resource Core maintains a library of over 1,000 metabolites. Based on the reactivity of BzCl towards amines, phenols, thiols, and some alcohols, we estimate it could be used to label approximately 25% of these compounds. BzCl labeling is fast and simple to implement. Benzoylation improves

sensitivity, retention, and quantification via easily generated internal standards with few drawbacks compared to direct detection of analytes.

References

(1) Knee, J. M.; Rzezniczak, T. Z.; Barsch, A.; Guo, K. Z.; Merritt, T. J. S. *J. Chromatogr. B Anal. Technol. Biomed. Life Sci.* **2013**, *936*, 63–73.

(2) Michopoulos, F.; Whalley, N.; Theodoridis, G.; Wilson, I. D.; Dunkley, T. P. J.; Critchlow, S. E. *J. Chromatogr. A* **2014**, *1349*, 60–68.

(3) Virgiliou, C.; Sampsonidis, I.; Gika, H. G.; Raikos, N.; Theodoridis, G. A. *Electrophoresis* **2015**, *36* (18), 2215–2225.

(4) Wei, R.; Li, G.; Seymour, A. B. *Anal. Chem.* **2010**, *82* (13), 5527–5533.

(5) Yan, Z.; Yan, R. *Anal. Chim. Acta* **2015**, *894*, 65–75.

(6) Yuan, M.; Breitkopf, S. B.; Yang, X.; Asara, J. M. *Nat. Protoc.* **2012**, *7* (5), 872–881.

(7) Dettmer, K.; Aronov, P. A.; Hammock, B. D. *Mass Spectrom. Rev.* **2007**, *26* (1), 51–78.

(8) Gummer, J.; Banazis, M.; Maker, G.; Solomon, P.; Oliver, R.; Trengove, R. *Aust. Biochem.* **2009**, *40* (3), 5–8.

(9) Song, P.; Mabrouk, O. S.; Hershey, N. D.; Kennedy, R. T. *Anal. Chem.* **2012**, *84*, 412–419.

(10) Zheng, X.; Kang, A.; Dai, C.; Liang, Y.; Xie, T.; Xie, L.; Peng, Y.; Wang, G.; Hao, H. *Anal. Chem.* **2012**, *84* (22), 10044–10051.

(11) Cox, J. M.; Butler, J. P.; Butzke, B. S.; Jones, B. A.; Buckholz, J. E.; Biondolillo, R.; Talbot, J. A.; Chernet, E.; Svensson, K. A.; Ackermann, B. L. *Bioanalysis* **2015**, *7* (19), 2461–2475.

(12) Aflaki, F.; Ghoulipour, V.; Saemian, N.; Salahinejad, M. *Anal. Methods* **2014**, *6* (4), 1482–1487.

(13) Özdestan, Ö.; Üren, A. *Talanta* **2009**, *78* (4–5), 1321–1326.

(14) Asan, A.; Isildak, I. *J. Chromatogr. A* **2003**, *988*, 145–149.

(15) Gao, S.; Wilson, D. M.; Edinboro, L. E.; McGuire, G. M.; Williams, S. G. P.; Karnes, H. T. *J. Liq. Chromatogr. Relat. Technol.* **2003**, *26* (20), 3413–3431.

(16) Cai, H. L.; Zhu, R. H.; Li, H. D. *Anal Biochem* **2010**, *396* (1), 103–111.

(17) Dai, W.; Huang, Q.; Yin, P.; Li, J.; Zhou, J.; Kong, H.; Zhao, C.; Lu, X.; Xu, G. *Anal. Chem.* **2012**, *84* (23), 10245–10251.

(18) Guo, K.; Li, L. *Anal. Chem.* **2009**, *81* (10), 3919–3932.

(19) Zhang, M.; Fang, C.; Smagin, G. *J. Pharm. Biomed. Anal.* **2014**, *100*, 357–364.

(20) Bhandare, P.; Madhavan, P.; Rao, B. M.; Someswar Rao, N. *J. Chem. Pharm. Res.* **2010**, *2* (22), 372–380.

(21) Buck, K.; Voehringer, P.; Ferger, B. *J. Neurosci. Methods Methods* **2009**, *182* (1), 78–84.

(22) West, C.; Fougere, L.; Elfakir, C.; Chirita-Tampu, R.-I. *LC-GC Eur.* **2013**, *26* (3), 128–

140.
(23) González, R. R.; Fernández, R. F.; Vidal, J. L. M.; Frenich, A. G.; Pérez, M. L. G. *J. Neurosci. Methods* **2011**, *198* (2), 187–194.
(24) Tufi, S.; Lamoree, M.; de Boer, J.; Leonards, P. *J. Chromatogr. A* **2015**, *1395*, 79–87.
(25) Zhang, L.-H.; Cai, H.-L.; Jiang, P.; Li, H.-D.; Cao, L.-J.; Dang, R.-L.; Zhu, W.-Y.; Deng, Y. *Anal. Methods* **2015**, *7* (9), 3929–3938.
(26) Zhang, X.; Rauch, A.; Lee, M.; Xiao, H.; Rainer, G.; Logothetis, N. K. *Rapid Commun. Mass Spectrom.* **2007**, *21* (22), 3621–3628.
(27) Wardlaw, S. L.; Burant, C. F.; Klein, S.; Meece, K.; White, A.; Kasten, T.; Lucey, B. P.; Bateman, R. J. *J. Clin. Endocrinol. Metab.* **2014**, *99* (7), 2540–2548.
(28) Jiang, L.; He, L.; Fountoulakis, M. *J. Chromatogr. A* **2004**, *1023* (2), 317–320.
(29) Park, S.; Alfa, R. W.; Topper, S. M.; Kim, G. E. S.; Kockel, L.; Kim, S. K. *PLoS Genet.* **2014**, *10* (8).
(30) Novotny, M.; Alasandro, M.; Konishi, M. *Anal. Chem.* **1983**, *55* (14), 2375–2377.
(31) Redmond, J. W.; Tseng, A. *J. Chromatogr. A* **1979**, *170* (2), 479–481.
(32) Higa, S.; Suzuki, T.; Hayashi, A.; Tsuge, I.; Yamamura, Y. *Anal. Biochem.* **1977**, *77* (1), 18–24.
(33) Greene, T. W. In *Greene's Protective Groups in Organic Synthesis*; John Wiley & Sons, Inc.: Hoboken, NJ, USA, 2006; pp 367–430.
(34) Scheline, R. R. *Acta Chem. Scand.* **1966**, *20*, 1182–1182.
(35) Hillemann, H. *Berichte der Dtsch. Chem. Gesellschaft (A B Ser.* **1938**, *71* (1), 34–41.
(36) El-Kholy, S.; Stephano, F.; Li, Y.; Bhandari, A.; Fink, C.; Roeder, T. *Cell Tissue Res.* **2015**, *361* (3), 669–684.
(37) Evans, P. D.; Maqueira, B. *Invertebr. Neurosci.* **2005**, *5* (3–4), 111–118.
(38) Livingstone, M. S.; Tempel, B. L. *Nature* **1983**, *303* (5912), 67–70.
(39) Monastirioti, M.; Linn, C. E.; White, K. *J. Neurosci.* **1996**, *16* (12), 3900–3911.
(40) Zucchi, R.; Chiellini, G.; Scanlan, T. S.; Grandy, D. K. *British Journal of Pharmacology*. Blackwell Publishing Ltd January 29, 2006, pp 967–978.
(41) Berry, M. D. *Journal of Neurochemistry*. Blackwell Science Ltd July 1, 2004, pp 257–271.
(42) Evans, P. H.; Fox, P. M. *J. Insect Physiol.* **1975**, *21*, 343–353.
(43) Finocchiaro, L.; Callebert, J.; Launay, J. M.; Jallon, J. M. *J. Neurochem.* **1988**, *50* (2), 382–387.
(44) Paxon, T. L.; Powell, P. R.; Lee, H.-G.; Han, K.-A.; Ewing, A. G. *Anal. Chem.* **2005**, *77* (16), 5349–5355.
(45) Savitz, J.; Drevets, W. C.; Smith, C. M.; Victor, T. A.; Wurfel, B. E.; Bellgowan, P. S.; Bodurka, J.; Teague, T. K.; Dantzer, R. *Neuropsychopharmacology* **2015**, *40* (2), 463–471.
(46) Pegg, A. E.; Casero, R. A. *Methods in molecular biology (Clifton, N.J.)*. 2011, pp 3–35.
(47) Lewandowski, N. M.; Ju, S.; Verbitsky, M.; Ross, B.; Geddie, M. L.; Rockenstein, E.;

Adame, A.; Muhammad, A.; Vonsattel, J. P.; Ringe, D.; Cote, L.; Lindquist, S.; Masliah, E.; Petsko, G. A.; Marder, K.; Clark, L. N.; Small, S. A. *Proc. Natl. Acad. Sci. U. S. A.* **2010**, *107* (39), 16970–16975.

(48) Morrison, L. D.; Kish, S. J. *Neurosci. Lett.* **1995**, *197* (1), 5–8.

(49) Aldini, G.; Orioli, M.; Carini, M.; Facino, R. M. In *Journal of Mass Spectrometry*; John Wiley & Sons, Ltd., 2004; Vol. 39, pp 1417–1428.

(50) Boldyrev, A. A.; Aldini, G.; Derave, W. *Physiol. Rev.* **2013**, *93* (4), 1803–1845.

(51) Gawryluk, J. W.; Wang, J. F.; Andreazza, A. C.; Shao, L.; Young, L. T. *Int. J. Neuropsychopharmacol.* **2011**, *14* (1), 123–130.

(52) Edison, P.; Ahmed, I.; Fan, Z.; Hinz, R.; Gelosa, G.; Ray Chaudhuri, K.; Walker, Z.; Turkheimer, F. E.; Brooks, D. J. *Neuropsychopharmacology* **2013**, *38* (6), 938–949.

(53) Mosconi, L.; Pupi, A.; De Leon, M. J. In *Annals of the New York Academy of Sciences*; Blackwell Publishing Inc, 2008; Vol. 1147, pp 180–195.

(54) Peppard, R. F.; Martin, W. R. W.; Clark, C. M.; Carr, G. D.; McGeer, P. L.; Calne, D. B. *J. Neurosci. Res.* **1990**, *27* (4), 561–568.

(55) Vander Borght, T.; Minoshima, S.; Giordani, B.; Foster, N. L.; Frey, K. A.; Berent, S.; Albin, R. L.; Koeppe, R. A.; Kuhl, D. E. *J. Nucl. Med.* **1997**, *38*, 797–802.

(56) Armbruster, D. A.; Pry, T. *Clin. Biochem. Rev.* **2008**, *29 Suppl 1* (August), S49-52.

(57) Matos Santos, S.; Garcia-Nimo, L.; Sá Santos, S.; Tavares, I.; Cocho, J. A.; Castanho, M. A. R. B. *Front. Aging Neurosci.* **2013**, *5*, 1–6.

(58) Ueda, H.; Shiomi, H.; Takagi, H. *Brain Res.* **1980**, *198* (2), 460–464.

(59) Ribeiro, M. M. B.; Pinto, A. R. T.; Domingues, M. M.; Serrano, I.; Heras, M.; Bardaji, E. R.; Tavares, I.; Castanho, M. A. *Mol. Pharm.* **2011**, *8* (5), 1929–1940.

(60) Sigrist, S. J.; Andlauer, T. F. M. In *Nature Neuroscience*; 2011; Vol. 14, pp 124–126.

(61) Yang, Z.; Yu, Y.; Zhang, V.; Tian, Y.; Qi, W.; Wang, L. *Proc. Natl. Acad. Sci.* **2015**, *112* (16), 5219–5224.

(62) Canelas, A. B.; Ten Pierick, A.; Ras, C.; Seifar, R. M.; Van Dam, J. C.; Van Gulik, W. M.; Heijnen, J. J. *Anal. Chem.* **2009**, *81* (17), 7379–7389.

(63) Dietmair, S.; Timmins, N. E.; Gray, P. P.; Nielsen, L. K.; Krömer, J. O. *Anal. Biochem.* **2010**, *404* (2), 155–164.

(64) Mushtaq, M. Y.; Choi, Y. H.; Verpoorte, R.; Wilson, E. G. *Phytochemical Analysis*. July 1, 2014, pp 291–306.

CHAPTER 4

Plasma metabolomics with benzoyl chloride derivatization reveals metabolic effects of Parkinson's disease

Introduction

Metabolomics can play an important role in understanding disease. In Chapters 2 and 3, we developed targeted metabolomic methods for neurochemicals in biological samples using benzoyl chloride (BzCl) derivatization. In this chapter, we explore the application of these methods to the study of Parkinson's disease (PD) with the goal of identifying metabolic perturbations resulting from the disease which may lead to the identification of putative biomarkers.

A biomarker is a measurable characteristic which is used to predict a biological outcome. Biomarkers can range from DNA sequences or specific patterns in brain scans to biomolecules such as proteins or metabolites.[1–3] They can be used for diagnostic purposes or for risk prediction, e.g. likelihood to develop a disease. The ideal metabolite biomarker would be readily accessible, meaning minimally invasive measurement and at detectable concentrations. The biomarker must be sensitive enough to distinguish between diseased and control groups. Selectivity is required to distinguish one disease state from another. Additionally, a biomarker should be stable enough to not be influenced by external factors such as diet.[4,5]

Many studies are quick to define differential metabolites as "biomarkers," but further validation is required to establish metabolites as robust biomarkers, so these differential

metabolites are best thought of as putative biomarkers.[4,6] Even identifying putative metabolite biomarkers can be challenging, however. The metabolome is susceptible to external influences, so finding a metabolite robust enough to avoid these influences is difficult.

With a hypothesis generating goal, metabolite biomarker identification is generally performed using untargeted methods.[4,5] Some work has been done with "pseudotargeted" metabolomics, which will be described in more depth in Chapter 7.[7,8] The limited scope of targeted methods can reduce the likelihood of discovering unexpected changes in metabolites, but the use of a "widely" targeted method, such as that described in Chapter 3, can increase the odds. The increased sensitivity afforded by BzCl derivatization adds the potential to identify changes in low abundance metabolites which may be overlooked by other methods.

In this chapter, we use BzCl metabolomics to investigate PD. PD is a neurodegenerative disease characterized by the death of dopamine neurons in the substantia nigra, along with the buildup of aggregates of α-synuclein, which are termed "Lewy bodies."[9–12] Physical symptoms include rigidity, resting tremor, and postural instability. Cognitive decline and psychiatric disturbances are also common. Though some genes have been linked with hereditary PD, the exact cause remains unknown.[13–15] Despite the fact that PD is the second most prevalent neurodegenerative disease, it is not well understood and diagnosis relies heavily on clinical measures and response to treatment.[16]

The discovery of biomarkers for PD could serve many purposes. A predictive biomarker would inform patients of their risk of developing the disease, and could help elucidate the cause of PD. A sensitive, diagnostic biomarker could allow for earlier, more accurate diagnosis, allowing for appropriate treatment before symptoms become severe. Thus, there is significant interest in identifying biomarkers for PD. The Michael J. Fox Foundation (MJFF) for Parkinson's

Research sponsors several studies for furthering the understanding of PD, including the BioFIND project.[17]

The BioFIND project is a collaborative study across academic sites intended to compliment its clinical counterpart, the Parkinson's Progression Markers Initiative.[18] Clinical samples are provided to researchers across various sites to search for putative biomarkers. Available samples include DNA, plasma, urine, and cerebrospinal fluid (CSF), and as a multi-site collaborative project, a variety of techniques can be used to screen for biomarkers. The work in this chapter was performed as part of the BioFIND project, with the goal of identifying metabolites which are correlated with PD. Plasma samples were used, which unlike CSF, is easily collected, and unlike urine, does not require normalization. These factors make plasma a convenient matrix for diagnostic purposes.

We used the 70 compound method described in Chapter 3 as an initial screen for this study. It was observed that many of these metabolites were either undetected or showed no change between groups. Most of the metabolites which differed between groups were outside of the calibration range. Based on these results, we developed a more specific method with a faster analysis time and a suitable calibration range for the samples. For this method, we chose to focus on polyamines,[19–21] dopamine metabolites,[22–24] and homocysteine metabolites,[25–27] which showed differences in the initial screen and have all been previously implicated in PD. These results were used to identify metabolic differences in the plasma of PD patients and healthy controls.

Experimental

Clinical data used in this study were obtained from the Fox Investigation for New Discovery of Biomarkers (BioFIND) database. For up-to-date information on the study, visit www.michaeljfox.org/biofind.

Chemicals and reagents

All chemicals were purchased from Sigma Aldrich (St. Louis, MO) unless otherwise noted. Water and acetonitrile are Burdick & Jackson HPLC grade from VWR (Radnor, PA). Stock solutions were prepared of 50 mM Arg, Cit, Met, Orn (Acros Organix, Geel, Belgium), Phe; 10 mM 3-OMD (MP Biomedicals, Santa Ana, CA), βAla, DOPAC (Acros Organics), HCY, HVA (Tocris, Bristol, UK), Spm; 5 mM 3MT, Agm, DA, DOPA, NAP, NE, Put, Spd, TyrA; 2 mM Tyr in HPLC water and stored at -80 °C. A standard mixture was prepared in artificial cerebrospinal fluid (aCSF) consisting of 145 mM NaCl, 2.68 mM KCl, 1.4 mM $CaCl_2$, 1 mM $MgSO_4$, 1.55 mM Na_2HPO_4, and 0.45 mM NaH_2PO_3 adjusted to pH 7.4 with NaOH. Calibration standards and internal standards were prepared as described previously.[28] Single use aliquots of each were stored at -80 °C. On the day of use, an internal standard aliquot was thawed and diluted 100-fold in 20% (v/v) acetonitrile containing 1% (v/v) sulfuric acid. This mixture is referred to as the internal standard solution. A fresh BzCl solution was prepared daily.

QC sample preparation

Pooled human serum from the American Red Cross Detroit National Testing Lab was provided by the Michigan Regional Comprehensive Metabolomics Resource Core (MRC^2). To ensure all targeted metabolites were detectable in the serum, select standards were spiked in to a final concentration of 2.5 µM for HCY, HVA, DOPA; 500 nM for 3-OMD; 250 nM for DOPAC;

125 nM for TyrA; 25 nM for Agm, 3MT, NE, and DA. Single use aliquots of the spiked serum were prepared and stored at -80 °C. On the day of use, a 10 µL aliquot of spiked serum was thawed, and 40 µL of ice cold acetonitrile were added to precipitate proteins. The mixture was vortexed briefly, and centrifuged for 10 min at 12,100g. 40 µL of supernatant were transferred to an HPLC autosampler vial, and derivatized by sequential addition of 20 µL 100 mM sodium carbonate, 20 µL 2% (v/v) BzCl in acetonitrile, 20 µL internal standard solution, and 100 µL water. The derivatized QC sample was run every 10 injections.

Plasma sample preparation

Plasma from healthy controls (n = 76) and PD patients (n = 98) was provided by the BioFIND Project of the Michael J. Fox Foundation. Demographics for the patients are listed in Table 1. Plasma was collected in the early morning prior to medication, following a fasting period of at least 8 hours. Upon receipt, plasma was stored at -80 °C until use. On the day of use, 40 µL of ice cold acetonitrile were added to 10 µL of plasma. After vortexing, the mixture was centrifuged for 10 min at 12,100g. 20 µL of the supernatant were transferred to an HPLC autosampler vial, and derivatized by sequential addition of 10 µL 100 mM sodium carbonate, 10 µL 2% (v/v) BzCl in acetonitrile, 10 µL internal standard solution, and 100 µL water. Calibration

Diagnosis	Gender	Age Range	# Samples
HC	F	55-82	37
	M	55-84	39
PD	F	55-82	35
	M	57-81	63

Table 4-1: Sample demographics for healthy controls (HC) and Parkinson's patients (PD) used in this study.

standards were prepared in aCSF and diluted in acetonitrile to match the solvent composition of the plasma samples. Standards were derivatized in the same manner as the plasma. A new calibration was prepared each day. Derivatized plasma was analyzed in triplicate. Researchers were blinded to sample identity until all data collection was completed.

LC-MS analysis

Derivatized samples were analyzed using a Waters nanoAcquity UPLC (Milford, MA) coupled to an Agilent 6410B triple quadrupole mass spectrometer (Santa Clara, CA) operating in dynamic MRM mode. An example chromatogram is shown in Figure 4-1. The injection volume was 5 µL. An Acquity UPLC HSS T3 C18 column (100 x 1 mM, 1.8 µM, 100 Å) was used. Mobile phase A was 10 mM ammonium formate with 0.15% formic acid in water, and mobile phase B was acetonitrile. The flow rate was 100 µL/min, and the gradient was: Initial, 0% B; 0.1 min, 25% B; 1.5 min, 26% B; 1.51 min, 49% B; 4.00 min, 49% B; 4.01 min, 68% B; 4.99 min, 68% B; 5.00 min, 100% B; 6.00 min, 100% B; 6.01 min, 0% B; 8 min, 0% B. The autosampler was kept at ambient temperature, and the column was at 27 °C. Electrospray ionization was used in positive ion mode at 4 kV. The gas temperature was 350 °C, gas flow was 11 L/min, and nebulizer was at 15 psi. MRM conditions are listed in Table 2. Automated peak integration was performed using

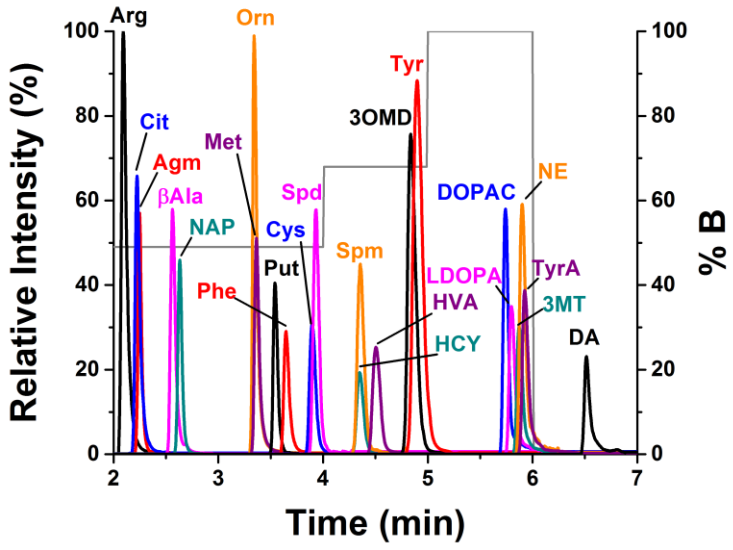

Figure 4-1: Extracted ion chromatogram of Parkinson's related metabolites in standard solution. Gradient is overlaid as % B.

Metabolite	Precursor (m/z)	Product (m/z)	Fragmentor (V)	Collision Energy (V)	Retention Time (min)
Bz-3MT	376	105	120	20	5.78
$^{13}C_6$-Bz-3MT	388	111			
Bz-3OMD	420	105	140	30	4.63
$^{13}C_6$-Bz -3OMD	432	111			
Bz-Agm	235	105	110	30	2.24
$^{13}C_6$-Bz -Agm	241	111			
Bz-Arg	279	105	135	30	2.09
$^{13}C_6$-Bz -Arg	285	111			
Bz-B-Ala	194	105	120	20	2.53
$^{13}C_6$-Bz -B-Ala	200	111			
Bz-Cit	280	105	120	20	2.23
$^{13}C_6$-Bz -Cit	286	111			
Bz-Cys	330	105	120	20	3.81
$^{13}C_6$-Bz -Cys	342	111			
Bz-DA	466	105	140	20	6.44
$^{13}C_6$-Bz -DA	484	111			
Bz-DOPAC	394	105	140	20	5.65
$^{13}C_6$-Bz -DOPAC	406	111			
Bz-HCY	344	105	120	20	4.23
$^{13}C_6$-Bz -HCY	356	111			
Bz-HVA	304	105	120	15	4.37
$^{13}C_6$-Bz -HVA	310	111			
Bz-LDOPA	510	360	120	30	5.71
$^{13}C_6$-Bz -LDOPA	528	372			
Bz-Met	254	105	120	15	3.33
$^{13}C_6$-Bz -Met	260	111			
Bz-NAP	235	105	135	20	2.59
$^{13}C_6$-Bz -NAP	241	111			
Bz-NE	482	105	140	30	5.8
$^{13}C_6$-Bz -NE	500	111			
Bz-Orn	341	174	120	15	3.31
$^{13}C_6$-Bz -Orn	353	180			
Bz-Phe	270	120	120	10	3.6
$^{13}C_6$-Bz -Phe	276	120			
Bz-Put	297	105	120	30	3.5
$^{13}C_6$-Bz -Put	309	111			
Bz-Spd	458	162	120	30	3.84
$^{13}C_6$-Bz -Spd	476	168			
Bz-Spm	619.6	497.2	135	25	4.21
$^{13}C_6$-Bz -Spm	643.6	515.2			
Bz-TyrA	346	105	135	25	5.83
$^{13}C_6$-Bz -TyrA	358	111			
Bz-Tyr	390	105	120	30	4.69
$^{13}C_6$-Bz -Tyr	402	111			

Table 4-2: MRM conditions for benzoylated metabolites and internal standards. Cell accelerator voltage was at 4 V for all metabolites.

Agilent MassHunter Workstation Quantitative Analysis for QQQ, version B.05.00. All peaks were manually inspected to ensure proper integration. Calibration curves were prepared using the ratio of analyte peak area to internal standard peak area.

Data processing

Calculated concentrations were corrected for day-to-day variability using the average of the QC concentration that day relative to the overall average of all QC samples. No correction was performed for intra-day variability, as little variance was observed in same-day QC samples. Limits of detection (LOD) were calculated from triplicate calibrations using Armbruster's method.[29] Results from triplicate analysis were averaged, and values below the LOD were discarded and imputed with half the LOD.

Statistical analysis

Unpaired, two-tailed Student's t-tests and single factor ANOVA were performed in Microsoft Office Excel 2007, and differences were deemed significant if $P \leq 0.05$, subject to Holm-Bonferroni correction.

Results and discussion

Figures of merit

LODs and linearity were calculated from six point calibrations in aqueous standards diluted in acetonitrile. Relative standard deviations (RSD) were calculated for QC standards to show both intra- and inter-day repeatability (Table 3). These LODs are higher than those reported for similar BzCl methods using aqueous dialysate samples, but are comparable to LODs

previously reported for other proteinaceous samples.[28,30] All metabolites produced linear calibration curves ($R^2 \geq 0.99$).

Intra- and inter-day reproducibility was determined as the RSD of the calculated concentration in the QC samples. For each day, the RSD for all QC runs (n = 7-13) was calculated. The average intra-day RSD over the six days of analysis was below 10% for each metabolite. Inter-day reproducibility was calculated for all QC runs (n = 60) over the course of the experiment. RSDs were below 10% for all but eight metabolites, and all RSDs were below 20%.

Metabolite	LOD (nM)	Linearity (R^2)	Repeatability (%)	
			Intra-day	Inter-day
Arg	100	0.999	4.04	10.9
Agm	0.5	0.999	6.39	11.7
Cit	200	0.999	1.92	11
BAla	30	0.999	8.36	16.4
NAP	2	0.999	3.78	6.4
Orn	50	0.999	1.53	9.51
Met	500	0.999	1.25	4.58
Put	1	0.997	4.81	10.2
Phe	1000	0.999	2.89	4.58
Cys	20	0.998	2.34	10.5
Spd	0.5	0.998	2.33	8.28
Spm	1	0.994	4.04	11.4
HCY	40	0.998	3.87	10.7
HVA	30	0.999	2.51	5.17
3OMD	10	0.999	4.13	5.3
Tyr	400	0.999	1.86	3.19
DOPAC	20	0.996	3.75	6.56
DOPA	100	0.996	5.67	10.2
3MT	1	0.999	5.06	6.56
NE	1	0.999	5.42	6.64
TyrA	5	0.999	1.6	4.39
DA	2	0.998	3.26	9.96

Table 4-3: Figures of merit for the method. LODs were calculated from triplicate calibration curves. Linearity as R^2 was calculated from the same calibrations. Repeatability was calculated as the RSD of calculated QC concentrations over each day and over the entire course of the experiment.

Metabolite differences between healthy controls and PD patients

Significant increases in β-alanine, N-acetylputrescine, putrescine, HVA, and 3-OMD were observed in the plasma of PD patients relative to controls (Figure 4-2). None of the metabolites assayed were found to decrease in PD patients. Polyamines, especially putrescine, spermidine, and spermine, have been previously implicated in PD.[19–21] Expression of the catabolic enzyme, spermidine/spermine N1-acetyl-transferase (SAT1) was found to be decreased in the dorsal motor nucleus of the vagus (DMNV) in PD.[20] In the periphery, polyamines were found to be increased in red blood cells of PD patients.[19] Serum levels of N8-acetylspermidine were found to be increased in rapidly progressing PD.[21] The effect on other plasma polyamines in PD has not yet been reported. Here, we observed no significant difference in spermidine or spermine, but putrescine and N-acetylputrescine were increased in PD patients, further confirming that polyamines are implicated in PD. Polyamines are essential to development and have been shown to have both neuroprotective and neurotoxic effects,[20,31,32] so the exact role of polyamines in PD and other neurodegenerative diseases remains under investigation.

β-Alanine is involved in the production of carnosine, an antioxidative neuropeptide which is reported to increase PD treatment efficacy.[33,34] Additionally, β-alanine is a side product of polyamine metabolism. The reactive aldehyde 3-aminopropanal is produced when spermine oxidase (SMOX) converts spermine back to spermidine. 3-Aminopropanal can then be converted to β-alanine via aldehyde dehydrogenase. Reactive aldehydes have been found to play a role in neurodegenerative diseases, and 3-aminopropanal specifically is known to cause neuronal cell death.[35,36] It is unclear why this increase in β-alanine is observed, but the connection to carnosine and polyamines support that β-alanine is somehow implicated in PD.

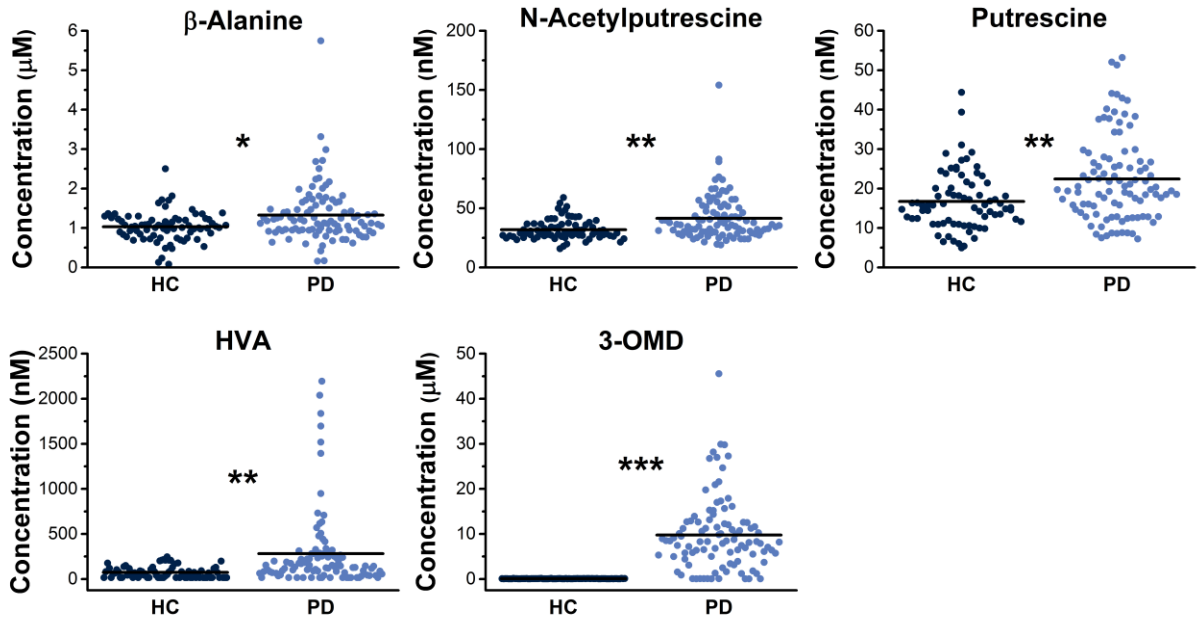

Figure 4-2: Plasma metabolite concentrations between healthy controls (HC, n = 76) and Parkinson's patients (PD, n = 98). Each point represents an individual, and the line is at the mean. The Holm-Bonferroni correction was used for statistics. * $p \leq 0.05$; ** $p \leq 0.01$; *** $p \leq 0.001$.

We observed a significant increase in plasma homovanillic acid (HVA) in PD patients relative to healthy controls. HVA is a metabolite of dopamine, and is decreased in the CSF of PD patients.[37] Currently, the main treatment for PD is dopamine replacement therapy via its precursor, L-DOPA. Dopamine cannot cross the blood-brain barrier, but L-DOPA can; as a result, taking L-DOPA orally can increase dopamine concentrations in the brain. L-DOPA is also metabolized in the periphery, leading to a reported increase of HVA in the plasma of L-DOPA treated PD patients.[24] No increase in HVA has been observed in the plasma of PD patients prior to or withdrawn from L-DOPA treatment.[23] Our data supports these trends; the majority of the PD patients in this study were treated with L-DOPA, and a significant increase in plasma HVA was observed in PD patients relative to healthy controls.

3-O-Methyldopa (3-OMD) was also found to be elevated in PD patients relative to healthy controls. 3-OMD is a major metabolite of L-DOPA via catechol-O-methyl transferase (COMT). L-DOPA has a half life of roughly two hours in plasma, so increases are short-lived

and may not be observed depending on sampling time frame.[38] 3-OMD, on the other hand, has a much longer half life, so increases in 3-OMD can reflect an earlier increase in L-DOPA. The majority of the PD patients were treated with L-DOPA, so this likely explains the increase in 3-OMD.

No increase in homocysteine was observed in PD patients. Homocysteine is part of a metabolic cycle with S-adensoylmethionine (SAM), which acts as a methyl transferase in the conversion of L-DOPA to 3-OMD. Increases in the plasma of PD patients treated with L-DOPA have been reported.[25–27] The patients in this study were withdrawn from their most recent treatments prior to plasma sampling. The effect of L-DOPA withdrawal on homocysteine levels has not been established. If homocysteine levels return to normal after L-DOPA withdrawal, this would explain why no change was observed in this study.

Metabolite correlations to Hoehn and Yahr score

The Hoehn and Yahr (HY) scale is a means of ranking PD severity based on specific clinical criteria.[9] A HY score is assigned following assessment of the patient for the presence and severity of a variety of PD symptoms by a physician. A higher HY score corresponds to more severe PD. In this study, the most severe PD cases corresponded to an HY score of 4. Single factor ANOVA was used to compare each HY score to healthy controls. Of the 22 metabolites studied, 13 were found to be elevated in at least one group of PD patients separated by HY score. These include putrescine, N-acetylputresceine, β-alanine, HVA, and 3-OMD, as well as ornithine, spermidine, DOPAC, DOPA, 3MT, norepinephrine, tyramine, and dopamine (Figure 4-3). All of these except ornithine, were elevated in the most severe PD cases (HY = 4) relative to healthy controls.

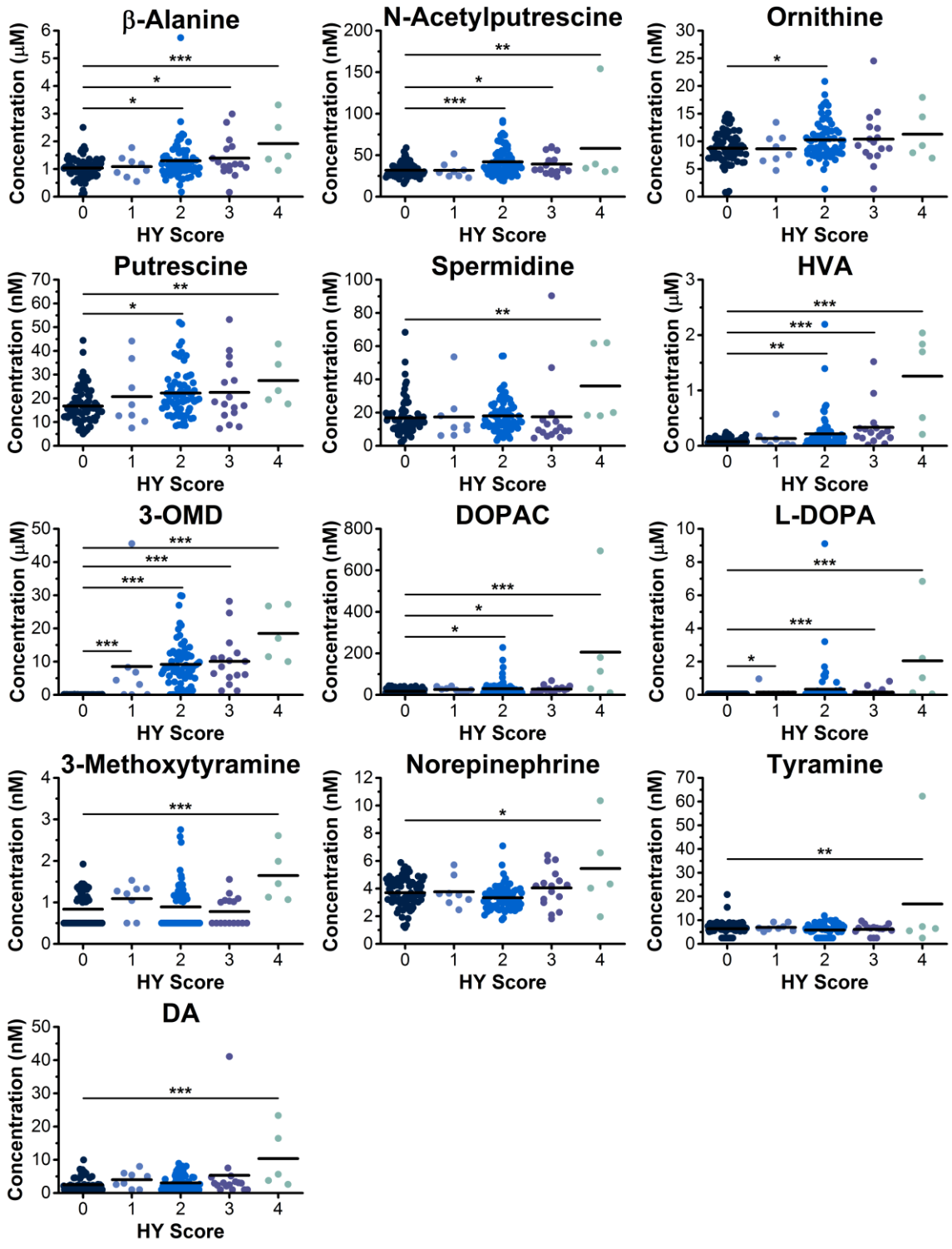

Figure 4-3: Metabolite concentrations as a function of Hoehn and Yahr (HY) score. A score of 0 corresponds to healthy controls (HC, n = 76), and a higher score corresponds to increasing disease severity (1, n = 8; 2, n = 69; 3, n = 16; 4, n = 5). Each point corresponds to an individual, and the line is at the mean. Single factor ANOVA was used with post hoc Holm-Bonferroni correction. * $p \leq 0.05$; ** $p \leq 0.01$; *** $p \leq 0.001$.

Ornithine is a precursor to the polyamines. Elevated plasma concentrations of putrescine and N-acetylputrescine in this work already suggests polyamines are implicated in PD and this elevation in ornithine relative to healthy controls further supports the hypothesis. Although ornithine trends towards upregulated in HY = 4 PD patients, the difference was not significant, most likely due to the small sample size (n = 5) relative to healthy controls (n = 76). Spermidine, another polyamine, was found to be elevated in the most severe PD cases. Although many of the polyamines were elevated in PD, this was not observed with spermine, a metabolite of spermidine. A decrease in spermine synthase could explain these results, but an increase in spermine oxidase (SMOX) activity could also lead to an increase in spermidine.

While L-DOPA has a relatively short half-life, high doses administered for severe PD could lead to detectable levels of L-DOPA even after withdrawal from treatment. As such, L-DOPA was below the LOD for all healthy controls, but was increasingly detected in PD patients with increasing disease severity. Dopamine is a direct metabolite of L-DOPA, and DOPAC, 3MT, and norepinephrine are metabolites of dopamine via various catabolic enzymes. It is unsurprising that these metabolites are elevated following peripheral treatment with L-DOPA.

Tyramine is a naturally occurring trace amine in humans that is a particular concern in PD patients. Monoamine oxidase (MAO) inhibitors are common treatments for PD to prevent premature catabolism of dopamine. MAO is one of the primary catabolic enzymes for tyramine, so inhibitors can lead to a build-up of tyramine in PD patients. This can lead to hypertensive crisis and potentially death, so care must be taken to avoid dietary excess of tyramine. As medication doses increase with PD severity, it is not unexpected that tyramine catabolism would be reduced, explaining the observed increase in severe PD.

Metabolite correlation to L-DOPA treatment

As has been noted, several of the metabolite increases in PD can be explained as a result of L-DOPA treatment. The majority of PD patients tested in this study were taking L-DOPA, but a small number were not. To investigate whether L-DOPA treatment was linked to these changes, we compared metabolite concentrations between healthy controls (n = 76), PD patients without L-DOPA treatment (PD - DOPA, n = 10), and PD patients with L-DOPA treatment (PD + DOPA, n = 88). Using single-factor ANOVA, we found that in addition to the five metabolites which were different between healthy controls and PD patients as a whole, ornithine was significantly increased in PD + DOPA patients relative to healthy controls (Figure 4-4). However, no metabolites were found to be significantly different between healthy controls and PD - DOPA patients.

The link between L-DOPA treatment to increases in 3-OMD and HVA is straightforward, as 3-OMD is a direct metabolite and HVA is a metabolite of dopamine, for which L-DOPA is a precursor. The connection between L-DOPA and the increased polyamine concentrations is less clear. One study reported an increase in putrescine in the brain and liver of rats treated with L-DOPA.[39] The mechanism for this increase was unclear, but an increase in ornithine decarboxylase (ODC), which converts ornithine to putrescine, was proposed. An increase in ODC would explain the increase in putrescine and N-acetylputrescine observed in our results, but would not explain the observed increase in ornithine. There is no

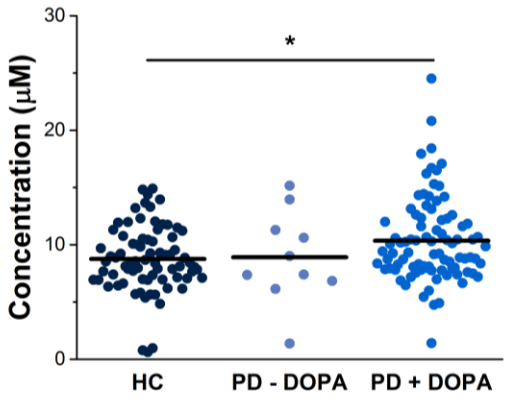

Figure 4-4: Ornithine concentration in healthy controls (HC, n = 76), Parkinson's patients not treated with L-DOPA (PD - DOPA, n - 10), and Parkinson's patients treated with L-DOPA (PD + DOPA, n = 88). Each point represents and individual, and the line is at the mean. The Holm-Bonferroni correction was used. * $p \leq 0.05$.

direct metabolic link between L-DOPA and ornithine or other urea cycle metabolites, so further investigation is needed to explain this finding.

We compared metabolite concentrations in PD + DOPA patients to total daily L-DOPA dosage (Figure 4-5). Unsurprisingly, the direct metabolite 3-OMD was found to be correlated to L-DOPA dosage. However, no other metabolites were found to be dependent on L-DOPA dosage. This observation suggests a more complex mechanism for their increase than simply by-products of L-DOPA metabolism. Additionally, slight trends were observed in the PD-D samples compared to healthy controls which were not statistically significant due to the small sample size, but could be significant if a larger body of untreated samples was analyzed.

These findings illustrate an interesting challenge in studying PD. Response to L-DOPA treatment is typically a factor in diagnosing PD, so it is uncommon to have samples from untreated patients. Indeed, many investigations have a relatively small set of untreated patients relative to treated or treatment-withdrawn patients.[23–26] To deconvolute effects of the disease from effects of treatment, larger cohorts of untreated patients will need to be compared to healthy controls. The information from treated patients still has value, however. Long term treatment with L-DOPA causes debilitating dyskinesias which are not yet fully understood.[40,41] Gaining insight of the molecular mechanism leading to this could allow for treatment or even prevention of L-DOPA induced dyskinesia.

Conclusions

Dopamine metabolism, as well as polyamine and homocysteine metabolism are frequently implicated in the study of PD. The effect of PD on these metabolites in the periphery (i.e. plasma) has not been well studied; targeted metabolomic methods are often used which

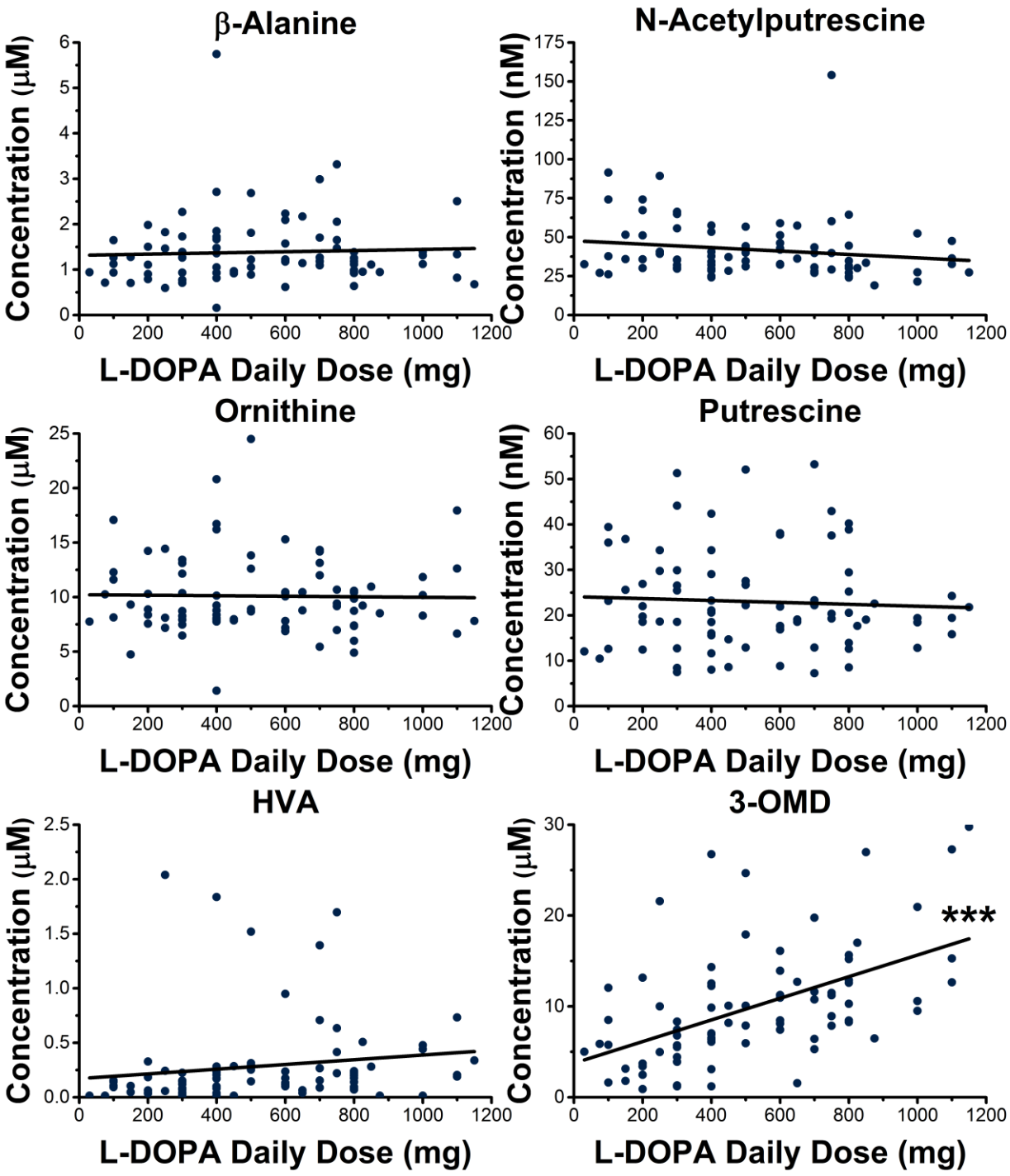

Figure 4-5: Metabolite concentrations as a function of total L-DOPA daily dose. Each point corresponds to an individual (n = 80). ANOVA was used to calculate linear fit. *** $p \leq 0.001$.

across these metabolic pathways to provide a more complete insight into these pathways. BzCl derivatization was used to increase retention and sensitivity of these metabolites in reversed

phase chromatography, as well as to easily create internal standards for each targeted metabolite. Internal standards account for instrument drift and matrix effects, leading to better quantification of metabolites.

Five metabolites were found to be significantly increased in PD patients relative to healthy controls. Seven more were significant when comparing healthy controls to only the most severe PD cases in this study. None of these implicated metabolites were found to be significantly elevated in PD patients who were not treated with L-DOPA, though this may be due to the limited availability of samples from untreated PD patients. Only 3-OMD was found to correlate to L-DOPA in a dose-dependent manner, which suggests the observed metabolite increases are more than just a byproduct of increased L-DOPA metabolism. A larger sample set from untreated PD patients could help confirm this hypothesis.

While the effects of PD alone on the plasma metabolome have been obscured by L-DOPA, the results are not without value. L-DOPA has negative side effects, ranging from drowsiness and gastrointestinal distress to dyskinesias with long term treatment. By determining the metabolic effects of L-DOPA treatment, it may be possible to identify specific causes of these side effects. Co-therapies may be developed to minimize or eliminate the negative effects while maintaining the therapeutic potential of L-DOPA. Diagnostic biomarkers for PD could not be identified in this study, however, demonstrating the need for tightly controlled studies for biomarker discovery.

While we chose to focus on dopamine, polyamine, and homocysteine metabolism for this work, BzCl derivatization has previously been demonstrated for 70 metabolites across a wide variety of metabolic pathways.[28] Dansyl chloride, a derivatization reagent with similar reactivity to BzCl, has been used for untargeted metabolomics to cover an even larger number of

metabolites and has recently been used to evaluate metabolic changes associated with PD.[42,43] This method could be expanded to cover more metabolites and could easily be adapted to investigate many other neurological disorders.

Acknowledgements

We thank the MRC[2] for providing pooled human serum and access to metabolite standards, and Prof. Charles Burant for help with data interpretation. BioFIND is funded by The Michael J. Fox Foundation for Parkinson's Research and the National Institute of Neurological Disorders and Stroke.

References

(1) Schwarz, E.; Bahn, S.; Mallei, A.; Giambelli, R.; Khoury, A. El; Gruber, S. H. M.; Musazzi, L.; Barbiero, V. S.; Tardito, D.; Vollmayr, B.; Gass, P.; Mathé, A. a; Racagni, G.; Popoli, M. *Biomarkers for Psychiatric Disorders*; Springer US: Boston, MA, 2009.
(2) Strimbu, K.; Tavel, J. A. *Curr Opin HIV AIDS* **2011**, *5* (6), 463–466.
(3) Mayeux, R. *NeuroRx* **2004**, *1* (2), 182–188.
(4) Koulman, A.; Lane, G. A.; Harrison, S. J.; Volmer, D. A. *Anal. Bioanal. Chem.* **2009**, *394* (3), 663–670.
(5) Monteiro, M. S.; Carvalho, M.; Bastos, M. L.; Guedes de Pinho, P. *Curr. Med. Chem.* **2013**, *20* (2), 257–271.
(6) Goodsaid, F. M.; Frueh, F. W.; Mattes, W. *Toxicology* **2008**, *245*, 219–223.
(7) Chen, S.; Kong, H.; Lu, X.; Li, Y.; Yin, P.; Zeng, Z.; Xu, G. *Anal. Chem.* **2013**, *85* (17), 8326–8333.
(8) Shao, Y.; Zhu, B.; Zheng, R.; Zhao, X.; Yin, P.; Lu, X.; Jiao, B.; Xu, G.; Yao, Z. *J. Proteome Res.* **2015**, *14* (2), 906–916.
(9) Hoehn, M. M.; Yahr, M. D. *Neurology* **1967**, *17* (5), 427–442.
(10) Moore, D. J.; West, A. B.; Dawson, V. L.; Dawson, T. M. *Annu. Rev. Neurosci.* **2005**, *28* (1), 57–87.
(11) Agid, Y. *Lancet* **1991**, *337* (8753), 1321–1324.
(12) Fahn, S.; Oakes, D.; Shoulson, I.; Kieburtz, K.; Rudolph, A.; Lang, A.; Olanow, C. W.; Tanner, C.; Marek, K. *N. Engl. J. Med.* **2004**, *351* (24), 2498–2508.
(13) Polymeropoulos, M. H. *Science (80-.).* **1997**, *276* (5321), 2045–2047.

(14) Klein, C.; Westenberger, A. *Cold Spring Harb. Perspect. Med.* **2012**, *2* (1), a008888.
(15) Chang, D.; Nalls, M. A.; Hallgrímsdóttir, I. B.; Hunkapiller, J.; van der Brug, M.; Cai, F.; Kerchner, G. A.; Ayalon, G.; Bingol, B.; Sheng, M.; Hinds, D.; Behrens, T. W.; Singleton, A. B.; Bhangale, T. R.; Graham, R. R. *Nat. Genet.* **2017**, *49* (10), 1511–1516.
(16) Tysnes, O. B.; Storstein, A. *Journal of Neural Transmission*. 2017, pp 901–905.
(17) Kang, U. J.; Goldman, J. G.; Alcalay, R. N.; Xie, T.; Tuite, P.; Henchcliffe, C.; Hogarth, P.; Amara, A. W.; Frank, S.; Rudolph, A.; Casaceli, C.; Andrews, H.; Gwinn, K.; Sutherland, M.; Kopil, C.; Vincent, L.; Frasier, M. *Mov. Disord.* **2016**, *31* (6), 924–932.
(18) Marek, K.; Jennings, D.; Lasch, S.; Siderowf, A.; Tanner, C.; Simuni, T.; Coffey, C.; Kieburtz, K.; Flagg, E.; Chowdhury, S.; Poewe, W.; Mollenhauer, B.; Sherer, T.; Frasier, M.; Meunier, C.; Rudolph, A.; Casaceli, C.; Seibyl, J.; Mendick, S.; Schuff, N.; Zhang, Y.; Toga, A.; Crawford, K.; Ansbach, A.; de Blasio, P.; Piovella, M.; Trojanowski, J.; Shaw, L.; Singleton, A.; Hawkins, K.; Eberling, J.; Russell, D.; Leary, L.; Factor, S.; Sommerfeld, B.; Hogarth, P.; Pighetti, E.; Williams, K.; Standaert, D.; Guthrie, S.; Hauser, R.; Delgado, H.; Jankovic, J.; Hunter, C.; Stern, M.; Tran, B.; Leverenz, J.; Baca, M.; Frank, S.; Thomas, C. A.; Richard, I.; Deeley, C.; Rees, L.; Sprenger, F.; Lang, E.; Shill, H.; Obradov, S.; Fernandez, H.; Winters, A.; Berg, D.; Gauss, K.; Galasko, D.; Fontaine, D.; Mari, Z.; Gerstenhaber, M.; Brooks, D.; Malloy, S.; Barone, P.; Longo, K.; Comery, T.; Ravina, B.; Grachev, I.; Gallagher, K.; Collins, M.; Widnell, K. L.; Ostrowizki, S.; Fontoura, P.; La-Roche, F. H.; Ho, T.; Luthman, J.; van der Brug, M.; Reith, A. D.; Taylor, P. *Prog. Neurobiol.* **2011**, *95* (4), 629–635.
(19) Gomes-Trolin, C.; Nygren, I.; Aquilonius, S.-M.; Askmark, H. *Exp. Neurol.* **2002**, *177* (2), 515–520.
(20) Lewandowski, N. M.; Ju, S.; Verbitsky, M.; Ross, B.; Geddie, M. L.; Rockenstein, E.; Adame, A.; Muhammad, A.; Vonsattel, J. P.; Ringe, D.; Cote, L.; Lindquist, S.; Masliah, E.; Petsko, G. A.; Marder, K.; Clark, L. N.; Small, S. A. *Proc. Natl. Acad. Sci. U. S. A.* **2010**, *107* (39), 16970–16975.
(21) Roede, J. R.; Uppal, K.; Park, Y.; Lee, K.; Tran, V.; Walker, D.; Strobel, F. H.; Rhodes, S. L.; Ritz, B.; Jones, D. P. *PLoS One* **2013**, *8* (10).
(22) Campanella, G.; Algeri, S.; Cerletti, C.; Dolfini, E.; Jori, A.; Rinaldi, F. *Eur. J. Clin. Pharmacol.* **1977**, *11* (4), 255–261.
(23) Chia, L.-G.; Cheng, F.-C.; Kuo, J.-S. *J. Neurol. Sci.* **1993**, *116* (2), 125–134.
(24) Dethy, S.; Laute, M. A.; Van Blercom, N.; Damhaut, P.; Goldman, S.; Hildebrand, J. *Clin. Chem.* **1997**, *43* (5), 740–744.
(25) O'Suilleabhain, P. E.; Sung, V.; Hernandez, C.; Lacritz, L.; Dewey, R. B.; Bottiglieri, T.; Diaz-Arrastia, R. *Arch. Neurol.* **2004**, *61* (June), 865–868.
(26) Hassin-Baer, S.; Cohen, O.; Vakil, E.; Sela, B.-A.; Nitsan, Z.; Schwartz, R.; Chapman, J.; Tanne, D. *Clin. Neuropharmacol.* **2006**, *29* (6), 305–311.
(27) Helane Doherty, G. *J. Neurol. Disord.* **2013**, *1* (1), 1–9.
(28) Wong, J. M. T.; Malec, P. A.; Mabrouk, O. S.; Ro, J.; Dus, M.; Kennedy, R. T. *J.*

Chromatogr. A **2016**, *1446*, 78–90.
(29) Armbruster, D. A.; Pry, T. *Clin. Biochem. Rev.* **2008**, *29 Suppl 1* (August), S49-52.
(30) Song, P.; Mabrouk, O. S.; Hershey, N. D.; Kennedy, R. T. *Anal. Chem.* **2012**, *84*, 412–419.
(31) Pegg, A. E. *IUBMB Life* **2009**, *61* (9), 880–894.
(32) Bell, M. R.; Belarde, J. A.; Johnson, H. F.; Aizenman, C. D. *Nat. Neurosci.* **2011**, *14* (4), 505–512.
(33) Boldyrev, A.; Fedorova, T. N.; Stepanova, M.; Dobrotvorskaya, I.; Koslova, E.; Boldanova, N.; Bagyeva, G.; Ivanova-Smolenskaya, I. *Rejuvenation Res.* **2008**, *11* (4), 821–827.
(34) Solis, M. Y.; Cooper, S.; Hobson, R. M.; Artioli, G. G.; Otaduy, M. C.; Roschel, H.; Robertson, J.; Martin, D.; Painelli, V. S.; Harris, R. C.; Gualano, B.; Sale, C. *PLoS One* **2015**, *10* (4).
(35) Ivanova, S.; Batliwalla, F.; Mocco, J.; Kiss, S.; Huang, J.; Mack, W.; Coon, A.; Eaton, J. W.; Al-Abed, Y.; Gregersen, P. K.; Shohami, E.; Connolly, E. S.; Tracey, K. J. *Proc. Natl. Acad. Sci. U. S. A.* **2002**, *99* (8), 5579–5584.
(36) Matveychuk, D.; Dursun, S.; Wood, P.; Baker, G. *Bull. Clin. Psychopharmacol.* **2011**, *21* (2), 1.
(37) Johansson, B.; Roos, B.-E. *Life Sci.* **1967**, *6*, 1449–1454.
(38) Mena, M. A.; Casarejos, M. J.; Solano, R. M.; de Yébenes, J. G. *Curr. Top. Med. Chem.* **2009**, *9* (10), 880–893.
(39) Harik, S. I. *Eur. J. Pharmacol.* **1979**, *54*, 235–242.
(40) Thanvi, B.; Lo, N.; Robinson, T. *Postgrad. Med. J.* **2007**, *83* (980), 384–388.
(41) Bargiotas, P.; Konitsiotis, S. *Neuropsychiatric Disease and Treatment*. 2013, pp 1605–1617.
(42) Guo, K.; Li, L. *Anal. Chem.* **2009**, *81* (10), 3919–3932.
(43) Han, W.; Sapkota, S.; Camicioli, R.; Dixon, R. A.; Li, L. *Mov. Disord.* **2017**, *0* (0), 1–9.

CHAPTER 5

Determination of amines and phenolic acids in wine with benzoyl chloride derivatization and liquid chromatography - mass spectrometry

Introduction

Consumers, regulators, and producers are increasingly interested in obtaining information on the characteristics and the quality of food products.[1] This interest has spawned development of a wide variety of methods for analyzing consumable goods (e.g., wine, honey, tea, olive oil and juices).[2] With respect to wine, various national organizations require strict control over factors such as geographical origin and grape varieties to maintain consistency and quality.[3] Thus, characterization methods are required to assess authenticity and detect wine fraud. Separation techniques such as LC and GC have been widely used for wine characterization and classification. Two important families of LC-amenable wine components are phenols and biogenic amines. Compositional profiles of phenolic and/or amino species have been correlated with significant factors such as organoleptic properties, wine-making practices, and grape varieties.[4,5] In this work, we describe a new approach to assay of phenols and amines in wine using derivatization followed by LC-MS/MS for separation and quantification.

Phenols are a family of bioactive compounds found in wine that have drawn significant attention over the last few years. These aromatic secondary metabolites are ubiquitous in the plant kingdom. They comprise a complex family of more than 8,000 substances with highly

diverse structures and sizes from <100 Da to >30,000 Da for highly polymerized polyphenolic species. The main reasons for the interest in phenols are their antioxidant properties, great abundance in our diet, probable role in the prevention of various diseases, and contribution to sensorial properties.[6–8] Wine is an excellent natural source of various phenols that range from phenolic acids like benzoic- or cinnamic-like derivatives to different classes of polyphenolic flavonoids such as flavones, flavan-3-ols, flavonols and anthocyanins.[9] For this reason, analytical methods such as comprehensive LC techniques have been exploited over the last few years especially to quantify phenols in wine.[10–12]

In addition to phenols, biogenic amines have also been the subject of some studies.[13–18] Some of the biogenic amines usually found in wines are agmatine, spermine, spermidine, putrescine, cadaverine, histamine, and tyramine. These compounds are all produced by microorganisms during fermentation via decarboxylation of free amino acids. The consumption of some of them, e.g., histamine and tyramine, can lead to headaches, nausea, hot flushes, skin rashes, sweating, respiratory distress, and cardiac/intestinal problems[19] Because these components may be responsible for the biological responses to wine consumption, their measurement in different wine varieties of various origins has great importance.

LC with UV detection has been widely used for the determination of amines and phenolic compounds in wine and other beverages. Phenols can be detected in their native state,[11,20–22] while amines require derivatization to be compatible with UV detection.[23–26] Although these methods are adequate for measuring a few metabolites, the limited selectivity makes it difficult to characterize a large (e.g., 20+) panel of metabolites, especially in complex mixtures. Mass spectrometry (MS) detection offers a way to overcome these limitations. MS has much better selectivity than UV detection, making it possible to distinguish many more metabolites, even co-

eluting compounds, in complex mixtures. Using tandem mass spectrometry (MS/MS) allows for greater confidence in peak identification from unique fragmentation patterns. Additionally, MS/MS is more sensitive than UV, allowing for the measurement of trace metabolites which may not be detected with UV. Mass spectrometry does suffer from instrument drift and matrix effects, but this problem can be corrected through the use of internal standards labeled with stable isotopes.

Some work has been done for the analysis of native amines and phenolic compounds in wine with LC-MS.[12,27–29] However, there are still challenges which much be addressed. Polar amines are poorly retained with reversed phase chromatography, and sensitivity for some trace metabolites may still be limiting. Some of the same derivatization techniques used in UV detection of amines can be beneficial to mass spectrometry and help overcome these challenges. Tagging metabolites with a hydrophobic moiety increases retention of polar metabolites, while also increasing ESI ionization efficiency up to 10,000-fold.[30,31] Additionally, derivatization makes it easy to generate internal standards for each targeted metabolite through the use of stable isotope labeled derivatizing reagents. Labeling improves quantification by accounting for instrument drift and matrix effects, and can aid in peak selection in the presence of background peaks and retention time drift.

Several reagents have been reported that have use for amines and phenols by LC-MS. Derivatization with 1,2-naphthoquinone-4-sulfonate has been used with LC-MS for wine analysis previously.[17] Dansyl chloride derivatization has been used in wine for LC-UV analysis.[24] This same reagent has recently been promoted for the determination of phenols and amine metabolites with LC-MS in a variety of samples including urine, cerebrospinal fluid, and plasma.[31–34] Benzoyl chloride (BzCl) has also been used for LC-UV[35–38] as well as LC-MS.[30,39]

Like dansyl chloride, this reagent reacts with amines, phenols, and some hydroxyls. BzCl may have advantages, though, over other reagents for food analysis. The reaction is near instantaneous at room temperature and produces photostable derivatives.[30,39] Furthermore, ^{13}C labeled reagent is readily available at a reasonable cost enabling routine creation of internal standards for all analytes. Here, we demonstrate the application of BzCl derivatization with LC-MS/MS for determination of 56 amine and phenol metabolites in wine. To our knowledge, this method is unique in its capability to measure both amines and phenols in wine in a single, quick assay. Furthermore, the method assays a much larger panel of compounds than other methods, is shown to provide accurate quantitative data, and may enable distinguishing of varietals and location of production for wine.

Experimental

Chemicals and reagents

All chemicals were purchased from Sigma-Aldrich (St. Louis, MO) unless otherwise noted. Water and acetonitrile were Burdick & Jackson HPLC grade purchased from VWR (Radnor, PA). Stock solutions of 2 M Glc; 1 M Ch; 50 mM Pro; 10 mM ACh, Ala, Arg, Asn, Asp, βAla, Cad, Cit, Cys, DA, DOMA, DOPA, DOPAC (Acros Organics, Geel, Belgium), DOPEG, ETA, GABA, Gln, Glu, Gly, His, Hist, HVA (Tocris, Bristol, UK), Leu, Lys, Met, MOPEG, NAP, Orn (Acros Organics, Geel, Belgium), Phe, PhEt (MP Biomedicals, Santa Ana, CA), Put, Ser, Spd, Spm, Tau, Thr, TyrA Val, VMA; 5 mM Ado, Trp; 2 mM Tyr; 250 μM TrpA, and 20 nM d4-ACh and d4-Ch (C/D/N Isotopes, Pointe-Claire, Canada) were prepared in water and stored at -80 °C. Stock solutions of 10 mM Caf, Cou (TCI Chemicals, Philadelphia, PA), Fer, Gal (Acros Organics, Geel, Belgium), PCA, Sin, TOH, VA, and VN were prepared in ethanol

and stored at -20 °C. Wine was purchased from a local retailer. The varietals selected were Cabernet Sauvignon and Merlot, each from California and Australia.

A standard mixture was prepared in water for use in calibration standards. Preparation of calibration standards and internal standards has previously been described.[30,39] Calibration ranges for each metabolite are listed in Table 5-1. Single-use aliquots of calibration standards and internal standards were prepared and stored at -80 °C. On the day of use, an internal standard aliquot was thawed, diluted 100-fold in 20% (v/v) acetonitrile containing 1% (v/v) sulfuric acid, and spiked with deuterated acetylcholine and choline to a final concentration of 20 nM. A fresh BzCl solution was prepared daily.

Sample preparation and derivatization

Three aliquots of 500 μL from each wine sample were filtered through Amicon Ultra spin filters (30k MWCO, Millipore Sigma, Billerica, MA) by centrifugation for 5 min at 12,100 g. The filtered wine was diluted 10-fold in water. Filtered, diluted wine was derivatized by sequential addition of 10 μL 100 mM sodium carbonate, 10 μL 2% (v/v) BzCl in acetonitrile, and 10 μL internal standard solution. Calibration standards were prepared in water and derivatized in the same manner.

Metabolite analysis by LC-MS/MS

Analysis was performed using a Waters (Milford, MA) nanoAcquity UPLC. An Acquity HSS T3 C18 column (1 mm x 100 mm, 1.8 μm, 100 Å pore size) was used. The autosampler was kept at ambient temperature, and the column was kept at 27 °C. The injection size was 5 μL using partial loop injection mode. Mobile phase A was 10 mM ammonium formate with 0.15%

formic acid. Mobile phase B was acetonitrile. The flow rate was 100 µL/min, and the gradient used was: initial, 0% B; 0.01 min, 15% B; 0.5 min, 17% B; 14 min, 55% B; 14.5 min, 70% B; 18 min, 100% B; 19 min, 100% B; 19.1 min, 0% B; 20 min, 0% B. A 10 minute re-equilibration period followed each injection.

Compound	Calibration Range (µM)	Compound	Calibration Range (µM)
ACh	0.0025 - 0.5	Hist	0.05 - 10
Ado	0.00025 - 0.05	HVA	0.005 - 1
Agm	0.0005 - 0.1	Leu	0.25 - 50
Ala	0.25 - 50	Lys	0.1 - 20
Arg	0.1 - 20	Met	0.025 - 5
Asn	0.05 - 10	MOPEG	0.00025 - 0.05
Asp	0.1 - 20	NAP	0.0025 - 0.5
βAla	0.025 - 5	Orn	0.025 - 5
Cad	0.005 - 1	PCA	0.025 - 5
Caf	0.025 - 5	Phe	0.05 - 10
Ch	0.25 - 50	PhEt	0.005 - 1
Cit	0.005 - 1	Pro	10 - 2000
Cou	0.025 - 5	Put	0.05 - 10
Cys	0.0005 - 0.1	Ser	0.05 - 10
DA	0.00025 - 0.05	Sin	0.0005 - 0.1
DOMA	0.00025 - 0.05	Spd	0.0025 - 0.5
DOPA	0.00025 - 0.05	Spm	0.00025 - 0.05
DOPAC	0.00025 - 0.05	Tau	0.0025 - 0.5
DOPEG	0.00025 - 0.05	Thr	0.025 - 5
ETA	0.1 - 20	TOH	0.25 - 50
Fer	0.25 - 50	Trp	0.005 - 1
GABA	0.1 - 20	TrpA	0.0001 - 0.02
Gal	0.25 - 50	Tyr	0.025 - 5
Glc	5 - 1000	TyrA	0.025 - 5
Gln	0.0005 - 0.1	VA	0.025 - 5
Glu	0.25 - 50	Val	0.05 - 10
Gly	0.25 - 50	VMA	0.00025 - 0.05
His	0.0005 - 0.1	VN	0.0025 - 0.5

Table 5-1: Calibration ranges for each metabolite.

Detection was performed on an Agilent (Santa Clara, CA) 6410B triple quadrupole mass spectrometer in dynamic multiple reaction monitoring (dMRM) mode. Electrospray ionization

was used in positive mode at 4 kV. The gas temperature was 350 °C, gas flow was 11 L/min, and the nebulizer was at 15 psi. MRM conditions are listed in Table 5-2. Peak integration was performed using Agilent MassHunter Quantitative Analysis for QQQ, version B.05.00. All peaks were visually inspected to ensure proper integration.

Compound	Precursor (m/z)	Product (m/z)	Fragmentor (V)	Collision Energy (V)	Retention Time (min)
Ch	104	60	120	20	1.25
	108	60	120	20	1.25
ACh	146	87	120	15	1.37
	150	91	120	15	1.37
Bz-His	260	110	130	20	2.44
	266	110	130	20	2.44
Bz-Tau	230	105	120	10	2.57
	236	111	120	10	2.57
Bz-Arg	279	105	135	30	2.61
	285	111	135	30	2.61
Bz-Hist	216	105	120	20	2.65
	222	111	120	20	2.65
Bz-Asn	237	105	120	20	2.66
	243	111	120	20	2.66
Bz-Gln	251	105	120	20	2.76
	257	111	120	20	2.76
Bz-Ser	210	105	120	20	2.78
	216	111	120	20	2.78
Bz-Cit	280	105	120	20	2.89
	286	111	120	20	2.89
Bz-Agm	235	176	110	30	2.96
	241	182	110	30	2.96
Bz-Asp	238	105	120	10	2.97
	244	111	120	10	2.97
Bz-ETA	166	105	120	20	2.97
	172	111	120	20	2.97
Bz-Glc	307	185	130	20	3.07
	313	185	130	20	3.07
Bz-Gly	180	105	120	10	3.1
	186	111	120	10	3.1
Bz-Glu	252	105	120	20	3.22
	258	111	120	20	3.22
Bz-BAla	194	105	120	20	3.5
	200	111	120	20	3.5
Bz-NAP	235	176	135	20	3.6
	241	182	135	20	3.6
Bz-Ala	194	105	120	20	3.7
	200	111	120	20	3.7

Compound	Precursor (m/z)	Product (m/z)	Fragmentor (V)	Collision Energy (V)	Retention Time (min)
Bz-GABA	208	105	120	10	3.79
	214	111	120	10	3.79
Bz-Pro	220	105	120	20	4.05
	226	111	120	20	4.05
Bz-Ado	372	136	120	30	5.35
	378	136	120	30	5.35
Bz-Val	222	105	120	30	5.94
	228	111	120	30	5.94
Bz-Met	254	105	120	15	6
	260	111	120	15	6
Bz-Orn	341	174	120	15	6.4
	353	180	120	15	6.4
Bz-Lys	355	188	120	20	7.11
	367	194	120	20	7.11
Bz-Put	297	105	120	30	7.53
	309	111	120	30	7.53
Bz-Xle	236	105	120	30	8.12
	242	111	120	30	8.12
Bz-Phe	270	120	120	10	8.37
	276	120	120	10	8.37
Bz-Thr	224	105	140	20	8.39
	230	111	140	20	8.39
Bz-VMA	320	105	120	10	8.4
	326	111	120	10	8.4
Bz-Trp	309	159	120	10	8.5
	315	159	120	10	8.5
Bz-MOPEG	306	105	120	20	8.55
	312	111	120	20	8.55
Bz-Cad	311	105	130	30	8.56
	323	111	130	30	8.56
Bz-Cys	330	105	120	20	10.1
	342	111	120	20	10.1
Bz-Spd	458	162	120	30	10.43
	476	168	120	30	10.43
Bz-PhEt	226	105	120	15	10.94
	232	111	120	15	10.94
Bz-TrpA	265	144	130	30	10.99
	271	144	130	30	10.99
Bz-HVA	304	105	120	15	11.75
	310	111	120	15	11.75
Bz-TOH	243	105	120	20	11.77
	249	111	120	20	11.77
Bz-DOMA	410	105	130	20	11.95
	422	111	130	20	11.95
Bz-VA	273	105	120	20	12
	279	111	120	20	12

Compound	Precursor (m/z)	Product (m/z)	Fragmentor (V)	Collision Energy (V)	Retention Time (min)
Bz-Spm	619.6	497	135	25	12.1
	643.6	515.6	135	25	12.1
Bz-DOPEG	396	105	120	20	12.2
	408	111	120	20	12.2
Bz-Tyr	390	105	120	30	12.78
	402	111	120	30	12.78
Bz-Cou	269	105	120	20	12.89
	275	111	120	20	12.89
Bz-Fer	299	105	120	20	13
	305	111	120	20	13
Bz-Sin	329	105	130	20	13.03
	335	111	130	20	13.03
Bz-VN	257	105	120	20	13.8
	263	111	120	20	13.8
Bz-DOPAC	394	105	140	20	14.22
	406	111	140	20	14.22
Bz-PCA	380	105	120	20	14.4
	392	111	120	20	14.4
Bz-DOPA	510	360	120	30	14.53
	528	372	120	30	14.53
Bz-TyrA	346	105	135	25	14.67
	358	111	135	25	14.67
Bz-Caf	406	105	120	20	14.9
	418	111	120	20	14.9
Bz-Gal	500	105	140	30	16
	518	111	140	30	16
Bz-DA	466	105	140	20	16.02
	484	111	140	20	16.02

Table 5-2: MRM conditions for benzoylated metabolites and their internal standards.

Method evaluation

Limits of detection (LOD) were calculated as three standard deviations of the blank, using a six point calibration with three replicates. Limits of quantification (LOQ) were calculated as ten standard deviations of the blank. The same calibration was used to determine linearity for each metabolite. Repeatability was defined as the RSD for triplicate analysis of an aqueous standard at relevant metabolite concentrations. Recovery was determined by spiking three aliquots each of 200 μL wine with 40 μL of either water or 5X concentrated standards. The

spiked wine was prepared and analyzed as described previously. The expected concentration was determined by adding the known, spiked concentration to the measured concentration of the sample spiked with water. Recovery was calculated by comparing the concentration of the standard spiked wine to the expected concentration.

Statistical analysis

Single factor ANOVA and unpaired, two-tailed student's *t*-tests were performed. Differences were deemed significant if $P \leq 0.05$ following Holm-Bonferroni correction.

Results and discussion

Metabolite selection

We have previously described BzCl derivatization of 70 amine and phenol metabolites in biological samples.[39] We used that previous work as a basis for developing a method for analysis of wine to test the utility of this approach for food analysis. Of the 70 compounds previously assayed, 46 were selected as potentially relevant in wine. An additional 10 metabolites were chosen to add to the method: hydroxybenzoic acids gallic acid, protocatechuic acid, and vanillic acid; hydroxycinnamic acids caffeic acid, ferulic acid, *p*-coumaric acid, and sinapic acid; phenolic aldehyde vanillin; phenylethanoid tyrosol; and polyamine cadaverine. These metabolites were selected based on their relevance in wine and availability. In principle, BzCl derivatization could be used for the assay of additional phenolic acids as well.

Attempts to extend the method to some other polyphenols revealed some limitations. Due to the excess of reagent in the reaction mixture, the BzCl reaction typically goes to completion. In the case of sinapic acid, a low yield of underivatized product was observed, which we believe

is due to steric hindrance of the 4-phenol. Linear calibrations were still achieved, so this did not appear to limit quantification.

Additionally, flavonols did not appear to label efficiently with BzCl. Quercetin, for example, has five potential labeling sites. Unlabeled, singly labeled, and doubly labeled quercetin were the primary species detected. This finding is in contrast with metabolites like dopamine, which has three labeling sites, and only triply labeled dopamine is detected. We believe the poor reaction efficiency is due to resonance stabilization and hydrogen bonding between the phenols. While the conditions used here are not compatible with flavonol detection, these metabolites can be detected directly using LC-MS,[12] or with dansyl chloride,[33] where the harsher reaction conditions allow for derivatization of flavonols.

Figures of merit

After pilot experiments revealed that the 56 target compounds could be labeled with BzCl, we developed a LC-MS/MS method that utilized gradient elution and multiple reaction monitoring with optimized MS/MS for each compound. Figure 5-1 shows that reasonable separation was achieved using a 20 min gradient. No differences in peak shape were observed between aqueous standards and wine. LODs, repeatability, recovery, and linearity for each metabolite are listed in Table 5-3. LODs for all but 12 of the studied metabolites were below 10 nM, and all were below 1 μM. Every metabolite studied was above the limit of detection in the wines. Thus, the sensitivity of the method is appropriate for wine analysis, and could even be applied to wine subject to greater dilution. RSDs were below 10% for all metabolites except vanillin, vanillic acid, agmatine, and vanillymandelic acid. RSDs for these metabolites were

below 15%. All metabolites produced linear calibrations (R^2 > 0.99), allowing for reliable quantification.

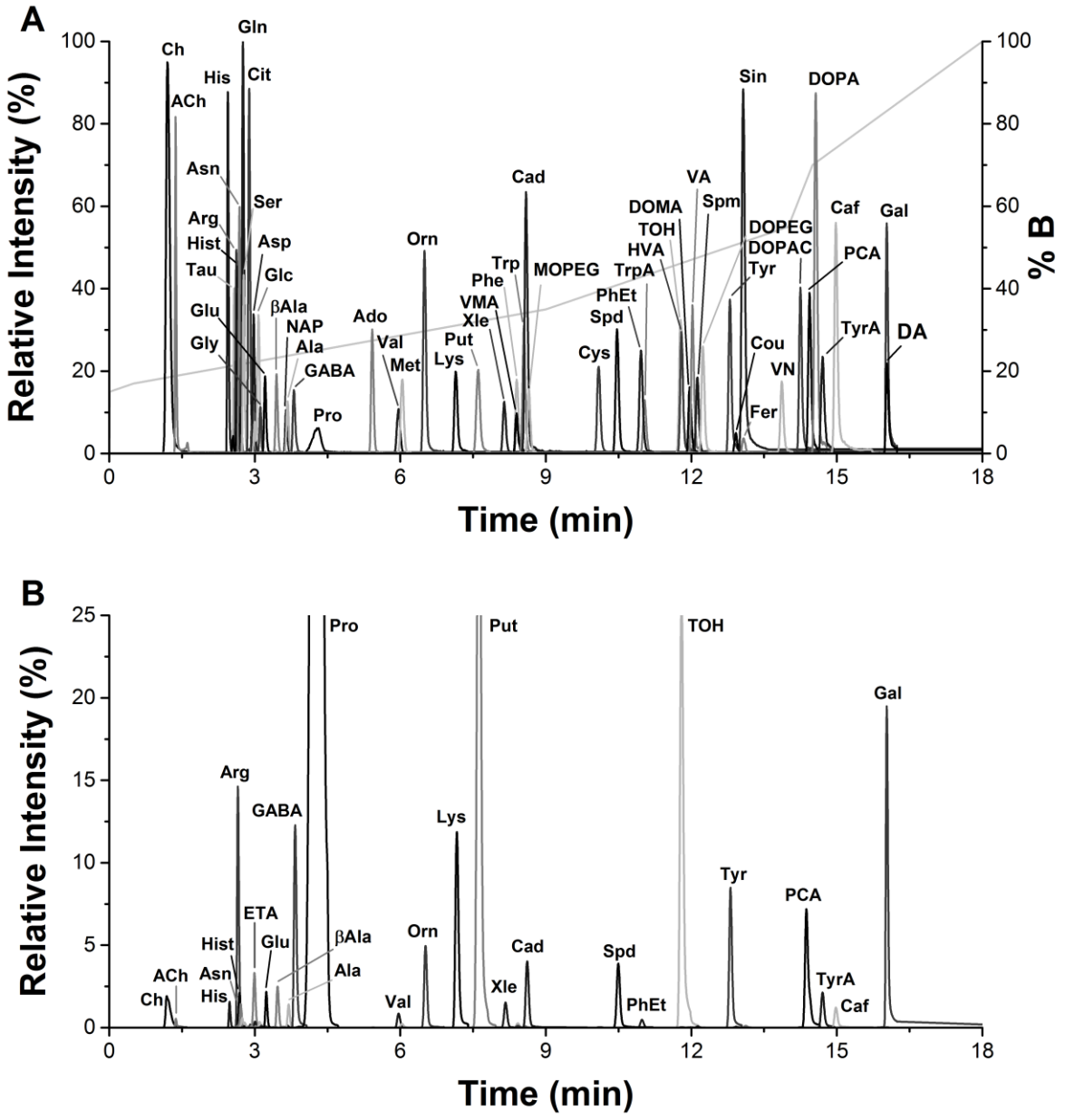

Figure 5-1: Extracted ion chromatogram of 56 amine and phenolic metabolites. A. Standards in aqueous solution. Gradient is overlaid as % B. B. Example chromatogram from filtered, diluted wine. No significant differences in peak shape or retention times were observed between standards and wine samples.

Compound	LOD (nM)	RSD (%)	Linearity (R^2)	Compound	LOD (nM)	RSD (%)	Linearity (R^2)
Ch	40	0.5	0.9995	Phe	2	0.7	0.9997
ACh	0.5	2	0.9998	Thr	2	5	0.9994
His	1	2	0.9927	VMA	1	13	0.9958
Tau	2	3	0.9996	Trp	4	2	0.995
Arg	2	2	0.9993	Cad	0.4	0.4	0.9996
Hist	1	2	0.9994	MOPEG	0.3	1	0.9993
Asn	1	0.4	0.9958	Cys	0.2	7	0.9996
Gln	0.4	2	0.9921	Spd	0.3	6	0.9958
Ser	60	3	0.9998	PhEt	0.9	2	0.9986
Cit	0.5	2	0.9999	TrpA	0.3	0.8	0.995
Agm	0.2	12	0.9939	TOH	40	3	0.9973
ETA	4	6	0.9995	HVA	0.7	4	0.9992
Asp	4	4	0.999	DOMA	0.3	5	0.9989
Glc	300	2	0.9999	VA	20	11	0.9905
Gly	8	3	0.9942	Spm	0.2	4	0.9903
Glu	5	0.5	0.999	DOPEG	1	2	0.9953
BAla	1	0.5	0.9999	Tyr	10	3	0.9997
NAP	0.2	5	0.9995	Cou	30	2	0.9961
Ala	8	0.6	0.9999	Fer	90	8	0.9993
GABA	3	6	0.9995	Sin	3	5	0.9971
Pro	200	4	0.9972	VN	4	11	0.994
Ado	0.3	0.7	0.9959	DOPAC	0.1	4	0.9999
Val	3	2	0.9973	PCA	20	9	0.9999
Met	1	2	0.9988	DOPA	0.5	7	0.9932
Orn	2	3	0.9997	TyrA	20	1	0.998
Lys	6	4	0.9947	Caf	70	0.1	0.9915
Put	3	6	0.9973	Gal	700	5	0.9999
Xle	7	4	0.9996	DA	0.7	5	0.9994

Table 5-3: Summary of limit of detection (LOD), repeatability (RSD), and linearity for a six point calibration using aqueous standards (n = 3).

All quantification was based on comparison to internal standards consisting of ^{13}C-BzCl labeled standards added to the samples. The significance of using internal standards was assessed by comparing concentrations calculated based on analyte peak area alone to analyte peak area normalized to internal standard peak area. Without internal standards, calculated concentrations ranged from 27% to 136% of the value determined through use of internal standards (Figure 5-2).

This result demonstrates the necessity of including internal standards for each metabolite for accurate quantification in complex samples. Individual internal standards are easily prepared for this method through the use of ^{13}C-BzCl.

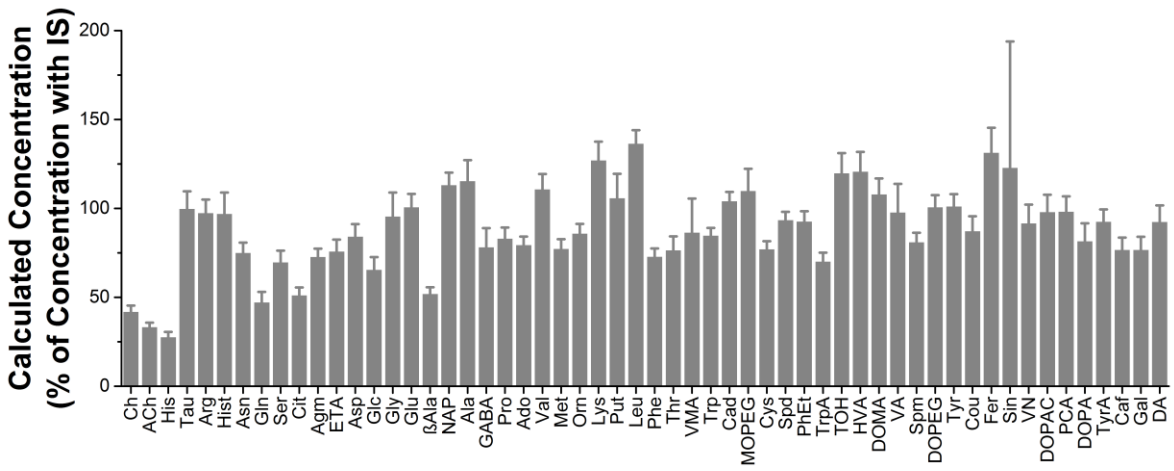

Figure 5-2: Accuracy of concentrations without internal standards relative to concentrations calculated with internal standards. Without internal standards, concentrations ranged from 27% to 136% of the concentrations normalized to internal standards. Data shown is average ± standard deviation (n = 3).

To assess accuracy and recovery of the method, wine was spiked with a known concentration of standards, and the calculated concentration was compared to the expected concentration. If the internal standards were not sufficiently accounting for matrix effects, we would expect low accuracy from this experiment. However, calculated recovery ranged from 80% to 150%, and average recovery was 101%. Of the 56 metabolites, 46 had recoveries within the range of 90% to 110%. Gallic acid had the lowest recovery of 80%, and adenosine, protocatechuic acid, and sinapic acid had the three highest recoveries, all at or above 130%. Inspection of the data revealed that each of these metabolites had a single deviant point contributing to the inaccuracy. Accuracy was greatly improved if this point is removed, so we expect that these problems were sample preparation errors and that a greater number of replicates would further improve these calculations. In general, recoveries were repeatable, further demonstrating that the method allows for accurate and reliable quantification.

Wine analysis

To demonstrate the suitability of the method for wine, we compared four: a Californian Merlot, a Californian Cabernet Sauvignon, an Australian Merlot, and an Australian Cabernet Sauvignon. These choices allowed us to determine if the method could distinguish between region of production or varietal based on the metabolites included. The wine was filtered prior to analysis to remove any particulate matter. No difference was observed in calculated concentrations after filtration with spin columns or syringe filters, so spin columns were chosen for the ability to prepare multiple samples simultaneously. Filtered wine was then diluted 10 or 100 fold in water prior to derivatization. We found that low abundance metabolites such as tryptamine and vanillylmandelic acid were undetectable after 100 fold dilution, so 10 fold dilution was selected for analysis. Calculated concentrations for each of the tested wines are listed in Table 5-4.

When compared by region of production, 24 of the 56 metabolites were found to be different ($P < 0.05$) between Australian and Californian wines (Figure 5-3). These distinguishing compounds were polyamines spermidine and spermine; phenolic acids caffeic acid, gallic acid, homovanillic acid, protocatechuic acid, and vanillic acid; amino acids asparagine, aspartate, histidine, leucine/isoleucine, lysine, phenylalanine, serine, threonine, tyrosine, and valine; and biogenic amines choline, DOPA, DOPEG, histamine, phenethylamine, tryptamine, and tyramine. All of these were found to be higher in Australian wines except homovanillic acid, spermine, and caffeic acid. Differences in amines and phenols based on geographic origin have been observed previously using LC with spectrophotometric detection [15,40], and may result from differences in climate, soil conditions, or fertilizers. Larger sample sizes would be required to determine if these differences are generalizable among the different regions. Further study would also be

required to determine the exact relationship between these metabolites and the location of production.

Of the 56 metabolites assayed, five were found to differ significantly ($P \leq 0.05$) based on varietal following Holm-Bonferroni correction (Figure 5-4). These included polyamines cadaverine, putrescine, and N-acetylputrescine; ferulic acid, and glutamic acid. The polyamines were higher in Cabernets, while ferulic acid and glutamate were higher in the Merlots. It is important to note that wines can be labeled as a particular varietal as long as that varietal makes

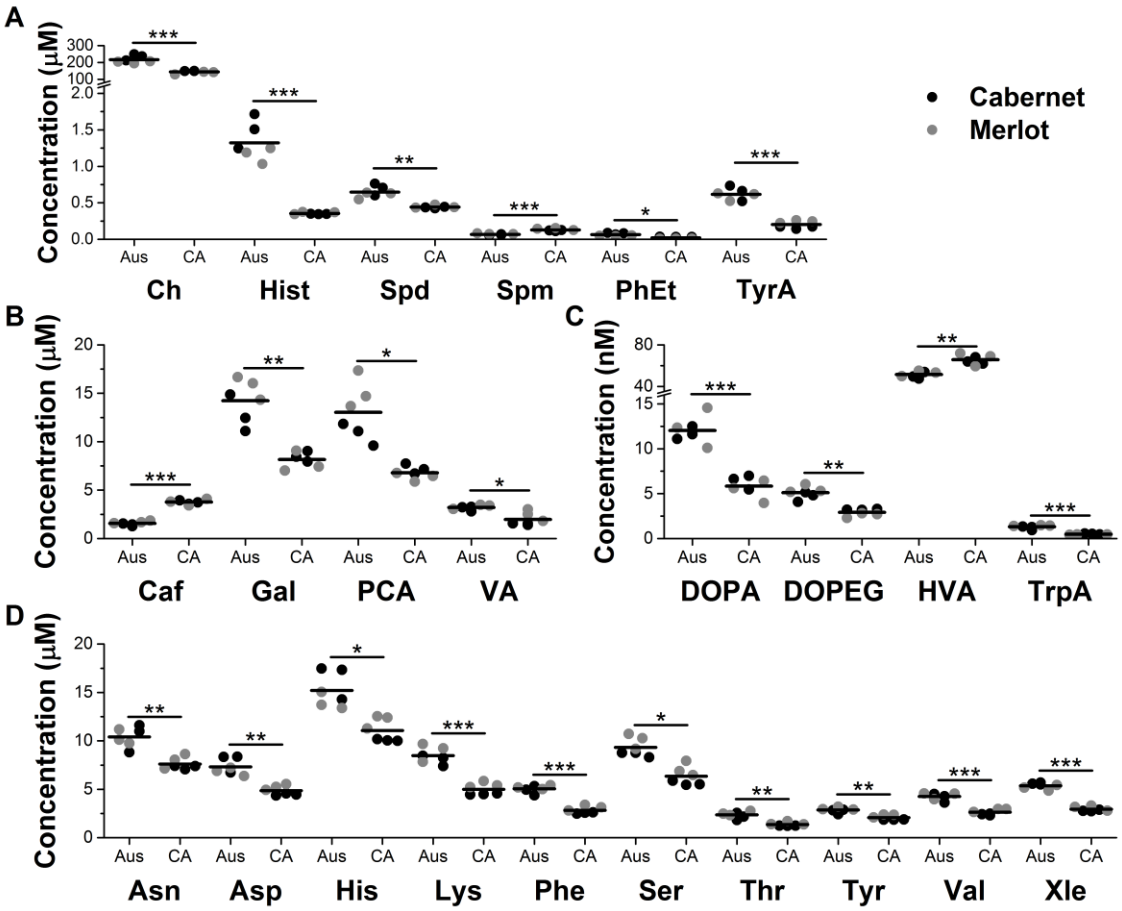

Figure 5-3: Metabolites showing significant differences between locations of production. A. Biogenic amines. B. Phenolic acids. C. Trace metabolites. D. Amino acids. Unpaired, two-tailed Student's *t*-tests were performed and the Holm-Bonferroni correction was used. Each point is a single sample, and the horizontal bar is the mean. Data shown is uncorrected for dilution. * $p \leq 0.05$; ** $p \leq 0.01$; *** $p \leq 0.001$. Aus: Australia; CA: California; Ch: choline; Hist: histamine; Spd: spermidine; Spm: spermine; PhEt: phenethylamine; TyrA: tyramine; Caf: caffeic acid; Gal: gallic acid; PCA: protocatechuic acid; VA: vanillic acid; DOPA: 3,4-dihydroxyphenylalanine; DOPEG: 3,4-dihydroxyphenylglycol; HVA: homovanillic acid; TrpA: tryptamine; Asn: asparagine; Asp: aspartic acid; His: histidine; Lys: lysine; Phe: phenylalanine; Ser: serine; Thr: threonine; Tyr: tyrosine; Val: valine; Xle: leucine/isoleucine.

Compound	Units	Australia Cabernet		Australia Merlot		California Cabernet		California Merlot	
ACh	nM	544 ± 34.6	(6.35)	467 ± 124	(26.6)	353 ± 8.87	(2.51)	356 ± 19.7	(5.53)
Ado	nM	52.3 ± 3.48	(6.56)	25.9 ± 2.65	(10.2)	15.8 ± 1.76	(11.1)	19.7 ± 2.12	(10.7)
Agm	nM	58.9 ± 2.96	(5.02)	35.9 ± 7.53	(21.0)	27.9 ± 3.15	(11.3)	16.0 ± 5.97	(37.3)
Ala	µM	35.0 ± 2.96	(8.48)	37.7 ± 2.23	(5.92)	21.7 ± 0.74	(3.42)	36.5 ± 2.79	(7.64)
Arg	µM	20.2 ± 2.02	(9.99)	18.7 ± 1.15	(6.16)	17.4 ± 0.38	(2.15)	15.4 ± 0.58	(3.74)
Asn	µM	10.5 ± 1.47	(14.0)	10.4 ± 0.74	(7.16)	7.29 ± 0.20	(2.70)	7.94 ± 0.75	(9.42)
Asp	µM	7.81 ± 0.93	(11.9)	6.82 ± 0.42	(6.16)	4.46 ± 0.11	(2.38)	5.24 ± 0.30	(5.74)
BAla	µM	17.9 ± 1.64	(9.20)	14.0 ± 1.20	(8.53)	15.7 ± 0.81	(5.15)	15.0 ± 0.93	(6.19)
Cad	nM	407 ± 40.9	(10.0)	53.8 ± 4.00	(7.44)	456 ± 4.11	(0.90)	45.3 ± 2.77	(6.11)
Caf	µM	1.42 ± 0.14	(9.53)	1.7 ± 0.14	(8.25)	3.75 ± 0.19	(5.11)	3.77 ± 0.34	(9.13)
Ch	µM	233 ± 18.7	(8.02)	202 ± 6.72	(3.33)	149 ± 0.91	(0.61)	139 ± 8.19	(5.90)
Cit	nM	392 ± 45.5	(11.6)	268 ± 27.0	(10.1)	428 ± 32.01	(7.47)	523 ± 14.6	(2.80)
Cou	µM	1.83 ± 0.20	(11.03)	1.37 ± 0.14	(10.3)	2.08 ± 0.03	(1.42)	1.82 ± 0.22	(11.9)
Cys	nM	252 ± 30.4	(12.1)	547 ± 44.9	(8.21)	518 ± 34.2	(6.61)	1250 ± 75.5	(6.06)
DA	nM	4.24 ± 0.77	(18.1)	4.56 ± 0.89	(19.4)	6.31 ± 1.53	(24.2)	4.35 ± 0.81	(18.5)
DOMA	nM	19.1 ± 2.78	(14.6)	17.2 ± 0.41	(2.36)	18.1 ± 1.04	(5.78)	14.7 ± 1.60	(10.9)
DOPA	nM	11.7 ± 0.71	(6.05)	12.3 ± 2.24	(18.1)	6.36 ± 0.80	(12.5)	5.33 ± 1.26	(23.7)
DOPAC	nM	9.95 ± 1.37	(13.8)	12.9 ± 0.67	(5.20)	11.1 ± 0.91	(8.20)	6.31 ± 0.45	(7.20)
DOPEG	nM	4.69 ± 0.54	(11.5)	5.51 ± 0.47	(8.45)	3.23 ± 0.06	(1.76)	2.60 ± 0.28	(10.7)
ETA	µM	23.1 ± 2.68	(11.6)	26.6 ± 3.21	(12.1)	26.8 ± 1.65	(6.17)	26.7 ± 2.34	(8.77)
Fer	µM	14.5 ± 1.90	(13.1)	27.8 ± 3.85	(13.9)	13.9 ± 1.60	(11.5)	22.9 ± 1.49	(6.50)
GABA	µM	29.7 ± 4.44	(14.9)	18.9 ± 1.20	(6.37)	12.0 ± 0.28	(2.29)	14.4 ± 1.14	(7.97)
Gal	µM	12.8 ± 1.91	(14.9)	15.7 ± 1.21	(7.71)	8.47 ± 0.55	(6.47)	7.83 ± 1.08	(13.8)
Glc	mM	1.54 ± 0.13	(8.54)	1.55 ± 0.06	(3.85)	1.15 ± 0.06	(5.63)	1.58 ± 0.10	(6.61)
Gln	nM	485 ± 37.3	(7.69)	417 ± 49.1	(11.8)	357 ± 10.5	(2.95)	512 ± 58.6	(11.5)
Glu	µM	12.8 ± 1.06	(8.28)	15.5 ± 0.58	(3.71)	11.7 ± 0.27	(2.34)	17.6 ± 1.43	(8.10)
Gly	µM	18.9 ± 1.68	(8.90)	20.8 ± 1.71	(8.22)	13.01 ± 1.03	(7.90)	20.2 ± 3.35	(16.6)
His	µM	16.4 ± 1.80	(11.0)	14.1 ± 0.88	(6.23)	10.07 ± 0.09	(0.90)	12.1 ± 0.69	(5.70)
Hist	µM	1.49 ± 0.24	(15.8)	1.16 ± 0.11	(9.57)	0.35 ± 0.003	(0.94)	0.36 ± 0.02	(4.33)
HVA	nM	50.2 ± 3.22	(6.41)	52.7 ± 2.62	(4.98)	64.6 ± 3.13	(4.85)	66.7 ± 6.51	(9.76)

Compound	Units	Australia Cabernet		Australia Merlot		California Cabernet		California Merlot	
Lys	μM	8.03 ± 0.57	(7.09)	8.92 ± 0.96	(10.8)	4.50 ± 0.06	(1.34)	5.49 ± 0.33	(5.94)
Met	nM	946 ± 99.6	(10.5)	981 ± 54.6	(5.57)	799 ± 12.9	(1.61)	911 ± 67.5	(7.40)
MOPEG	nM	9.84 ± 1.15	(11.7)	15.0 ± 2.35	(15.7)	13.6 ± 1.42	(10.5)	13.2 ± 2.64	(20.1)
NAP	nM	406 ± 32.3	(7.96)	171 ± 26.2	(15.3)	402 ± 5.57	(1.39)	170 ± 7.09	(4.18)
Orn	μM	4.01 ± 0.42	(10.4)	4.04 ± 0.32	(7.90)	5.13 ± 0.05	(0.93)	7.76 ± 0.53	(6.89)
PCA	μM	10.8 ± 1.14	(10.6)	15.2 ± 1.89	(12.4)	7.20 ± 0.51	(7.06)	6.36 ± 0.45	(7.03)
Phe	μM	4.89 ± 0.47	(9.66)	5.20 ± 0.20	(3.87)	2.55 ± 0.07	(2.88)	3.11 ± 0.29	(9.38)
PhEt	nM	79.9 ± 10.5	(13.1)	49.7 ± 4.79	(9.64)	34.3 ± 1.38	(4.03)	9.89 ± 0.86	(8.74)
Pro	mM	2.57 ± 0.20	(7.66)	2.52 ± 0.17	(6.58)	3.16 ± 0.19	(5.92)	2.51 ± 0.12	(4.76)
Put	μM	8.23 ± 1.01	(12.2)	4.30 ± 0.55	(12.7)	11.5 ± 0.24	(2.08)	4.50 ± 0.46	(10.1)
Ser	μM	8.61 ± 0.27	(3.14)	10.1 ± 0.79	(7.87)	5.62 ± 0.23	(4.08)	7.09 ± 0.77	(10.8)
Sin	nM	38.3 ± 16.9	(44.2)	35.6 ± 11.7	(32.9)	46.4 ± 8.10	(17.5)	35.9 ± 0.84	(2.34)
Spd	nM	690 ± 82.6	(12.0)	605 ± 51.3	(8.48)	434 ± 10.4	(2.39)	450 ± 22.5	(5.00)
Spm	nM	61.0 ± 8.37	(13.7)	75.3 ± 6.27	(8.33)	119 ± 7.44	(6.24)	141 ± 14.6	(10.4)
Tau	nM	167 ± 20.9	(12.6)	174 ± 16.5	(9.50)	239 ± 37.3	(15.6)	165 ± 19.2	(11.7)
Thr	μM	2.18 ± 0.37	(17.0)	2.53 ± 0.23	(8.89)	1.24 ± 0.01	(0.73)	1.49 ± 0.18	(12.0)
TOH	μM	34.6 ± 5.53	(16.0)	29.4 ± 0.32	(1.08)	28.2 ± 1.90	(6.75)	19.0 ± 1.93	(10.2)
Trp	nM	467 ± 57.6	(12.4)	717 ± 17.3	(2.42)	286 ± 23.7	(8.28)	508 ± 35.5	(6.98)
TrpA	nM	1.17 ± 0.21	(17.6)	1.44 ± 0.04	(3.04)	0.52 ± 0.05	(9.81)	0.44 ± 0.03	(6.55)
Tyr	nM	2.71 ± 0.26	(9.45)	3.01 ± 0.16	(5.22)	1.87 ± 0.01	(0.57)	2.28 ± 0.16	(6.85)
TyrA	nM	640 ± 108	(16.9)	591 ± 58.2	(9.85)	163 ± 17.0	(10.4)	244 ± 20.2	(8.29)
VA	μM	3.10 ± 0.26	(8.41)	3.31 ± 0.22	(6.75)	1.50 ± 0.08	(5.36)	2.45 ± 0.60	(24.5)
Val	μM	4.14 ± 0.46	(11.2)	4.37 ± 0.34	(7.75)	2.40 ± 0.09	(3.78)	2.86 ± 0.17	(6.09)
VMA	nM	53.3 ± 9.79	(18.4)	49.4 ± 8.24	(16.7)	36.3 ± 7.32	(20.2)	55.6 ± 0.77	(1.39)
VN	nM	128 ± 22.9	(17.9)	235 ± 23.4	(9.93)	101 ± 1.81	(1.79)	120 ± 7.86	(6.53)
Xle	μM	5.59 ± 0.10	(1.79)	5.16 ± 0.29	(5.71)	2.79 ± 0.08	(2.84)	3.10 ± 0.27	(8.71)

Table 5-4: Concentrations of amine and phenolic metabolites in wine. Concentrations are not corrected for dilution. Data is average ± standard deviation (RSD), n = 3.

up 75% of the composition in the United States, or 85% in Australia. Without knowing what the remaining composition is, we cannot draw conclusions of the relationship between these metabolites and the specific varietals. Larger sample sizes would be required to determine if these differences are generalizable among the different varietals; however, these results show the feasibility of distinguishing the different types of wine used here by the 56 compounds measured.

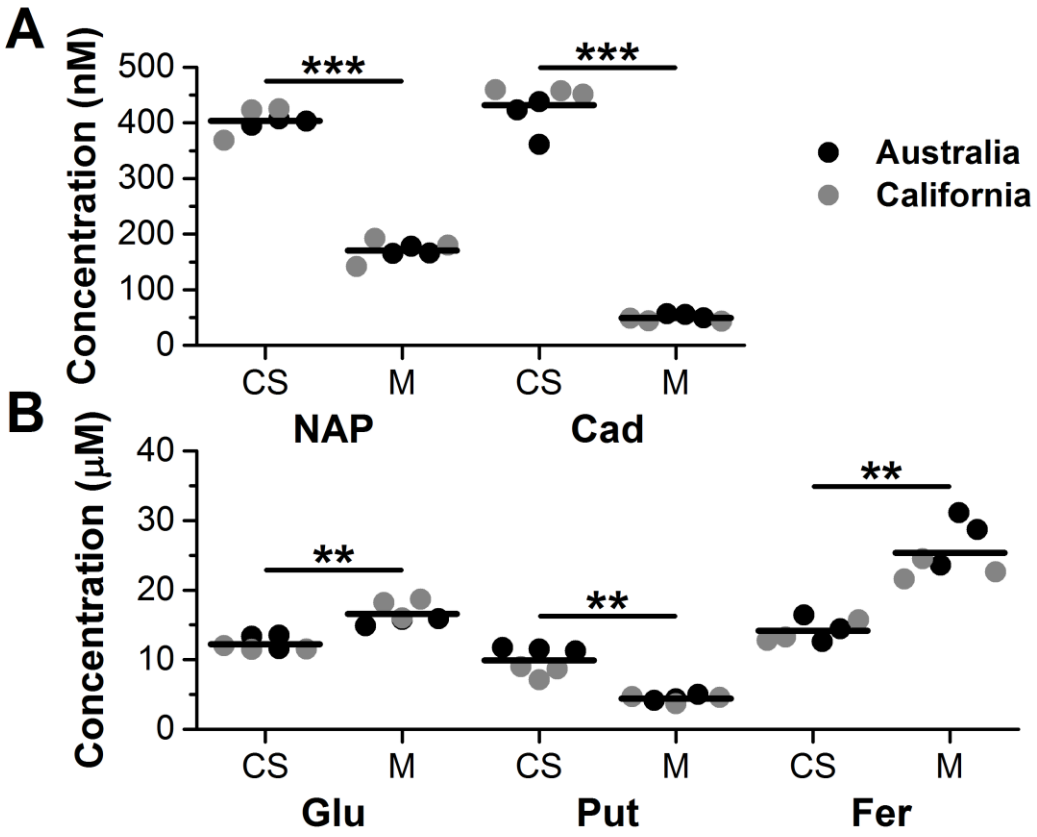

Figure 5-4: Metabolites showing significant differences between wine varietals. A. Metabolites at nanomolar concentrations. B. Metabolites at micromolar concentrations. Unpaired, two-tailed *Student's t*-tests were performed and the Holm-Bonferroni correction was used. Data shown is uncorrected for dilution. * $p \leq 0.05$; ** $p \leq 0.01$; *** $p \leq 0.001$. CS: Cabernet Sauvingnon; M: Merlot; NAP: N-acetylputrescine; Cad: cadaverine; Glu: glutamic acid; Put: putrescine; Fer: ferulic acid.

Comparison to current methods

Comparison of the BzCl-LC-MS/MS method to other methods used for measurement of phenols and amines in wine reveals that it has substantial advantages for quantitative,

multiplexed assays that can provide significant information on the wine. LC-UV is a commonly used technique for the analysis of amines and phenols in wine. It is particularly well suited to phenols, which are naturally UV active. Methods for up to 20 phenols have been established.[22] 2D-LC can increase selectivity, at the cost of analysis time and complexity of the fluidics.[11] Amines can be detected by UV after derivatization, and methods for up to 33 amines have been established.[23] UV detection is simple and inexpensive, but LC-MS/MS offers greater flexibility, because both amines and phenols can be detected. Additionally, while trace amines such as tryptamine, phenethylamine, and agmatine are not consistently detected with UV, these metabolites were above our LODs in all samples tested.

Studies on using LC-MS for analysis of wine have been reported as the technique is becoming more widely available. Untargeted metabolomics has been performed in wine,[29] though we have focused on targeted methods as they are more reproducible and allow for absolute quantification. As with LC-UV, existing targeted LC-MS methods focus on either amines or phenols. Biogenic amine analysis has been limited to fewer than 10 amines while still requiring 20 min for separation.[17,28] Over 40 phenols have been detected in wine using 2D-LC-MS, but analysis time is over 60 min.[12] Our assay covers a combination of 56 amines and phenols with a 20 minute gradient. Benzoyl chloride derivatization allows for accurate quantification using easily generated stable isotope labeled internal standards, while adding minimal time for sample preparation per sample. Additionally, with the low limits of detection afforded by mass spectrometry and benzoyl chloride derivatization, we were able to detect trace metabolites, such as tryptamine, which are not routinely detected with other methods.

Conclusions

Benzoyl chloride derivatization with LC-MS/MS is a powerful technique for determination of amine and phenol metabolites in biological samples. To demonstrate its potential in wine, we have developed a quantitative assay for 56 metabolites in wine. It is likely that the method can be extended to many more amines and phenols in wine (and other foods) as needed for a given application. Combining phenols and amines in one assay is useful because they provide complementary information on the wine. Phenolic acids contribute to the flavor and aroma of wine, and are believed to have positive health benefits as well. High concentrations of biogenic amines are associated with spoilage and poor quality.

As a proof of concept, we applied our method to four wines of two varietals and from two locations of production. We identified five metabolites which were significantly different based on varietal, and twenty-four which were significantly different based on location. A broader, more rigorous study may allow for the distinction of wines by varietal and location of production using the observed metabolite profiles.

As previously demonstrated with biological samples, BzCl derivatization with LC-MS/MS is a powerful technique for food analysis. The derivatization process improves sensitivity and quantification, which is well worth the minimal added sample preparation time. Wine was selected for analysis; however, this method could be easily adapted to other beverages or even solid foods following appropriate extraction techniques.

References

(1) Luykx, D. M. A. M.; van Ruth, S. M. *Food Chem.* **2008**, *107* (2), 897–911.

(2) Reid, L. M.; O'Donnell, C. P.; Downey, G. *Trends Food Sci. Technol.* **2006**, *17* (7), 344–353.

(3) Arvanitoyannis, I. S.; Katsota, M. N.; Psarra, E. P.; Soufleros, E. H.; Kallithraka, S. *Trends Food Sci. Technol.* **1999**, *10* (10), 321–336.

(4) Makris, D. P.; Kallithraka, S.; Kefalas, P. *J. Food Compos. Anal.* **2006**, *19* (5), 396–404.

(5) Ancín-Azpilicueta, C.; González-Marco, A.; Jiménez-Moreno, N. *Crit. Rev. Food Sci. Nutr.* **2008**, *48* (3), 257–275.
(6) Manach, C.; Scalbert, A.; Morand, C.; Rémésy, C.; Jiménez, L. *American Journal of Clinical Nutrition*. American Society for Nutrition May 2004, pp 727–747.
(7) Scalbert, A.; Manach, C.; Morand, C.; Rémésy, C.; Jiménez, L. *Crit. Rev. Food Sci. Nutr.* **2005**, *45* (4), 287–306.
(8) Bach-Faig, A.; Berry, E. M.; Lairon, D.; Reguant, J.; Trichopoulou, A.; Dernini, S.; Medina, F. X.; Battino, M.; Belahsen, R.; Miranda, G.; Serra-Majem, L. *Public Health Nutr.* **2011**, *14* (12A), 2274–2284.
(9) Antolovich, M.; Prenzler, P.; Robards, K.; Ryan, D. *Analyst* **2000**, *125* (5), 989–1009.
(10) Dugo, P.; Cacciola, F.; Herrero, M.; Donato, P.; Mondello, L. *J. Sep. Sci.* **2008**, *31* (19), 3297–3308.
(11) Dugo, P.; Cacciola, F.; Donato, P.; Airado-Rodríguez, D.; Herrero, M.; Mondello, L. *J. Chromatogr. A* **2009**, *1216* (44), 7483–7487.
(12) Donato, P.; Rigano, F.; Cacciola, F.; Schure, M.; Farnetti, S.; Russo, M.; Dugo, P.; Mondello, L. *J. Chromatogr. A* **2016**, *1458*, 54–62.
(13) Romero, R.; Sánchez-Viñas, M.; Gázquez, D.; Bagur, M. G. *J. Agric. Food Chem.* **2002**, *50* (16), 4713–4717.
(14) Csomós, E.; Héberger, K.; Simon-Sarkadi, L. *J. Agric. Food Chem.* **2002**, *50* (13), 3768–3774.
(15) Héberger, K.; Csomós, E.; Simon-Sarkadi, L. *J. Agric. Food Chem.* **2003**, *51*, 8055–8060.
(16) Kiss, J.; Sass-Kiss, A. *J. Agric. Food Chem.* **2005**, *53*, 10042–10050.
(17) García-Villar, N.; Hernández-Cassou, S.; Saurina, J. *J. Chromatogr. A* **2009**, *1216* (36), 6387–6393.
(18) Sass-Kiss, A.; Kiss, J.; Havadi, B.; Adányi, N. *Food Chem.* **2008**, *110* (3), 742–750.
(19) Bodmer, S.; Imark, C.; Kneubühl, M. *Inflammation Research*. Birkhäuser-Verlag June 17, 1999, pp 296–300.
(20) Kerem, Z.; Bravdo, B. A.; Shoseyov, O.; Tugendhaft, Y. *J. Chromatogr. A* **2004**, *1052* (1–2), 211–215.
(21) Burin, V. M.; Arcari, S. G.; Costa, L. L. F.; Bordignon-Luiz, M. T. *J. Chromatogr. Sci.* **2011**, *49* (8), 647–651.
(22) Aznar, Ó.; Checa, A.; Oliver, R.; Hernández-Cassou, S.; Saurina, J. *J. Sep. Sci.* **2011**, *34* (5), 527–535.
(23) Gómez-Alonso, S.; Hermosín-Gutiérrez, I.; García-Romero, E. *J. Agric. Food Chem.* **2007**, *55* (3), 608–613.
(24) Soufleros, E. H.; Bouloumpasi, E.; Zotou, A.; Loukou, Z. *Food Chem.* **2007**, *101* (2), 704–716.
(25) Preti, R.; Antonelli, M. L.; Bernacchia, R.; Vinci, G. *Food Chem.* **2015**, *187*, 555–562.
(26) Liu, T.; Li, B.; Zhou, Y.; Chen, J.; Tu, H. *J. Inst. Brew.* **2015**, *121* (1), 163–166.
(27) Alonso Borbalán, Á. M.; Zorro, L.; Guillén, D. A.; García Barroso, C. *J. Chromatogr. A*

2003, *1012* (1), 31–38.
(28) Millán, S.; Sampedro, M. C.; Unceta, N.; Goicolea, M. A.; Barrio, R. J. *Anal. Chim. Acta* **2007**, *584* (1), 145–152.
(29) Arbulu, M.; Sampedro, M. C.; Gómez-Caballero, A.; Goicolea, M. A.; Barrio, R. J. *Anal. Chim. Acta* **2015**, *858*, 32–41.
(30) Song, P.; Mabrouk, O. S.; Hershey, N. D.; Kennedy, R. T. *Anal. Chem.* **2012**, *84*, 412–419.
(31) Guo, K.; Li, L. *Anal. Chem.* **2009**, *81* (10), 3919–3932.
(32) Tseng, C.-L.; Li, L. *Sci. China Chem.* **2014**, *57* (5), 678–685.
(33) Achaintre, D.; Buleté, A.; Cren-Olivé, C.; Li, L.; Rinaldi, S.; Scalbert, A. *Anal. Chem.* **2016**, *88* (5), 2637–2644.
(34) Wu, Y.; Streijger, F.; Wang, Y.; Lin, G.; Christie, S.; Mac-Thiong, J.-M.; Parent, S.; Bailey, C. S.; Paquette, S.; Boyd, M. C.; Ailon, T.; Street, J.; Fisher, C. G.; Dvorak, M. F.; Kwon, B. K.; Li, L. *Sci. Rep.* **2016**, *6* (November), 38718.
(35) Paleologos, E. K.; Chytiri, S. D.; Savvaidis, I. N.; Kontominas, M. G. *J. Chromatogr. A* **2003**, *1010* (2), 217–224.
(36) Kirschbaum, J.; Rebscher, K.; Brückner, H. *J. Chromatogr. A* **2000**, *881* (1–2), 517–530.
(37) Sethi, R.; Chava, S. R.; Bashir, S.; Castro, M. E. *Am. J. Anal. Chem.* **2011**, *2* (4), 456–469.
(38) Aflaki, F.; Ghoulipour, V.; Saemian, N.; Salahinejad, M. *Anal. Methods* **2014**, *6* (4), 1482–1487.
(39) Wong, J. M. T.; Malec, P. A.; Mabrouk, O. S.; Ro, J.; Dus, M.; Kennedy, R. T. *J. Chromatogr. A* **2016**, *1446*, 78–90.
(40) Rodríguez-Delgado, M.-Á.; González-Hernández, G.; Conde-González, J.-E.; Pérez-Trujillo, J.-P. *Food Chem.* **2002**, *78* (4), 523–532.

CHAPTER 6

Combination of benzoyl chloride and benzylamine derivatization to increase coverage of targeted metabolomics with liquid chromatography - mass spectrometry

Introduction

Metabolomics is a rapidly growing field which can play an important role in biological studies as it can connect both internal and external effects to observed phenotypes. Despite the growing interest, no current instrumentation is capable of measuring the entire metabolome. The Human Metabolome Database (HMDB) contains entries for nearly 40,000 endogenous metabolites and over 70,000 total metabolites.[1] Physical properties of the metabolites are highly variable, ranging from small polar sugars to large hydrophobic steroids. Additionally, endogenous concentrations range from sub-nanomolar to millimolar in biological samples. This variability limits the scope of untargeted metabolomics. NMR is capable of unbiased detection but is limited in sensitivity. Mass spectrometry is better suited for analysis of trace metabolites, but detection is biased by the coupled separation technique.

Rather than try to detect all metabolites, targeted metabolomics methods focus on a pre-determined selection of metabolites. These methods are more limited in scope but provide better reproducibility and quantification. Advances in HPLC-MS/MS technologies have made it possible to measure as many as 300 metabolites within a single assay.[2–5] However, detection is still biased by the chosen separation technique. Reversed phase chromatography is widely used, but is a poor choice for the analysis of polar metabolites, while HILIC is unsuited for analysis of

hydrophobic metabolites. It is desirable to overcome this bias to further increase the scope of these targeted methods.

A relatively simple method to improve the polarity range that can be analyzed is to perform a biphasic metabolite extraction and analyze the aqueous and organic phases separately.[6–8] This strategy is effective but can increase analysis time as multiple column chemistries and ionization polarities are commonly used for each phase. Another commonly used technique is chemical derivatization.[5,9–14] Labeling polar functional groups with a hydrophobic tag makes it possible to separate polar metabolites using RPLC, while providing enhanced ionization efficiency and the capability to easily generate internal standards through the use of stable isotope labeled derivatization reagents. These internal standards account for instrument drift over time, improving quantification. A stable isotope labeled derivatizing reagent can be used with calibration standards to create internal standards for each targeted metabolite without needing to obtain a stable isotope labeled version of each metabolite. Such derivatization methods make it possible to detect a wider range of metabolites with RPLC, but analysis is typically limited to metabolites possessing a specific functional group. Derivatization reagents for several functional groups have been developed so it is possible to use multiple techniques on a single sample, but this requires separate reactions and analyses.

We have previously explored benzoyl chloride (BzCl) derivatization of amines and phenols for a number of applications.[5,11,15,16] BzCl has been valuable for monitoring neurochemicals, as nearly all common neurotransmitters and related metabolites contain an amine or phenol group. Although BzCl is useful, amines and phenols make up only a fraction of the metabolome, e.g., roughly 25%, based on the metabolite library at the Michigan Regional Comprehensive Metabolomics Resource Core (MRC^2). Other functional groups are more

common, such as carboxylic acids, which compose approximately 50% of the metabolite library. Several derivatization techniques have been established for carboxylic acids, but these methods often require synthesis of the reagent and long reaction times with heating.[9,12,17,18]

Of these reagents, aniline seems the most promising.[9,19] Aniline reacts with carboxylic acids through EDC-catalyzed amidation. The reaction requires only three reagents and no heating, so it is relatively simple. $^{13}C_6$-aniline is commercially available and can be used for internal standards. In addition to carboxylic acids, aniline reacts with carbonyls and phosphates, making its scope complimentary to BzCl. However, aniline suffers from poor solubility and is a toxic environmental pollutant. Additionally, compared to other amines, aniline has limited reactivity as a result of modest nucleophilicity due to resonance stabilization. We hypothesized that benzylamine (BnA), which is not resonance stabilized, would be a more reactive, greener alternative to aniline derivatization.

BnA derivatization has been reported previously for hydroxyindoles, catechols, and oligosaccharides, but not for carboxylic acids.[20,21] Here we report BnA as a derivatization reagent for carboxylic acids, carbonyls, and phosphates. d2-BnA is commercially available and is used to create individual internal standards for each targeted metabolite. Additionally, BnA derivatization can be used in conjunction with BzCl for simultaneous analysis of amines, phenols, and carboxylic acids. This combination has the potential to significantly increase the number of metabolites which can be determined quantitatively in a single LC-MS run.

Experimental

Chemicals and reagents

All chemicals were purchased from Sigma-Aldrich (St. Louis, MO) unless otherwise noted. Water and acetonitrile were Budick and Jackson HPLC grade from VWR (Radnor, PA). Stock solutions of 1 M glucose and $^{13}C_6$-glucose (Cambridge Isotope Laboratories, Andover, MA); 50 mM α-ketoglutarate, malate, citrate, isocitrate, and cis-aconitate; 20 mM glutamate, aspartate, succinate, glucose-6-phosphate, fructose-6-phosphate, fructose-1,6-bisphosphate, 3-phosphoglycerate, 2-phosphoglycerate, 6-phosphogluconate, and phenylpyruvate; 10 mM 2-hydroxyphenylacetate, 4-hydroxyphenylacetate, homogentisate, phenethylamine (MP Biomedicals, Santa Ana, CA), phenylalanine, and tyramine; 5 mM ATP, ADP, and phenylacetate; 2 mM tyrosine; 1 mM AMP were prepared in water and stored at -80 °C. A 20 mM stock of 4-hydroxyphenylpyruvate was prepared in ethanol and stored at -80 °C.

Standard mixtures were prepared in water for use in calibration standards. Internal standards were prepared by derivatizing standard mixtures using $^{13}C_6$-BzCl or d_2-BnA (CDN Isotopes, Pointe-Claire, Quebec, Canada). For internal standards, $^{13}C_6$-glucose was used instead of glucose. Single use aliquots of standards and internal standards were prepared and stored at -80 °C. On the day of use, internal standard aliquots were thawed and diluted 100-fold (BzCl) and 50-fold (BnA) into 20% (v/v) acetonitrile containing 1% (v/v) H_2SO_4. This is referred to as the internal standard solution. The BnA reagent was prepared by mixing 328 μL BnA, 972 μL water, and 258 μL HCl. The solution was then adjusted to pH 4.5. Fresh solutions of BzCl and N-dimethylaminopropyl-N'-ethylcarbodiimide (EDC) were prepared daily.

Benzylamine reaction optimization

A standard mixture of 100 μM α-ketoglutarate, malate, succinate, AMP, 2-phospoglycerate, and glucose was used for reaction optimization. BnA volume was optimized by

derivatizing 20 μL aliquots with 2 μL 200 mg/mL EDC followed by 1, 2, 4, or 10 μL of the BnA solution. Reaction time was optimized by allowing the reaction to proceed for 0, 30, 60, 120, and 240 minutes at room temperature. The reaction was stopped by addition of 1 μL triethylamine (TEA). Peak areas from LC-MS/MS analysis were used to compare reaction conditions.

Mobile phase A optimization

A mixture of 100 μM glucose, AMP, fructose-1,6-phosphate, 6-phosphogluconate, succinate, and α-ketoglutarate was used for mobile phase optimization. Standards were derivatized with BnA. Mobile phase A was either 0.1% formic acid, 10 mM ammonium formate with 0.15% formic acid, or 10 mM ammonium acetate with 0.1% acetic acid. Mobile phase B was acetonitrile. Peak area following LC-MS/MS analysis was used to compare mobile phase compositions.

Sample derivatization

The reaction scheme is shown in Figure 6-1a. For standalone BnA derivatization, 20 μL of samples or calibration standards were derivatized by addition of 2 μL 200 mg/mL EDC followed by addition of 10 μL of BnA solution. The mixture was incubated at room temperature for 1 h, with shaking. The reaction was stopped by addition of 1 μL of TEA. Internal standards were prepared in the same manner, using d_2-BnA. A 25 μL portion of each calibration standard or sample was mixed with 1 μL of the internal standards.

For dual derivatization, 20 μL of samples or calibration standards were derivatized by addition of 2 μL 200 mg/mL EDC followed by addition of 10 μL of BnA solution. The mixture was incubated at room temperature for 1 h, with shaking. While incubating, an additional 20 μL

aliquot was derivatized with BzCl by sequential addition of 10 µL 100 mM sodium carbonate, 10 µL 2% (v/v) BzCl in acetonitrile, and 10 µL of the internal standard solution. Following the 1 h incubation, the BnA reaction was stopped by addition of 3.5 µL of the internal standard solution. 5 µL of the BnA-derivatized sample was mixed with 25 µL of the BzCl-derivatized sample. This procedure is outlined in Figure 6-1b.

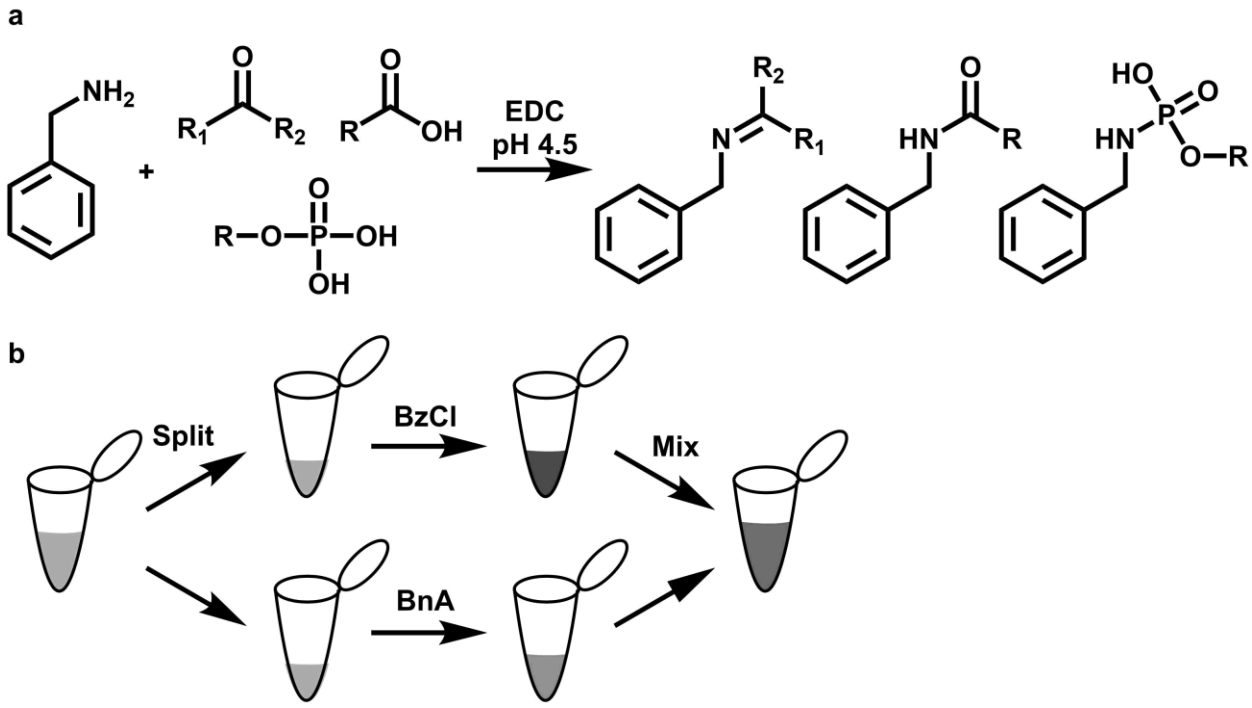

Figure 6-1: a. Schematic showing the reaction of benzylamine with carbonyls, carboxylic acids, and phosphates through EDC catalysis. b. Procedure for dual derivatization method. A sample is split, and portions are labeled with benzoyl chloride (BzCl) or benzylamine (BnA). After the reaction finishes, the two are mixed back together in a 5:1 BzCl:BnA ratio prior to LC-MS/MS analysis.

Metabolite analysis by LC-MS/MS

Analysis was performed using a Waters (Milford, MA) nanoAcquity UPLC. An Acquity HSS T3 C18 column (1 mm x 100 mm, 1.8 µm particle, 100 Å pore size) was used. The autosampler was at ambient temperature and the column was held at 27 °C. Partial loop injection mode was used for 5 µL injections. For standalone BnA samples, mobile phase A was 10 mM ammonium acetate with 0.1% acetic acid and mobile phase B was acetonitrile. The flow rate was

100 μL/min and the gradient was: initial, 0% B; 4.9 min, 80% B; 5 min, 100% B; 6 min, 100% B; 6.1 min, 0% B; 8 min, 0% B. For dual derivatization samples, mobile phase A was 10 mM ammonium formate with 0.15% formic acid, and mobile phase B was acetonitrile. The flow rate was 100 μL/min and the gradient was: initial, 0% B; 0.5 min, 45% B; 4 min, 55% B; 4.1 min; 65% B; 4.9 min, 75% B; 5 min, 100% B; 6 min, 100% B; 6.1 min, 0% B; 8 min, 0% B.

Detection was performed using an Aglient (Santa Clara, CA) G6410B triple quadrupole mass spectrometer in dynamic reaction monitoring (dMRM) mode. For standalone BnA derivatization, electrospray ionization was used in negative mode at -3 kV. For dual derivatized samples, electrospray ionization was used in positive mode at 4 kV. The gas temperature was 350 °C, gas flow was 11 L/min, and the nebulizer was at 15 psi. MRM conditions are listed in Supplemental 1. Automated peak integration was performed using Agilent MassHunter Quantitative Analysis for QQQ, version B.08.00. All peaks were visually inspected to ensure proper integration.

Method evaluation

Signal from BnA derivatization was determined by comparing peak area from a derivatized sample to an underivatized sample at the same concentration. Limits of detection (LOD) were calculated as three standard deviations of the blank using a six point calibration with three replicates. The same calibration was used to determine linearity (R^2). Repeatability was defined as the relative standard deviation (RSD) from triplicate runs of the calibration midpoint.

Sample preparation

Pooled human serum from the American Red Cross Detroit National Testing Lab was provided by the MRC[2]. Proteins were removed from 10 μL aliquots by addition of 40 μL of cold acetonitrile, followed by centrifugation at 12,100g for 5 min. The supernatant was removed and derivatized.

Pancreatic islets were isolated from C57BL/6 (B6) mice using previously described collagenase digestion. 100 islets were isolated per mouse and recovered in culture media (RPMI 1640, 1.7 mM glucose, 10% FBS) for two hours at 37 °C with 5% CO_2. Islets received either no treatment, L-DOPA treatment, or tyrosine treatment. The islets were then washed twice with PBS, and frozen with liquid nitrogen. Metabolite extraction was performed by addition of 50 μL 80% (v/v) acetonitrile followed by sonication. The resulting extract was centrifuged for 5 min at 12,100g. The supernatant was removed and derivatized.

Results and discussion

Benzylamine reaction optimization

We first aimed to determine suitable BnA reaction conditions for a range of metabolites. Carboxylic acids α-ketoglutarate, malate, and succinate; phosphates AMP and 2-phospoglycerate; and carbonyl glucose were selected as representatives of each functional group for optimzation of reaction time (0, 30, 60, 120, 240 min) and BnA reagent volume (1, 2, 4, 10 μL per 20 μL sample). Peak area for each metabolite at these conditions were compared to determine optimal reaction conditions (Figure 6-2a-b). For most metabolites tested, signal went up with increasing volume of BnA added. This increase was most prominent with glucose. For carboxylic acids malate and succinate, signal decreased with increasing BnA, likely due to increased sample dilution. This decrease was relatively small (< 20%) compared to the increase

for glucose (90%). Additionally, calibrations prepared with low BnA volumes were not consistently linear, likely due to an insufficient concentration of BnA. Thus, 10 µL of BnA, or a 2:1 ratio (v/v) of sample:BnA reagent, was determined to be optimal.

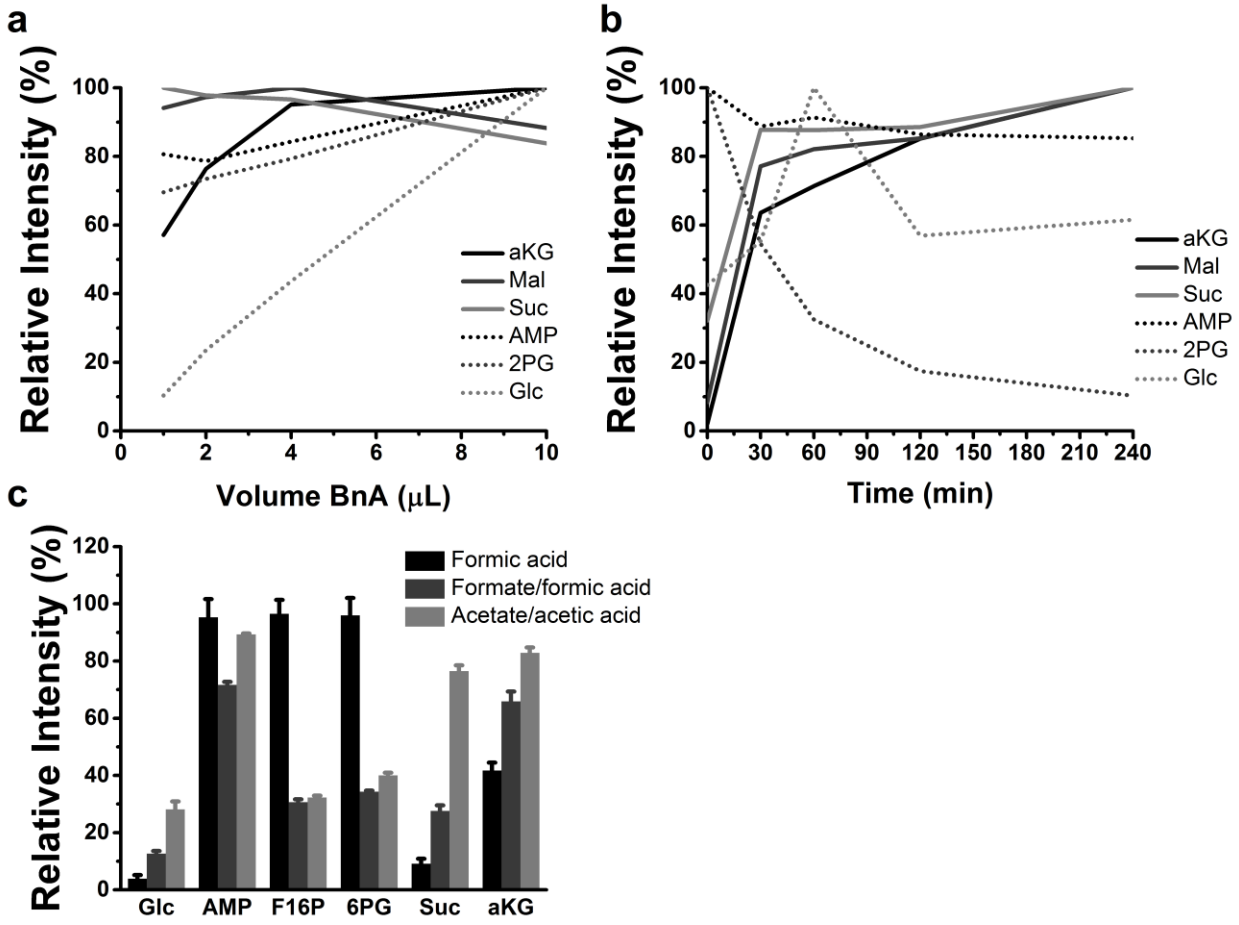

Figure 6-2: Optimization of benzylamine (BnA) derivatization. Reagent volume (a) and reaction time (b) were optimized for 20 µL samples of a 100 µM mix of α-ketoglutarate (aKG), malate (Mal), succinate (Suc), AMP, 2-phosphoglycerate (2PG), and glucose (Glc). Signal generally increased with additional reagent volume, while increasing reaction time had variable effects. A reagent volume of 10 µL and a reaction time of 60 min was selected as optimal. Mobile phase A (c) was optimized using a 100 µM mix of Glc, AMP, fructose-1,6-bisphosphate (F16P), 6-phosphogluconate (6PG), Suc, and aKG. Water with 0.1% formic acid was optimal for phosphates, but 10 mM ammonium acetate with 0.1% acetic acid performed better as a general purpose mobile phase than 10 mM ammonium formate with 0.15% formic acid.

For most metabolites, peak area increased with increasing reaction time. Low signal was generally observed with no incubation period, as expected, although phosphates AMP and 2-phosphoglycerate had highest signal at 0 min. For other metabolites, signal increased sharply

between 0 and 30 min, followed by a gradual increase thereafter. A small decrease was observed for AMP over time, while 2-phosphoglycerate signal dropped significantly. Further investigation is required to determine if this effect is general to all phosphates. Degradation of the derivatized phosphates in the acidic environment could explain this decrease with time. Once quenched to a basic pH, the phosphates appear stable and no decrease in signal was observed over the course of the injection batch. To maximize signal for most metabolites while not sacrificing too much signal for phosphates, a reaction time of 60 min was chosen.

Mobile phase A optimization

We next considered the effect of mobile phase A composition on signal for the derivatized analytes (Figure 6-2c). Glucose, AMP, fructose-1,6-bisphosphate, 6-phospogluconate, succinate, and α-ketoglutarate were selected as representatives of their functional groups. Water with formic acid, the general purpose mobile phase used by the MRC[2], gave the highest peak area for all phosphates tested, but the lowest area for carboxylic acids, and glucose was virtually undetectable. This mobile phase is recommended if only phosphates are of interest, but it is inadequate for a general purpose benzylamine method. Ammonium formate with formic acid, the mobile phase we prefer for BzCl derivatization, gave the lowest peak area for phosphates, and moderate performance for carboxylic acids and carbonyls.

Ammonium acetate with acetic acid, which was selected as an alternative additive to formate, performed better than the formate/formic acid mobile phase for all tested metabolites, so it was selected as the best general purpose mobile phase. The acetate/acetic acid mobile phase had the highest pH. Basic mobile phases are preferred for negative ESI mode, though too high of

a pH can degrade silica columns. The pH of the acetate/acetic acid mobile phase was 4.5, which seemed to be a good compromise between ESI efficiency and column integrity.

Method evaluation

Signal and chromatographic retention enhancement from BnA derivatization was evaluated for carbonyl glucose, phosphates AMP and glucose-6-phosphate, and carboxylic acids α-ketoglutarate, isocitrate, and citrate. Peak areas from unlabeled and labeled metabolites at the same concentration were compared (Figure 6-3). Retention time was increased for all metabolites tested. Signal was increased 10 - 2,000 fold for all metabolites except the phosphates, AMP and glucose-6-phosphate, though this decrease was less than 5 fold. It has been established that the selected mobile phase was not optimal for derivatized phosphates, so a more compatible mobile phase could be used if greater sensitivity is needed for phosphates. Even with a small decrease in signal, derivatization offers advantages in retention and quantification with easily generated internal standards.

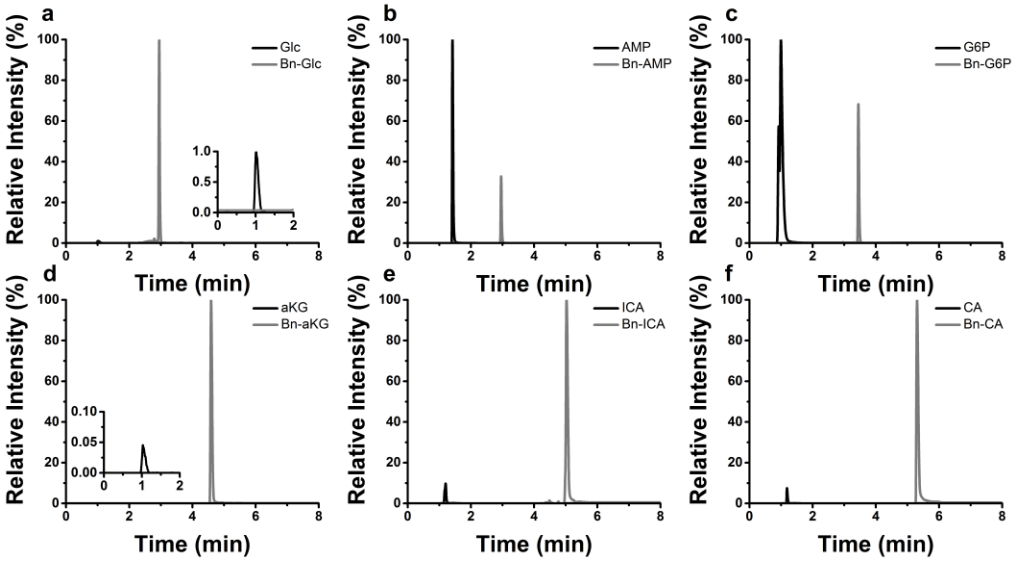

Figure 6-3: Comparison of retention time and signal between unlabeled and benzylamine labeled metabolites. All metabolites tested showed an increase in retention upon derivatization. Increases in signal of up to 2,000-fold were observed for a. glucose (Glc), d. α-ketoglutarate (aKG), e. isocitrate (ICA), and f. citrate (CA). Decreases in signal up to 3-fold were observered for phosphates b. AMP and c. glucose-6-phosphate (G6P).

The increase in retention time is especially important for energy metabolites, which tend to be very polar, as evidenced by only unlabeled AMP eluting significantly past the dead time with a 45% organic mobile phase. Increasing the retention time allows for less colelution and ion suppression, as well as better separation of isomers such as citrate and isocitrate. Unlabeled citrate and isocitrate coelute, while baseline resolution was achieved following derivatization (Figure 6-3e-f). The increase in signal allows for better detection of these metabolites which is particularly important in negative ESI where lower signal than in positive ESI is observed.

To test the utility of the BnA labeling, we developed two methods: 1) a standalone BnA derivatization method for TCA cycle metabolites and sugar phosphates, and 2) a dual derivatization method using BnA and BzCl derivatization for the analysis of phenylalanine metabolites. The selected energy metabolites demonstrate the broad applicability of BnA derivatization, as carboxylic acids, carbonyls, and phosphates are all represented. We also propose the combination of the two derivatization techniques within a single LC-MS/MS run as a means to increase the scope of targeted metabolomics using derivatization. The phenylalanine metabolic pathways demonstrates the need for such a method - a single derivatization method would not be sufficient to target all of the relevant metabolites in the pathway (Figure 6-4). Phenylalanine is an essential amino acid for humans and must be obtained through diet. Defects in phenylalanine metabolism can lead to seizures, learning disabilities, and mental disorders. By measuring the entire pathway, it would be possible to determine which step in the pathway is defective so appropriate treatment can be determined.[22] Example chromatograms for both methods are shown in Figure 6-5.

Figures of merit for the BnA energy metabolites method are listed in Table 6-1, while those for the phenylalanine dual derivatization method are listed in Table 6-2. Linearity was

good (R^2 > 0.98) for all metabolites in both methods. Repeatability, calculated as RSDs for the calibration midpoint, was below 11% for all metabolites. For the energy metabolites method, LODs were in the nanomolar or low micromolar range, with only fructose-6-phosphate, fructose-1,6-bisphosphate, and ATP having LODs over 10 μM. Using the fomic acid mobile phase instead of the acetate/acetic acid mobile phase would likely achieve lower LODs for these phosphates if greater sensitivity is needed.

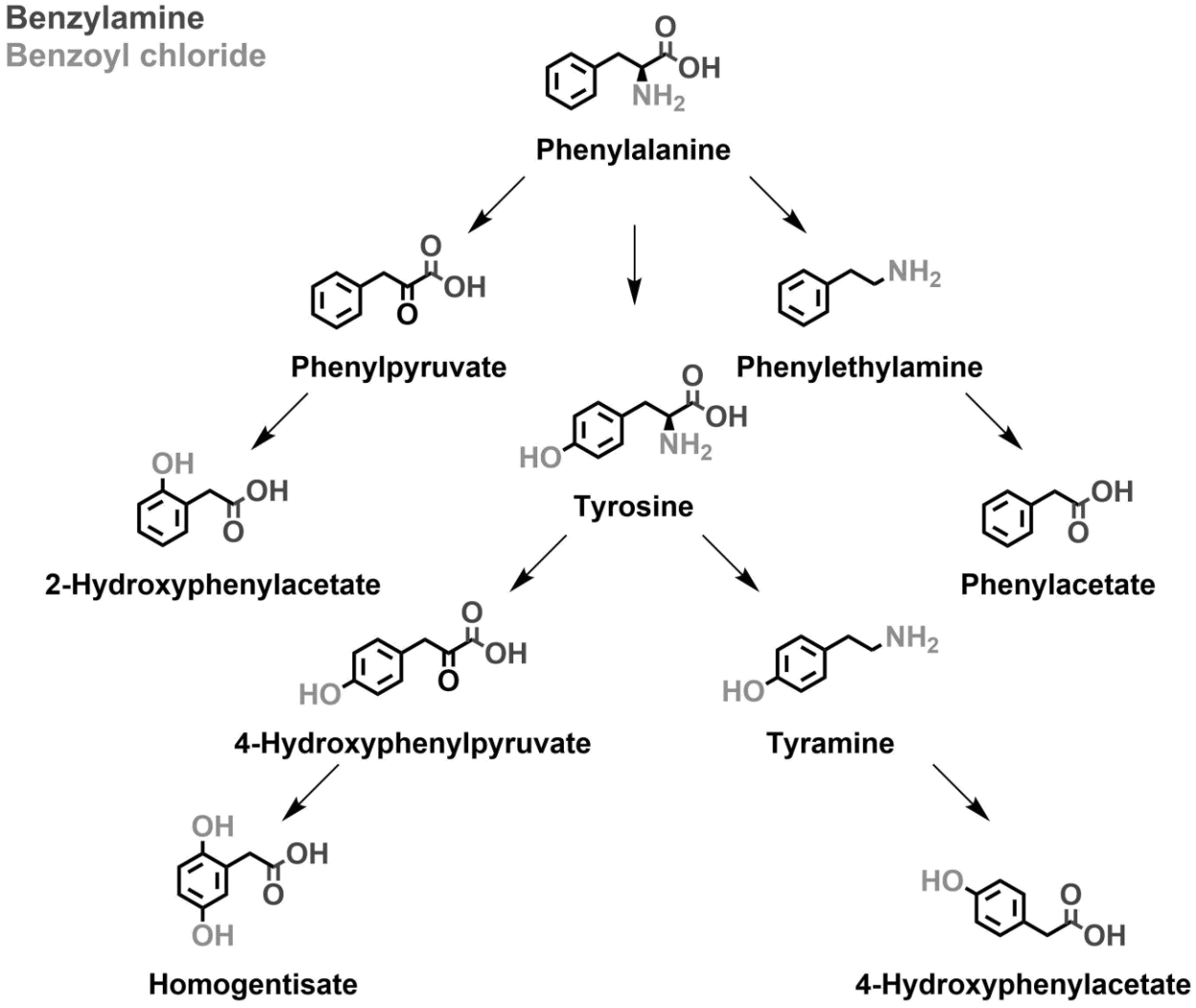

Figure 6-4: Metabolic pathway for catabolism of phenylalanine. Functional groups which are colored can be labeled by either benzylamine or benzoyl chloride. Neither reagent is capable of labeling the entire pathway, thus both techniques are required for full pathway coverage.

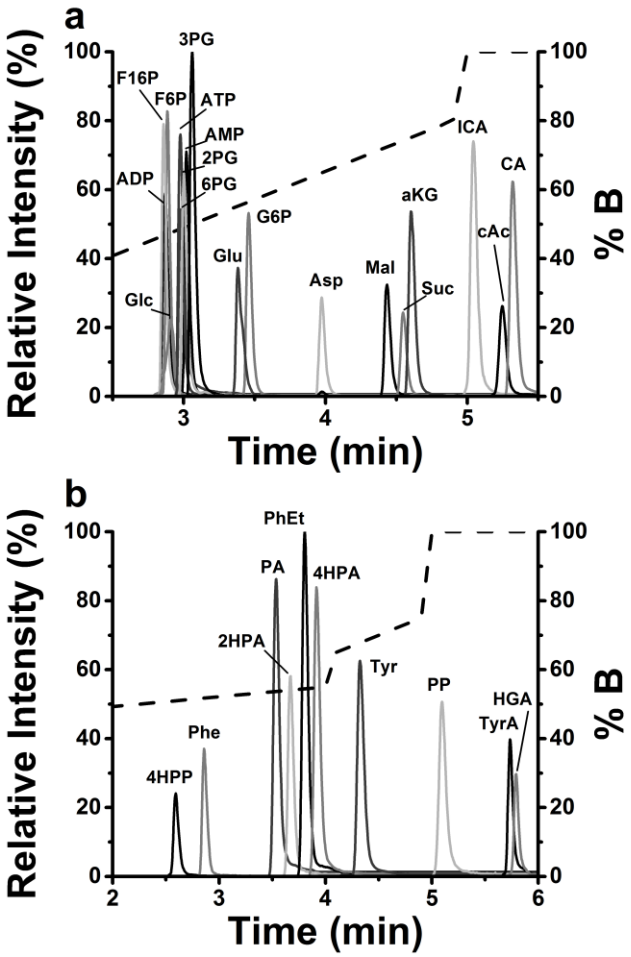

Figure 6-5: Example chromatograms from standards for the a. standalone benzylamine method for energy metabolites and b. the dual derivatization method for phenylalanine metabolites using benzylamine and BzCl. Elution gradients are overlaid as % B.

For the phenylalanine dual derivatization method, most metabolites had LODs between 50 nM and 2 μM. Only 4-hydroxyphenylpyruvate had an LOD over 2 μM. Balancing the ratio of BnA and BzCl derivatized samples when mixing back together for analysis can have a significant impact on resulting signal for each metabolite, so this can be adjusted if greater sensitivity for a specific metabolite is desired.

Metabolite analysis in biological samples

To demonstrate the application of these methods in biological samples, both were applied to pooled human serum. Calculated concentrations for the energy metabolites method are listed in Table 6-1, while concentrations for the phenylalanine dual derivatization method are in Table 6-2. While many of these concentrations for both methods fall within the range expected for serum according to the HMDB, some are lower than expected, particularly within the phosphates. The pooled serum used is several years old, so despite proper precautions being taken to store individual aliquots at -80 °C, it is possible some degradation of the sample has occurred.

Metabolite	LOD (µM)	RSD (%)	R^2	Serum Concentration (µM)
Fructose-1,6-bisphosphate	10	6.84	0.978	ND
ADP	2	3.03	0.999	ND
ATP	26	11.0	0.989	ND
2-Phosphoglycerate	2	4.58	0.998	ND
AMP	5	2.96	0.989	ND
Glucose	8	7.35	0.992	868 ± 61
Fructose-6-phosphate	25	2.17	0.994	ND
6-Phosphogluconate	1	8.51	0.999	ND
3-Phosphoglycerate	0.2	1.58	0.995	ND
Glutamate	2	8.35	0.999	65.7 ± 4.5
Glucose-6-phosphate	8	4.48	0.997	ND
Aspartate	0.9	3.55	0.999	25.8 ± 0.1
Malate	0.4	2.48	0.999	1.41 ± 0.13
Succinate	1	8.42	0.999	1.87 ± 0.23
α-Ketoglutarate	0.3	3.21	0.997	4.60 ± 0.30
Isocitrate	1	6.66	0.996	1.45 ± 0.05
cis-Aconitate	0.1	2.61	0.989	ND
Citrate	0.09	4.68	0.994	3.13 ± 0.41

Table 6-1: Figures of merit for standalone benzylamine derivatization of energy metabolites. Limits of detection (LOD), repeatability (RSD), and linearity (R^2) were calculated from triplicate calibration curves. Concentrations in serum are listed as average ± standard deviation. ND indicates not detected.

Alternatively, it is possible that the reaction and separation conditions are not well suited for analysis of phosphates in biological samples. The mobile phase and reaction time used were not optimal for phosphates, but these conditions were still adequate for phosphate standard solutions. It is possible a matrix component is interfering with ionization efficiency or limiting reaction yield. A standard addition of phosphates to serum could determine if the low concentrations in biological samples are the result of a matrix component.

Furthermore, to demonstrate the potential of the dual derivatization method for detecting changes, we also applied this method to islets of Langerhans from mice, exposed to different culture conditions. Of the ten tested metabolites, seven were detected in at least one of the samples, and five of these were found to be significantly different between the groups using single factor ANOVA (Figure 6-6). The islets treated with tyrosine showed an expected increase

in tyrosine, as well as the tyrosine metabolite tyramine. Islets treated with L-DOPA, a metabolite of tyrosine, also showed an increase in tyramine relative to untreated islets. A feedback mechanism may be present, shifting tyrosine metabolism towards tyramine to prevent an excess buildup of L-DOPA. Homogentisate was only observed in the islets treated with L-DOPA. Homogentisate and L-DOPA are not closely connected so further investigation is needed to explain this result.

Metabolite	LOD (µM)	RSD (%)	R^2	Serum Concentration (µM)
4-Hydroxyphenylpyruvate	25	7.5	0.995	ND
Phenylalanine	0.1	3.9	0.997	63.2 ± 6.8
Phenylacetate	0.2	0.084	0.992	0.29 ± 0.06
2-Hydroxyphenylacetate	0.1	6.2	0.999	ND
Phenethylamine	0.1	6.4	0.999	0.111 ± 0.004
4-Hydroxyphenylacetate	1	8.1	0.999	1.31 ± 0.04
Tyrosine	0.1	1.9	0.998	59.8 ± 6.5
Phenylpyruvate	2	3.9	0.994	ND
Tyramine	0.05	0.78	0.996	0.0183 ± 0.0013
Homogentisate	2	8.3	0.991	3.21 ± 0.66

Table 5-2: Figures of merit for benzylamine and BzCl dual derivatization of phenylalanine metabolites. Limits of detection (LOD), repeatability (RSD), and linearity (R^2) were calculated from triplicate calibration curves. Concentrations in serum are listed as average ± standard deviation. ND indicates not detected.

Comparison to other derivatization reagents

BnA derivatization is closely related to aniline derivatization. Both act as derivatization reagents through EDC-catalyzed reactions.[9,19] We anticipated that BnA would have greater reactivity than aniline, and this was observed as the BnA reaction time was optimized to 60 min, while 120 minute were required for aniline derivatization. Limits of detection for carboxylic acids were similar between aniline and BnA, but LODs were higher for phosphates with BnA than with aniline. A higher aniline concentration was used than BnA, so increasing the BnA concentration might compensate for this. Additionally, ion pairing reagents were added to the aniline mobile phase. Ion pairing in LC can aid in separation of polar metabolites with reversed

phase chromatography, but they are difficult to fully remove from the instrumentation. We choice to forego ion pairing reagents but they may be considered for future work with BnA. BnA has the advantage over aniline of being compatible with acid quenching; aniline crashes out of solution when acid is added. Quenching with acid makes BnA compatible with BzCl derivatization, so both reagents can be used for a single LC-MS/MS run.

2-Hydrazinoquinoline (2-HQ) is another reagent that has been used for LC-MS derivatization of carboxylic acids and carbonyls.[12] 2-HQ reacts with carbonyls to form hydrazones, and with carboxylic acids to form hydrazides following activation with 2,2'-dipyridyl disulfide and triphenylphosphine. Like aniline and BnA, 2-HQ is compatible with aqueous biological samples. Ion pairing reagents are not used and the reaction time is only an hour, which is consistent with BnA derivatization. However, the reaction mixture is heated, which may cause degradation of thermally sensitive metabolites. No stable isotope labeled version of 2-HQ is currently available for use in internal standards. Limits of detection were not evaluated for 2-HQ as the reagent was used to expand metabolome coverage rather than to increase sensitivity. This work was performed on a qTOF MS and MS/MS was only used to determine structural information. Our preliminary attempts at 2-HQ derivatization with a QQQ MS yielded poor fragmentation and inconsistent derivatization.

Phenylhydrazine has also been used for derivatization of carboxylic acids and phosphates.[23] This reaction takes two hours but does not require heating. Although not utilized in this work, deuterated phenylhydrazine is commercially available and could be used for internal standards. Limits of detection were also not evaluated. A major disadvantage of this method is its reliance on ion pairing reagents for the chromatography. While this allowed for the chromatographic separation of isomers such as glucose-6-phosphate and fructose-6-phosphate,

this was also achieved with aniline and BnA derivatization. Due to the difficulty of fully removing ion pairing reagents from instrumentation, we have not yet worked with phenylhydrazine as a potential derivatization reagent.

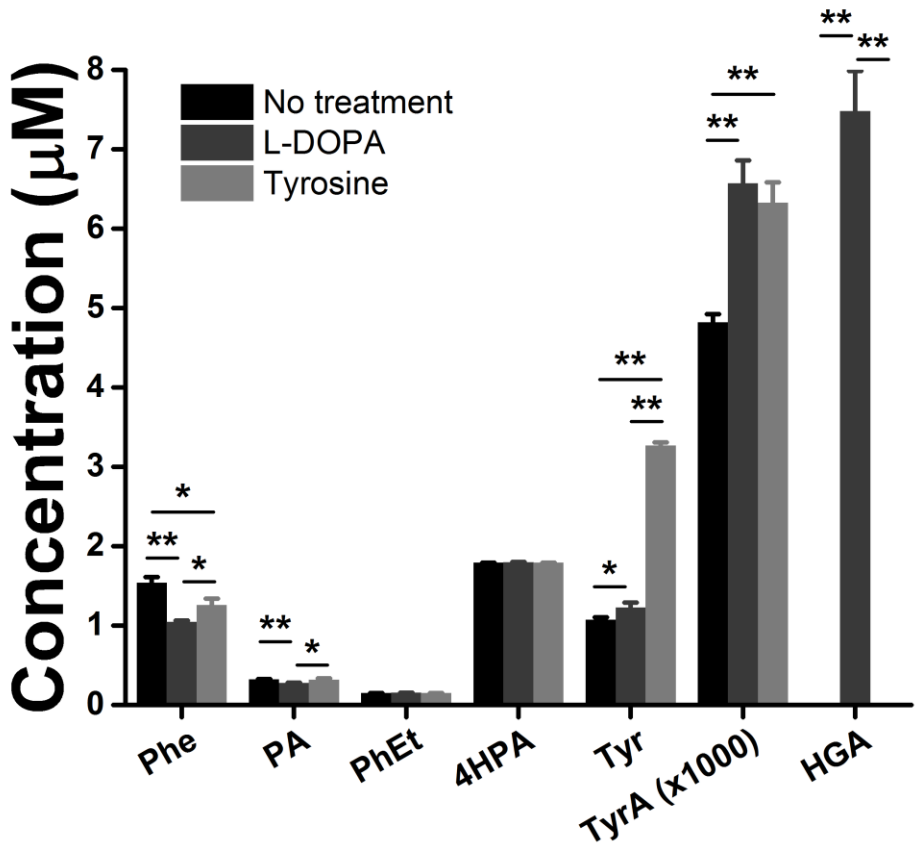

Figure 6-6: Concentrations of phenylalanine metabolites in extract from islets of Langerhans from mice with no treatment, L-DOPA treatment, or tyrosine treatement. Significant differences were observed between groups for phenylalanine (Phe), phenylacetate (PA), tyrosine (Tyr), tyramine (TyrA), and homogentisate (HGA). No differences were observed between phenethylamine (PhEt) or 4-hydroxyphenylacetate (4HPA). The remaining metabolites were not detected in any samples. * $p \leq 0.05$; ** $p \leq 0.01$

Conclusions

Reliable detection of a large number of metabolites is a persistent challenge in metabolomics. While a variety of approaches are being developed to address this, most require lengthy analysis times or suffer from poor sensitivity. Chemical derivatization is a way to increase the scope of targeted metabolomics while also increasing sensitivity. Methods are

limited to the functional groups which can be labeled, but the combination of complimentary reagents can greatly increase this. While any combination can be used for separate analysis, here we describe BnA as a novel derivatization reagent which can be used with BzCl derivatization within a single LC-MS/MS run.

A method for the analysis of 18 energy metabolites with BnA was developed. Furthermore, this reagent was combined with BzCl for the analysis of 10 metabolites related to phenylalanine metabolism, a pathway which could not be analyzed by either BnA or BzCl alone. These methods were demonstrated in both standard solutions and biological samples, though room for improvement remains. The methods described here are not particularly large in scope, and detection in biological samples, especially of phosphates, is still challenging. Comparison of additional mobile phases may find a solvent that works well for both carboxylic acids and phosphates. Further optimization of reaction conditions may also increase signal for phosphates. Samples can be extracted in lower volumes to achieve higher concentrations, or the extract could be dried down and reconstituted in a smaller volume to allow for preconcentration. If none of these options pan out, it may be best to focus solely on carboxylic acids and carbonyls.

Although these methods do not target a large number of metabolites, they demonstrate the potential of BnA as a derivatization reagent. Used alone with negative ESI, carboxylic acids, carbonyls, and phosphates can be labeled, though further optimization is needed for phosphates. More details on addressing the poor sensitivity for phosphates are provided in Chapter 7. With positive ESI, only carboxylic acids are detectable with BnA, but the derivatized samples are compatible with BzCl derivatized samples, allowing detection of amines and phenols in addition to carboxylic acids. The combination of these two reagents could allow for analysis of up to 75% of the metabolite library at the MRC^2.

References

(1) Wishart, D. S.; Feunang, Y. D.; Marcu, A.; Guo, A. C.; Liang, K.; Vázquez-Fresno, R.; Sajed, T.; Johnson, D.; Li, C.; Karu, N.; Sayeeda, Z.; Lo, E.; Assempour, N.; Berjanskii, M.; Singhal, S.; Arndt, D.; Liang, Y.; Badran, H.; Grant, J.; Serra-Cayuela, A.; Liu, Y.; Mandal, R.; Neveu, V.; Pon, A.; Knox, C.; Wilson, M.; Manach, C.; Scalbert, A. *Nucleic Acids Res.* **2017**.

(2) Bajad, S. U.; Lu, W.; Kimball, E. H.; Yuan, J.; Peterson, C.; Rabinowitz, J. D. *J. Chromatogr. A* **2006**, *1125* (1), 76–88.

(3) Yuan, M.; Breitkopf, S. B.; Yang, X.; Asara, J. M. *Nat. Protoc.* **2012**, *7* (5), 872–881.

(4) Gu, H.; Zhang, P.; Zhu, J.; Raftery, D. *Anal. Chem.* **2015**, *87* (24), 12355–12362.

(5) Wong, J. M. T.; Malec, P. A.; Mabrouk, O. S.; Ro, J.; Dus, M.; Kennedy, R. T. *J. Chromatogr. A* **2016**, *1446*, 78–90.

(6) Whiley, L.; Godzien, J.; Ruperez, F. J.; Legido-Quigley, C.; Barbas, C. *Anal. Chem.* **2012**, *84* (14), 5992–5999.

(7) Chen, S.; Hoene, M.; Li, J.; Li, Y.; Zhao, X.; Häring, H. U.; Schleicher, E. D.; Weigert, C.; Xu, G.; Lehmann, R. *J. Chromatogr. A* **2013**, *1298*, 9–16.

(8) Fei, F.; Bowdish, D. M. E.; McCarry, B. E. *Anal. Bioanal. Chem.* **2014**, *406* (15), 3723–3733.

(9) Yang, W.-C.; Sedlak, M.; Regnier, F. E.; Mosier, N.; Ho, N.; Adamec, J. *Anal. Chem.* **2008**, *80* (24), 9508–9516.

(10) Guo, K.; Li, L. *Anal. Chem.* **2009**, *81* (10), 3919–3932.

(11) Song, P.; Mabrouk, O. S.; Hershey, N. D.; Kennedy, R. T. *Anal. Chem.* **2012**, *84*, 412–419.

(12) Lu, Y.; Yao, D.; Chen, C. *Metabolites* **2013**, *3* (4), 993–1010.

(13) Esch, C.; Hui, D. S.; Lee, R.; Edwards, J. L. *Anal. Methods* **2015**, *7* (17), 7164–7169.

(14) Zhao, S.; Dawe, M.; Guo, K.; Li, L. *Anal. Chem.* **2017**, *89* (12), 6758–6765.

(15) Hershey, N. D.; Kennedy, R. T. *ACS Chem. Neurosci.* **2013**, *4* (5), 729–736.

(16) Malec, P. A.; Oteri, M.; Inferrera, V.; Cacciola, F.; Mondello, L.; Kennedy, R. T. *Journal of Chromatography A*. 2017, p Accepted.

(17) Ingalls, S. T.; Minkler, P. E.; Hoppel, C. L.; Nordlander, J. E. *J. Chromatogr. Res. Serv.* **1984**, *299891* (151).

(18) Guo, K.; Li, L. *Anal. Chem.* **2010**, *82* (21), 8789–8793.

(19) Jannasch, A.; Sedlak, M.; Adamec, J. In *Methods in Molecular Biology*; Metz, T. O., Ed.; 2011; Vol. 708, pp 159–171.

(20) Lemoine, J.; Chirat, F.; Domon, B. *J. Mass Spectrom.* **1996**, *31* (8), 908–912.

(21) Yoshitake, T.; Fujino, K.; Kehr, J.; Ishida, J.; Nohta, H.; Yamaguchi, M. *Anal. Biochem.* **2003**, *312* (2), 125–133.

(22) Blau, N.; Van Spronsen, F. J.; Levy, H. L. *Lancet* **2010**, *376* (9750), 1417–1427.

(23) Guo, L.; Worth, A. J.; Mesaros, C.; Snyder, N. W.; Glickson, J. D.; Blair, I. A. *Rapid Commun. Mass Spectrom.* **2016**, *30* (16), 1835–1845.

CHAPTER 7

Future directions

Optimization of benzylamine derivatization for phosphates

Reaction conditions for benzylamine derivatization were optimized and work well for carboxylic acids and carbonyls, but limits of detection for phosphates were relatively high and they were generally not detected in the biological samples tested. During optimization, sensitivity for phosphates was sacrificed to improve sensitivity for other metabolites, so further optimization may lead to conditions which are better suited for all functional groups.

Despite the lower sensitivity for phosphates, calibration standards still gave adequate signal. It is unclear whether the lack of signal in biological samples is because they simply are not present, or if matrix effects are limiting sensitivity. To test this, phosphate standards can be spiked into pooled serum, followed by protein precipitation and derivatization. If the spiked phosphates are undetectable, or at a lower concentration than expected, matrix effects are likely causing loss of signal. Using a different protein precipitation may help reduce matrix effects, or another extraction strategy, such as solid phase extraction, could be used.

It was also observed that signal for phosphates decreased with increasing reaction time, but the reason for this is unknown. Reaction progress was tracked by monitoring only the labeled species, so the labeled species may be converting back into the unlabeled species as reaction time increases. Tracking both the labeled and unlabeled species would help determine if this is the case or not. If an increase in the unlabeled species over time is not observed, the labeled species

may still be degrading into another product. Labeled species are stable in the final solution, which is basic, but the reaction occurs at acidic pH. If degradation is occurring, reaction time may need to be further reduced, or the reaction mixture could be optimized.

Additionally, while signal enhancement was observed for derivatized carboxylic acids and phosphates relative to unlabeled species, this was not the case for phosphates. For these experiments, only the labeled species was monitored, so it is unclear if the reaction is going to completion or not. If not, this could explain the decrease in signal. Monitoring both the labeled and unlabeled species would help determine if this is the case. If the reaction is not going to completion, adjusting reaction conditions may help increase the yield.

The mobile phase used was also not optimal for phosphates. Water with formic acid worked best for phosphates, but gave very poor signal for carboxylic acids and carbonyls. Ammonium formate with formic acid was chosen as a compromise. However, another mobile phase might work better for phosphates while maintaining adequate signal for the other metabolites. The tests outlined here would provide insight into the poor signal for phosphates and may allow for further optimization of reaction conditions to work for all functional groups. However, if the conditions required for phosphates are too different from those for carboxylic acids and carbonyls, it might be necessary to focus primarily on the carboxylic acids and carbonyls with benzylamine derivatization. When phosphates are of interest, a separate reaction can be used with conditions optimized specifically for the phosphates.

Development of derivatized metabolite library

Method development for targeted metabolomics can be slow, as MRMs must be determined and optimized for each metabolite of interest. Derivatized metabolites are well

retained with reversed phase chromatography, so time does not need to be spent comparing column chemistries. However, MRMs still must be determined for the derivatized metabolites. Currently, MRMs for derivatized metabolites are established on an "as needed" basis and general purpose methods are used for most applications. Using this approach, metabolites of interest for a particular study might not be measured while metabolites not relevant to the study are. Development of methods specific to each study would ensure that all relevant metabolites are being analyzed but the labor involved could create delays before sample analysis can occur.

To reduce method development time for custom targeted methods, a library of MRMs for derivatized metabolites using a general gradient could be established. When a specific method is desired, MRM conditions can be retrieved from the library, leaving only gradient optimization to be completed if the conditions used to create the library are inadequate. An approach like this would require significant effort up front, but could greatly reduce subsequent method development time.

MRMs for approximately 100 benzoylated metabolites have already been established. A potentially limiting factor for expanding upon that is standard availability. However, the Michigan Comprehensive Regional Metabolomics Resource Core (MRC^2) maintains a metabolite library with approximately 1,000 authentic standards. Roughly a quarter of the metabolites within this library can be derivatized with benzoyl chloride (BzCl), while up to two thirds could be derivatized with benzylamine (BnA). Accounting for overlap between these groups, a library of up to 750 metabolites could be established using standards from the MRC^2 alone. When a study requires a new method, MRMs for as many or a few metabolites as desired can be pulled from the library to create the method in a matter of minutes. The creation of such a

library would be beneficial for both in-lab and collaborative projects and could aid in metabolite identification if untargeted methods are used with derivatization.

Untargeted metabolomics with derivatization

All of the work in this dissertation has been targeted metabolomic methods, which quantify known metabolites based on MRMs developed using authentic standards. This approach leads to more reproducible results as well as simpler data analysis and the potential for absolute quantification. However, only known metabolites with accessible standards can be targeted, so novel or unexpected metabolites cannot be discovered. Thus, untargeted methods are still the gold standard for hypothesis generation.

Derivatization can still be used for untargeted methods with high resolution mass spectrometry (HRMS) to provide greater retention and ionization efficiency in reversed phase LC-MS. Data analysis and metabolite identification in untargeted metabolomics is challenging, however, and derivatization creates additional challenges. The information provided in HRMS is not sufficient to differentiate between unlabeled and labeled metabolites, nor can it tell how many labels are on a labeled metabolites. For BzCl, there is a correlation between number of labels and both retention time and precursor ion mass, but these factors are not enough to accurately assign a number of labels to each feature detected (Figure 7-1). If the goal is to distinguish groups based on metabolic profile, the number of labels should not matter, but metabolite identification becomes increasingly difficult without this information. Databases such as XCMS[1] or HMDB[2] do not include derivatized metabolites so they cannot be used without subtracting off a known number of labels.

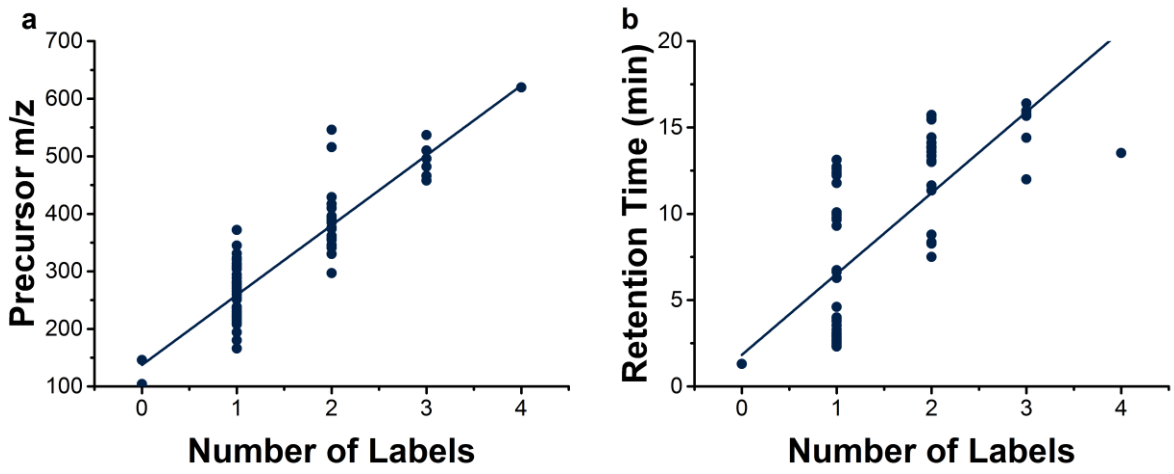

Figure 7-1: Factors such as precursor ion mass (a) and retention time (b) are correlated to the number of benzoyl groups on labeled metabolites

Liang Li's group has developed a number of approaches to overcome these challenges using dansyl chloride (DnsCl) derivatization for untargeted metabolomics.[3–5] By labeling a sample with both "light" DnsCl and "heavy" d2-DnsCl, a signature peak pair profile is created in the mass spectrum for any labeled metabolite. The difference between peak pairs will be a multiple of 2, based on the number of labels. From this data, it is easy to determine the number of labels on a specific feature. Additionally, software has been developed to automate peak pair picking, and a dansylated library has been developed to aid in metabolite identification.

A similar approach could be taken with BzCl. Using HRMS with ^{12}C and $^{13}C_6$ BzCl, the same peak pair profile could be created, though peak pairs would differ by a multiple of 6 instead of 2. The peak pair picking software is open source and factors could be modified to accommodate BzCl derivatization. Preliminary work on a q-TOF mass spectrometer using human plasma shows a number of peaks in the base peak chromatogram and the expected peak pair patterns in extracted mass spectra (Figure 7-2). The derivatized library described earlier would aid in metabolite confirmation though MS/MS fragmentation patterns, but HRMS would need to be used for these standards to obtain precise enough masses for initial searches.

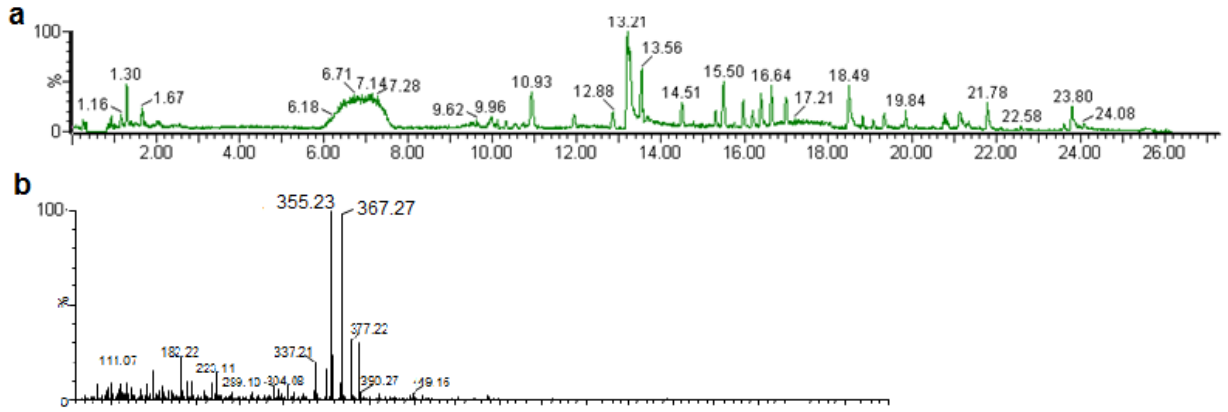

Figure 7-2: Untargeted metabolomics with benzoyl chloride (BzCl(derivatization using ultra high pressure liquid chromatography and qTOF mass spectrometry. a. Base peak chromatogram of human serum. b. Extracted mass spectrum from 15.7 min showing peak pair resulting from ^{12}C- and ^{13}C-BzCl derivatization.

Pseudotargeted metabolomics with benzoyl chloride

In addition to targeted and untargeted metabolomics, new approaches are being developed which combine features of each. One such approach, "widely targeted" metabolomics, has already demonstrated with BzCl. While widely targeted metabolomics still depends on authentic standards, another approach called "pseudotargeted" metabolomics does not.[6–9] Instead, pseudotargeted methods develop MRMs directly from the samples to be analyzed. Candidate precursor ions are selected though scanning methods or incremental SIMs. These precursors can then be fragmented and conditions can be optimized for the resulting MRMs. Method development in this manner can be time consuming, but it allows for a reproducible MRM method which does not depend on the availability of authentic standards.

Pseudotargeted metabolomics with derivatization has previously been described with ω-bromoacetonylquinolinium bromide (BQB), a derivatization reagent for thiols.[10,11] Using BQB and d7-BQB, peak pairs in the mass spectra were used to identify candidate thiols. However, rather than using a MS2 scan, a double precursor ion scan was used. BQB and d7-BQB labeled metabolites produce a characteristic product ions of 218 and 225 respectively. Precursor scans for each product ion were used to identify candidate precursor ions, limiting background from

unlabeled metabolites, and reducing method development time as product ions for the precursor ions do not need to be determined. Using this method, 103 thiol candidates have been discovered in human urine, and nearly 20 have been identified through the use of standards.

Based on the success of this method, we started to explore the potential of using this approach with BzCl derivatization, which produces characteristic product ions of 105 and 111 for light and heavy labeled metabolites. A double precursor scan method was established to cover a range of 100 - 600 m/z. This method was first applied to pooled human serum from the American Red Cross National Testing Lab, provided by the MRC[2]. Serum was derivatized with both ^{12}C- and ^{13}C-BzCl, and the resulting solutions were mixed in equal proportions. The resulting total ion chromatogram (TIC) is shown in Figure 7-3. Mass spectra were extracted for each observed peak in the TIC (7-3b). In the mass spectrum, five peak pairs can be identified with a difference of 6, corresponding to singly labeled metabolites. At a higher m/z, three peak pairs are seen with a difference of 12, corresponding to doubly labeled metabolites. From the serum, 62 potential precursor ions were identified.

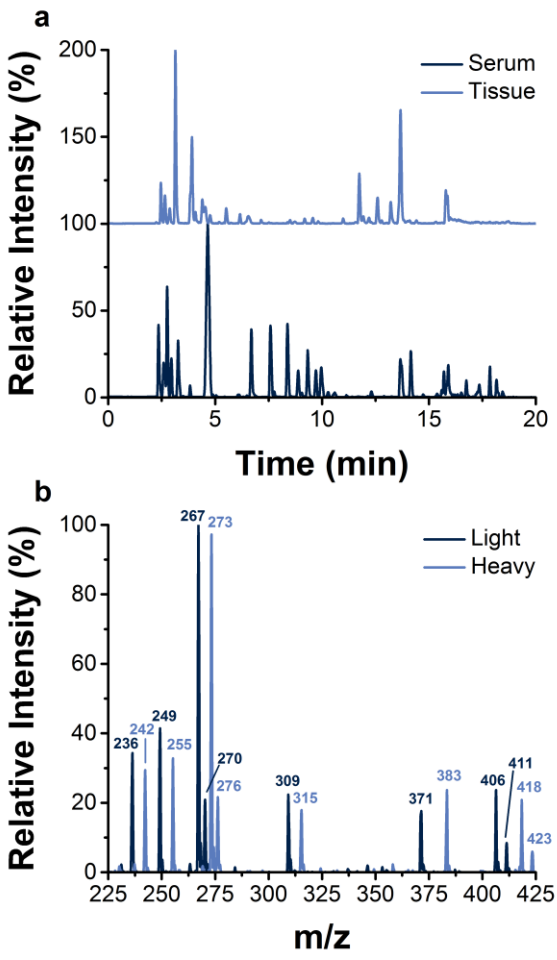

Figure 7-3: Pseudotargeted metabolomics with benzoyl chloride (BzCl) derivatization. a. Total ion chromatogram from human serum and mouse brain tissue. b. Extracted mass spectra from 9.9 min from serum. Separate spectra are extracted for ^{12}C- and ^{13}C-BzCl. Peak pairs are observed with m/z differences of 6 or 12, corresponding to singly or doubly labeled metabolites.

The double precursor scan was also applied to brain tissue extract. Samples from two brain regions, the hypothalamus and midbrain, were available from two strains of mice, B6 and CAST. Portions of each extract were pooled and the pooled extract was derivatized with both ^{12}C- and ^{13}C-BzCl. The resulting solutions were mixed in equal proportions. The TIC from the double precursor ion scan is shown in Figure 7-3. The brain tissue was less rich in metabolites than the serum, but 45 potential precursors were still identified. An MRM method was created based on these potential precursors. Individual brain tissue extracts were then labeled with ^{12}C-BzCl, and mixed with ^{13}C-BzCl derivatized pooled extract.

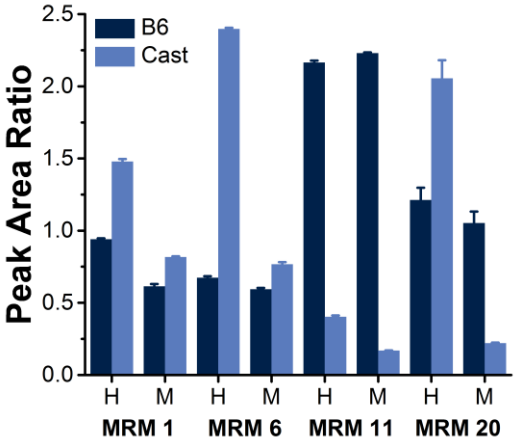

Figure 7-4: Relative quantification of pseudotargeted metabolomics in hypothalamus (H) and midbrain (M) tissue extract of B6 and CAST strains of mice. Individual samples were labeled with ^{12}C-BzCl and quantified relative to pooled tissue labeled with ^{13}C-BzCl. 30 of 45 candidate MRMs were detected, and four representative MRMs are shown.

Of the 45 potential MRMs, only 30 were reliably detected. Of these 30, all showed significant differences between the four sample types (Figure 7-4). Only preliminary work has been performed, so it is unclear why the remaining 15 were undetected. However, using narrower m/z ranges for the precursor ion scan and optimizing conditions for the resulting MRMs should increase sensitivity as well as the number of features detected. This approach combines the sensitive, reliable MRMs of targeted metabolomics with the ability to discover novel or unexpected metabolites typical of untargeted metabolomics and would be a powerful complement to the current targeted work done with BzCl derivatization.

References

(1) Gowda, H.; Ivanisevic, J.; Johnson, C. H.; Kurczy, M. E.; Benton, H. P.; Rinehart, D.; Nguyen, T.; Ray, J.; Kuehl, J.; Arevalo, B.; Westenskow, P. D.; Wang, J.; Arkin, A. P.; Deutschbauer, A. M.; Patti, G. J.; Siuzdak, G. *Anal. Chem.* **2014**, *86* (14), 6931–6939.

(2) Wishart, D. S.; Feunang, Y. D.; Marcu, A.; Guo, A. C.; Liang, K.; Vázquez-Fresno, R.; Sajed, T.; Johnson, D.; Li, C.; Karu, N.; Sayeeda, Z.; Lo, E.; Assempour, N.; Berjanskii, M.; Singhal, S.; Arndt, D.; Liang, Y.; Badran, H.; Grant, J.; Serra-Cayuela, A.; Liu, Y.; Mandal, R.; Neveu, V.; Pon, A.; Knox, C.; Wilson, M.; Manach, C.; Scalbert, A. *Nucleic Acids Res.* **2017**, *in press*.

(3) Guo, K.; Li, L. *Anal. Chem.* **2009**, *81* (10), 3919–3932.

(4) Zhou, R.; Tseng, C. L.; Huan, T.; Li, L. *Anal. Chem.* **2014**, *86* (10), 4675–4679.

(5) Huan, T.; Wu, Y.; Tang, C.; Lin, G.; Li, L. *Anal. Chem.* **2015**, *87* (19), 9838–9845.

(6) Chen, S.; Kong, H.; Lu, X.; Li, Y.; Yin, P.; Zeng, Z.; Xu, G. *Anal. Chem.* **2013**, *85* (17), 8326–8333.

(7) Shao, Y.; Zhu, B.; Zheng, R.; Zhao, X.; Yin, P.; Lu, X.; Jiao, B.; Xu, G.; Yao, Z. *J. Proteome Res.* **2015**, *14* (2), 906–916.

(8) Wang, Y.; Liu, F.; Li, P.; He, C.; Wang, R.; Su, H.; Wan, J.-B. **2016**.

(9) Gu, H.; Zhang, P.; Zhu, J.; Raftery, D. *Anal. Chem.* **2015**, *87* (24), 12355–12362.

(10) Liu, P.; Huang, Y. Q.; Cai, W. J.; Yuan, B. F.; Feng, Y. Q. *Anal. Chem.* **2014**, *86* (19), 9765–9773.

(11) Liu, P.; Qi, C.-B.; Zhu, Q.-F.; Yuan, B.-F.; Feng, Y.-Q. *Sci. Rep.* **2016**, *6* (1), 21433.